Addis Ababa University

Addis Ababa Institute of Technology

School of Electrical and Computer Engineering

Grid Connection and Synchronization Inverter Control for Solar Power System Using Synchronously Rotating Reference Frame

By

Wondimagegn Minda

A Thesis submitted to Addis Ababa Institute of Technology in partial fulfillment of the requirements for the Degree of Master of Science in Electrical and Computer Engineering (Control Engineering)

Advisor:

Mengesha Mamo (Associate Professor)

October, 2019

Addis Ababa, Ethiopia

Addis Ababa University

Addis Ababa Institute of Technology

School of Electrical and Computer Engineering

A Thesis submitted to Addis Ababa Institute of Technology in partial fulfillment of the requirements for the Degree of Master of Science in Electrical and Computer Engineering (Control Engineering)

By

Wondimagegn Minda

APPROVED BY BOARD OF EXAMINERS

_____	_____	_____
Chairman, Department of Graduate Committee	Signature	Date
_____	_____	_____
Advisor	Signature	Date
_____	_____	_____
Internal Examiner	Signature	Date
_____	_____	_____
External Examiner	Signature	Date

Declaration

I, the undersigned, declare that this thesis work is my original work, has not been presented for a degree in this or any other universities, and all sources of materials used for this thesis work have been fully acknowledged.

Wondimagegn Minda _____

Name Signature

Place: Addis Ababa Institute of Technology, Addis Ababa University, Addis Ababa

This thesis has been submitted for examination with my approval as a university advisor.

Dr. Mengesha Mamo _____

Advisor's Name Signature

Acknowledgement

First of all, I would like to express my deepest gratitude to the almighty God for helping me to accomplish this thesis work.

I would also like to gratitude my thesis advisor, Dr.Mengesha Mamo (Associate Professor) for his persistent support by sharing his knowledge and creative ideas until the completion of my thesis work.

Last but not least, I would like to thank my family for encouraging and supporting me during the period of my study.

Abstract

Grid connected solar PV systems are increasing dramatically from year to year due to the increase of global interest in renewable energy sources and growth in energy demand. In thesis work, the designing and modeling of grid connected PV system using synchronously rotating reference frame (SRRF) has been carried out. In this thesis, the important points and literature regarding the elements in a PV system, an inverter and grid connection system have been studied and reviewed.

The photovoltaic model is used to simulate actual PV array characteristics, and an MPPT method using incremental conductance method is proposed in order to control the DC-DC boost converter to extract the maximum power from the PV array. The inverter used in this thesis work is three-phase two-level voltage source inverter (VSI) which is controlled using synchronously d-q reference frame with space vector pulse width modulation (SVPWM). The control structure for the inverter is designed by synchronous reference frame with phase locked loop (PLL). The phase locked loop is used to acquire the available necessary information of grid voltage. An LCL-filter is used to interconnect the output of inverter to the grid and used to attenuate the total harmonics distortion (THD) present in the output current and voltage of the inverter. The system model is developed using MATLAB/SIMULINK environment.

The efficiency of the overall system is around 97% which is improved more than the previous related work whose efficiency is around 96%. The total harmonic distortion of the grid current is 0.88% which is less than the previous work that is 1.42%. For resistive load change, the THD of the grid current and inverter current are 0.88%, 0.91% and 0.93%, and 0.86%, 0.87% and 0.87% for a load of 1.5kW, 2.5kW and 3.5kW respectively. For a nonlinear load change, the THD of the grid current and inverter current are 0.61%, 0.51% and 0.50%, and 0.12%, 0.12% and 0.12% for a load of 100Ω, 125Ω and 320Ω and C = 3000μF respectively.

Keywords: DC-DC Converter, MPPT controller, Inverter control scheme, Grid synchronization, Phase locked loop (PLL), Grid connected solar PV system.

Table of Contents

List of Tables

List of Figures

List of Abbreviations

PLL	Phase Locked Loop
PWM	Pulse width modulation
PV	Photovoltaic
DC	Direct current
AC	Alternating current
MPPT	Maximum power point tracking
d-q	Direct-quadrature
PCU	Power conditioning unit
PI	Proportional integral controller
CSI	Current source inverter
VSI	Voltage source inverter
SVPWM	Space vector pulse width modulation
STC	Standard test condition
THD	Total harmonic distortion
FFT	Fast Fourier transforms
SRRF	Synchronously rotating reference frame
RF	Reference frame

Chapter One

Introduction

1.1. Background of the Thesis

In the past decade, the focus has shifted towards obtaining energy from renewable resources rather than from fossil fuels. This has led to the commencement of wide scale research in the fields of wind and solar energy as these never-ending resources provide clean and sustainable energy with minimal pollution. Many countries want to shift completely on renewable energy by the next few years. Wind power systems are generally employed for large scale power production in the form of wind farms, which are usually situated far from civilization as they produce noise [1] which may decline the quality of life for people residing nearby [2].

Solar Photovoltaic (PV) system is a system that employs solar cells to convert solar energy into electrical power. The solar cell, or the PV cell, is an electrical device that produces electricity directly from the sunlight. Solar PV system is one of the renewable and clean energy sources. The tremendous increase in energy demand, the growth of global interest in renewable and clean energy sources, and the advances in research and technology in solar PV, all led to significant advances in PV industry [3].

The necessity for having available sustainable energy systems for substituting gradually conventional ones requires changing the paradigm of energy supply by utilizing clean and renewable resources of energy. Among all renewables energy, solar energy characterizes as a clean, pollution free and inexhaustible energy source, which is also abundantly available anywhere in the world. These factors have contributed to make solar energy the fastest growing renewable technology in the world [4].

The input to the solar panel is temperature and solar irradiance as a DC input. Solar panel is provided to the DC-DC converter as an input. The function of this converter is to boost the voltage level and passes it to the type of inverter which is going to be used.

Distributed energy sources are connected to the grid through power electronic converters which besides transferring the generated dc power to the ac grid should also be able to exhibit advanced functions like dynamic control of active and reactive power, stationary operation within a range of voltage and frequency, voltage ride-through, reactive current injection during faults, participation in grid balancing act like primary frequency control, and so on [5].

1.2. Statement of problem

Utilization of renewable energy sources have been the most important and prospective field to acquire new energy sources to meet up the increasing demand in power all over the world especially in developing country like Ethiopia. The total harmonic distortion is the main concern and problem in a grid connected solar power system which degrades the power quality of the system. There are a lot of things which have to be considered such as high power density, high efficiency and reliability of the system along with the control objectives. The grid connected solar PV system is not like any other conventional distribution power generation system. It was very difficult to control the active and reactive power flow of the system effectively. Some different mechanisms are required to bring the system back to operate synchronously. Synchronously rotating reference frame technique plays a vital role to control the active and reactive power of the grid connected solar power system. This transformation technique works on the voltage and current of grid and it is very necessary to maintain and improve the efficiency, reliability, stability and power quality of the system by controlling active and reactive power of the system independently. Furthermore, the active power can be dissipated to the grid through inverter after reaching at the optimum point and similarly the reactive power can be reduced to the required level.

1.3. Objective of the thesis

This thesis work comprises of the following general and specific objectives.

1.3.1. General Objective

The general objective of the thesis is to model and control the grid connected solar power system using synchronously rotating reference frame technique in order to control the active and reactive power flow.

1.3.2. Specific objectives

The specific objectives of the thesis are:

- To study the mathematical model of the solar PV system.
- To study the maximum power point tracking to control the output of PV array.
- To control the flow of active and reactive power.
- To maintain synchronism for both voltage and current of inverter and grid.

1.4. Scope of the thesis

The scope of the thesis that the system is developed to control the flow of active and reactive power by applying rotating reference frame synchronously which includes the following points:

- Modelling and simulation of a PV array for grid connected system.
- Modelling and simulation of DC-DC boost converter with MPPT controller.
- Modelling and simulation of DC-AC inverter as well as its control.
- Modelling of active and reactive power control.
- Simulation of the overall system for grid connected PV system.
- The simulation model was done on MATLAB/SIMULINK.

1.5. Methodology

The proposed method is implemented based on the modeling and controlling of active power and reactive power injected into the grid. The total system consists of a solar/PV panel, boost converter with MPPT using incremental conductance method, three-phase voltage source inverter and the inverter control scheme applying the dq-reference frame which is used to transform the three phase quantities to the two phase quantities in rotating voltage and current synchronously to control active and reactive power flow from the PV inverter to the utility grid. The power control is implemented using synchronously rotating reference frame technique. The grid voltage and currents are transformed from three phase component (abc-frame) to two phase component (dq-frame) and (αβ-frame) using Park's and Clarke's transformation respectively. After the components are started rotating synchronously with the reference frame, the control variables become DC quantities. The active and reactive power flow depends on the direct and quadrature axis component of voltage and current. This facilitates individual control of active and reactive power flow.

The modeling and control is carried out using synchronously rotating reference frame technique. To achieve this system, MATLAB/SIMULINK is required to do all design on it.

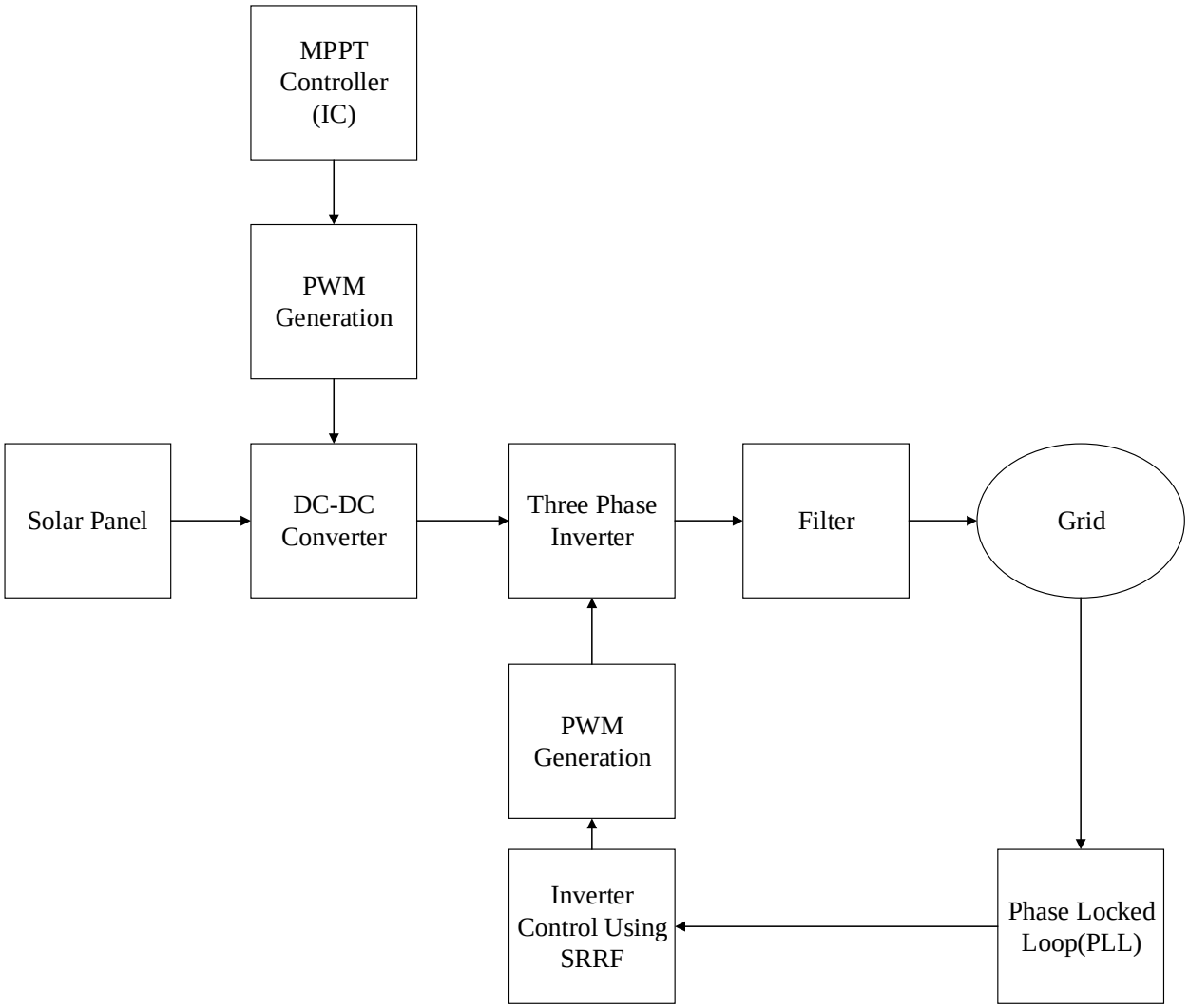

Figure 1.1 General Block diagram of Grid Connected PV system

1.6. Thesis Organization

The thesis is organized into six chapters including the introduction section. The remaining part of the thesis is organized in the following manner.

Chapter 2 describes the details of literature review of the grid connected solar PV systems.

Chapter 3 describes the details of mathematical modeling of the PV system, DC-DC boost converter, the space vector PWM control strategy and DC-AC inverter.

Chapter 4 describes the grid connected PV inverter systems which includes Clarke's and Park's transformations and their inverse transformation, the DC-link voltage controller, the current controller and the whole block diagram of the system.

Chapter 5 presents the simulation results and discussion of the proposed grid connected PV system and describes the results of the PV array and the overall system.

Chapter 6 describes the general conclusion and recommendation.

Chapter Two

Literature Review

The recent work mainly focuses on the grid interfacing behaviour, control performance and operation after connecting to renewable energy. The integration of renewable energy sources to the utility grid depends on the scale of power which is being generated. Different researchers have been worked on the grid connected PV system to improve the quality of power in different ways as well as to enhance the stability and efficiency of the system by employing various types of techniques and methods.

A. Angela Sheril and M. Ramesh Babu (Middle-East Journal of Scientific Research 25 (4): 864-870, 2017) have been demonstrated that the voltage, current and frequency of the grid connected photovoltaic system could be synchronized and controlled by using phase locked loops and stationary reference frame technique. But the active and reactive power flow from the output of inverter to the grid has not been controlled. Since the two powers are not being controlled independently, the stability and efficiency cannot be improved [6].

Manel Hammami, Rabeh Abbassi and Souad Chebbi (Conference Paper, January, 2014) proposed that the efficiency of the photovoltaic system is the serious issue in the world, so the rotating reference frame technique has been applied to control the active and reactive power depending on the currents in the d-q rotating reference system in order to improve the efficiency of the system [7]. However, the new proposed method which is going to apply depends on both voltage and current in the rotating system for controlling purpose.

Bhavesh M. Jesadia and Prof. Indrajit N.Trivedi have been applied instantaneous reactive power theory as a control strategy. According to this theory during the sunlight system send active power to grid and same time compensate the reactive power of load and compensate the harmonics. During no sunlight available system only compensate reactive power of load and harmonics. In this method, the synchronization control would not be applied to control the phase angle of the voltage of the grid [8]. So this leads the system to the faulty conditions. However, the aim of the proposed system is to control the required power of the system in parallel way using the technique depending on voltage and current.

2.1. Overview of Photovoltaic Cell

Photovoltaic cell is also known as solar cell is used to convert energy from the sun directly into electrical energy without any form of rotational parts. Photovoltaic cells represent the basic fundamental power conversion unit of solar PV system. These cells are made from semiconductors and like any other solid-state electronic devices e.g. diode, transistors and integrated circuit, they have also similar behavior. Photovoltaic cells are usually arranged into modules and array when applied practically [9].

2.1.1. Types of PV Cells

There are different types of photovoltaic cells available on the market and yet different other types of cells are under development [10].

2.1.1.1. Monocrystalline Solar Cell

They also known as "single crystalline" cells are readily known by their coloring. These cells are believed to be singular due to it is assumed constituted of very pure type of silicon. In the silicon world, efficiency of material depends on the purity of aligned molecules and its efficiency is around 20%. A solar cell is used to convert sunlight into electricity. They are constituted of what are called "silicon ingots," which is of a cylindrical pattern that aids in optimizing execution. In this way, panels are made up of monocrystalline cells with rounded edges instead of being square, like other types of solar cells. This is due to the fact fewer cells per unit of electrical output. Another advantage of these cells is that they also have highest longevity.

2.1.1.2. Polycrystalline Solar Cell

These cells do not require the cutting process as in the case of monocrystalline cells. Here, the silicon is of square shaped as silicon is disintegrated and poured into a square mold. In this way, these cells are very much economical as hardly any silicon is wasted during the manufacturing process. Generally, efficiency of this system is around 13-16% efficiency - main reason is due to lower purity of material.

2.1.1.3. Amorphous Solar Cell

This cell is made up of thin films. This thin films consist of amorphous silicon are generally employed for low power applications. A new method known as "stacking" is used for developing

multiple layers of amorphous silicon cells which leads to higher rates of efficiency (up to 8%) for these technologies; even though it is quite costly.

2.2. Types of Solar PV System

From application point of view, photovoltaic power systems are categorized into two types grid connected as well as off grid. They can be designed to produce DC and/or AC voltage, can function independent of grid or with grid [11].

2.2.1. Grid connected PV system

For grid-connected PV systems inverter, or power conditioning unit (PCU) is the primary component. The PV system produces very less DC power. Then this less DC power must be converted to AC power up to the level or the need of grid by means of inverter. So PV inverter plays very important role in grid connected PV system. In a grid connected system, all excess power is fed to grid. Also, during absence or inadequate sunshine, supply of power is maintained from the grid and thus battery is eliminated. As PV produce DC power is first converted to AC power by inverter, harmonics are filtered and then only AC power is fed into grid after adjusting the voltage level. Figure 2.1 describes about the block diagram of a grid connected PV system.

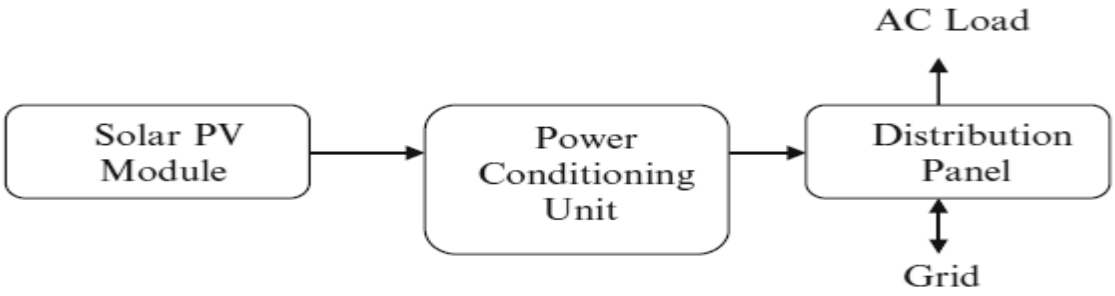

Figure 2.1 Block diagram of Grid connected solar PV system

2.2.2. Stand-Alone Photovoltaic Systems

Off-grid solar PV system can be used without power grid. Presently, such solar PV systems are usually set up at isolated sites where the power grid is far away, such as off-shore islands or rural areas. They can also be set up within the city when it is inconvenient or very expensive to tap electricity from the power grid. An off-grid solar PV system employs deep cycle rechargeable batteries such as nickel-cadmium, lead-acid or lithium-ion batteries used for accumulating electricity for use under various circumstances when there is no or little output from the solar PV system, essentially when it is dark. For low power applications, stand-alone PV systems are

generally used to supply certain DC and/or AC electrical loads. In order to operate the load during sunlight hours as well as night hours fed by PV power, electrical energy storing devices (batteries) are required, which makes the system costlier. Figure 2.2 depicts about the block diagram of standalone PV system where PV array is connected to DC and AC load through charge controller.

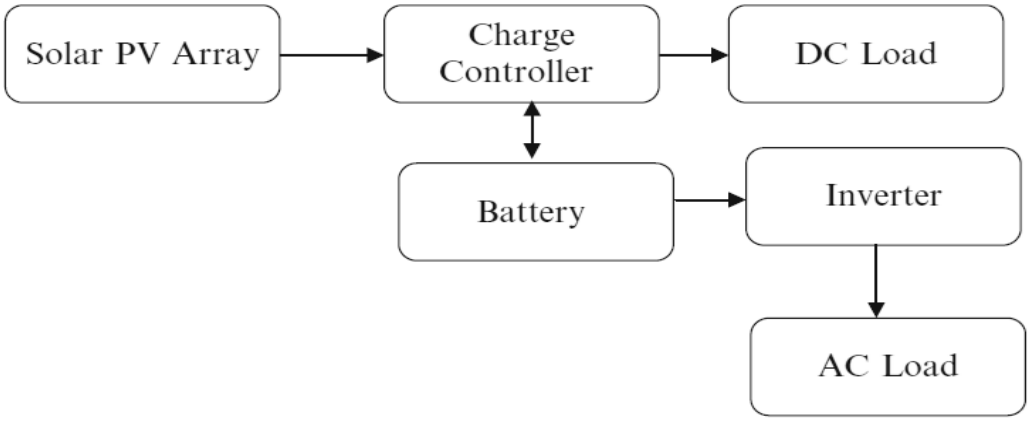

Figure 2.2 Block diagram of Standalone PV system with Battery storage

2.3. Maximum Power Point Tracking

The maximum power point tracking is the main part of the solar PV system. It is the most important part in solar PV system which is used to extract the maximum power from the PV array. The output power of the PV array is influenced by solar irradiance and temperature.

The most commonly used MPPT algorithms are briefly explained below.

2.3.1. Perturb and Observe Algorithm

This algorithm is based on perturbation of a control variable, which is either the output voltage of PV array, or duty cycle of the DC-DC converter switches. For the first case, a perturbation is applied to output voltage of PV array and a PI controller, consequently, adjusts the duty ratio of the converter. Tuning of PI controller in this case is done by using maximum power point value of PV array voltage [12]. In the case of direct duty cycle control, as the name suggests that a small perturbation is introduced in the duty ratio of DC-DC converter.

A major advantage of Perturb and Observe algorithm is that it is simple and easy to implement. Flowchart of direct duty ratio control P and O algorithm is shown in figure 2.3.

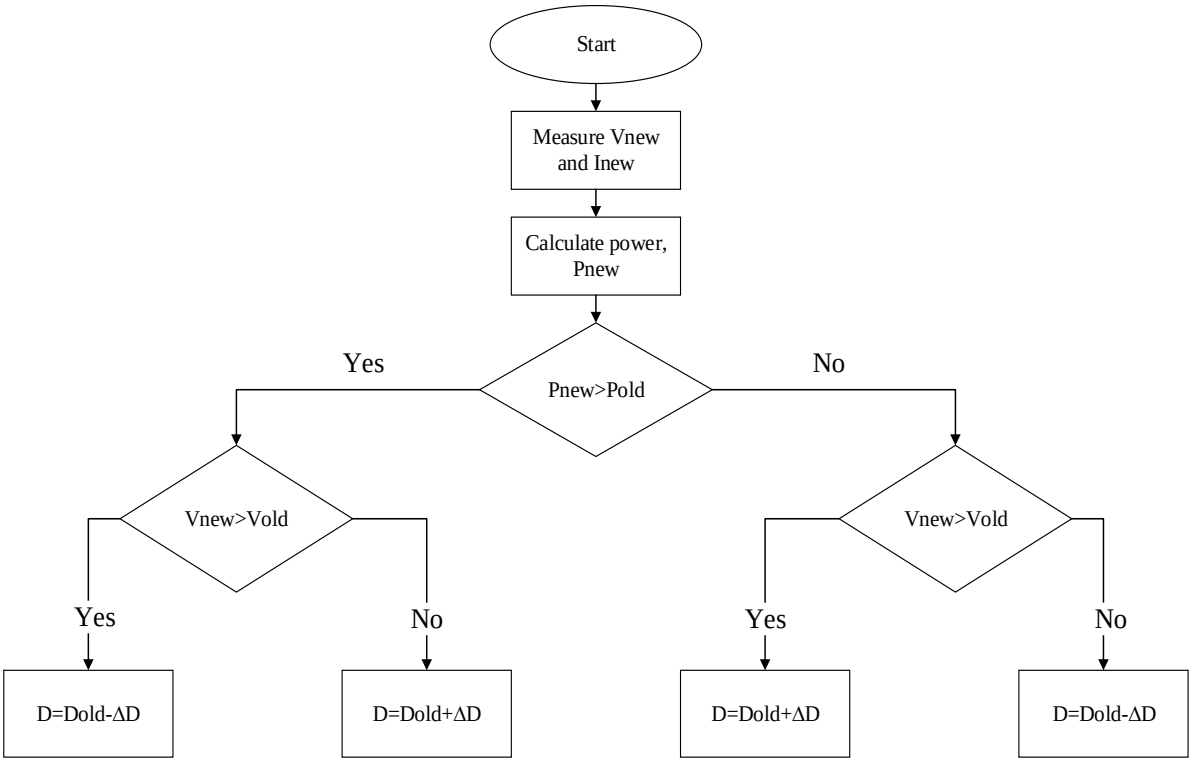

Figure 2.3 Flowchart of Perturb and Observe Algorithm [13]

2.3.2. Incremental Conductance Algorithm

In this algorithm, the power (product of voltage and current) of PV array is differentiated w.r.t the PV array voltage and set equal to zero, and based on the value of the differential, the actual operating point is found. In this algorithm, unlike perturb and observe, PV array power doesn't have to be computed. This algorithm provides very good transient performance i.e., when atmospheric conditions are changing. Flowchart of Incremental Conductance algorithm is shown in figure 2.4.

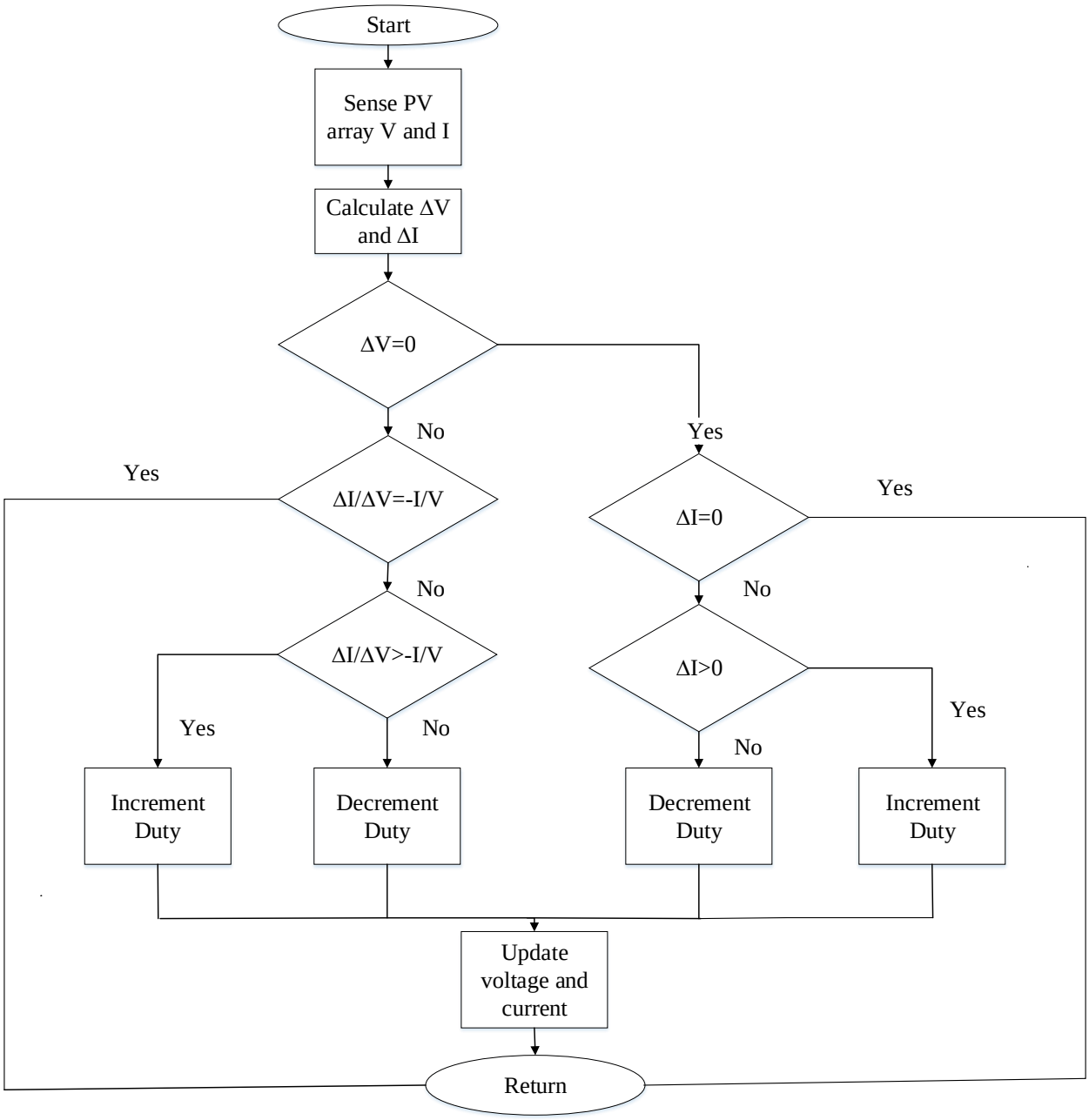

Figure 2.4 Flowchart of Incremental Conductance Algorithm [13]

The basic idea of incremental conductance method is that the slope of the power at the MPP with respect to the voltage equals zero. Also, the power is increasing with the voltage to the left of the MPP, and it is decreasing to the right of the MPP. Simply, the slope of P-V characteristics curve is zero at the MPP, positive on the left of the MPP and negative on the right of the MPP [14]. Figure 2.5 shows the incremental conductance method for MPPT.

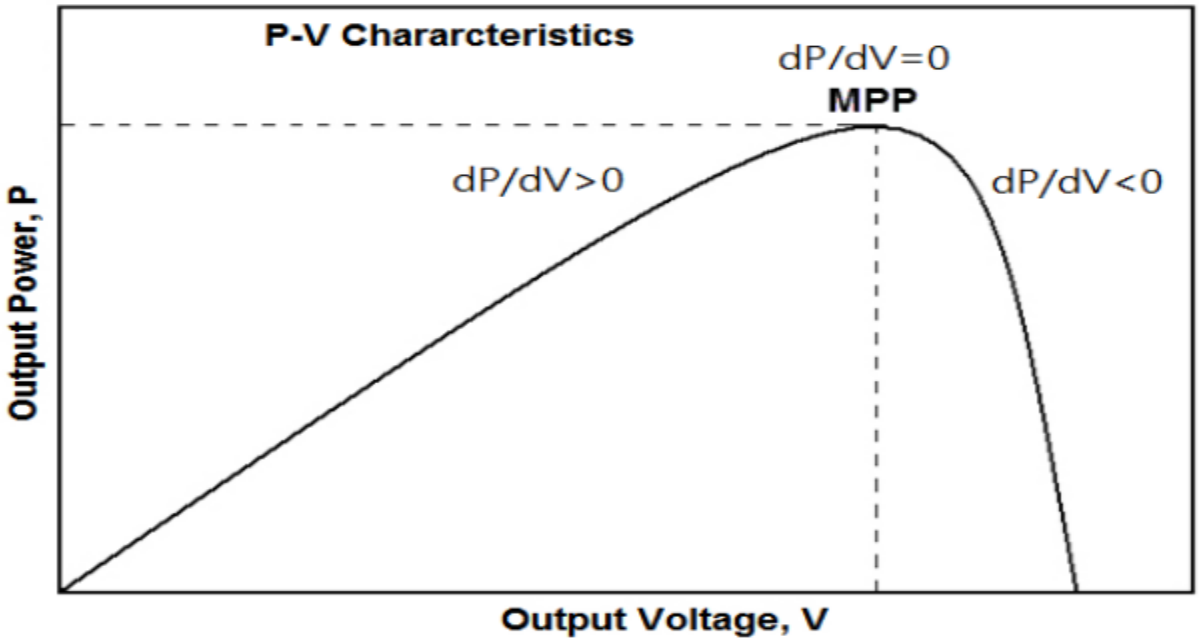

Figure 2.5 Incremental Conductance Method for MPPT

2.4. DC-DC Boost converter

The Boost converter is a power converter that generates output voltage greater than the input voltage. It consists of four main components: an inductor, a power electronic switch (e.g. an IGBT, MOSFET), a diode and a capacitor. The boost converter is controlled using Pulse Width Modulation (PWM) control strategy. PWM controls the boost converter by turning the switch ON or OFF at a high frequency (called the switching frequency) [15, 16].

2.5. DC-AC Inverter in PV System

Inverters used nowadays in a PV system are self-commutated. The switching devices used in them can be power BJTs, IGBTs or MOSFETs, depending on the switching frequency and power density of the system. The inverters can be broadly classified into two types which are current source inverters and voltage source inverters [17]. They are briefly explained below.

2.5.1. Current Source Inverter

In a current source inverter, the input side is a current source. The polarity of input current does not change and the direction of flow of power is determined by the input voltage. CSIs generate an alternating current wave at the output which has a fixed magnitude for a given input and adjustable time period. An inductor is connected at the input side of CSIs to maintain the current.

2.5.2. Voltage Source Inverter

The input side of a voltage source inverter is a voltage source; a large capacitor is used for this purpose. The polarity of input voltage does not change and therefore direction of power flow is determined by the DC current input. Contrary to CSIs, alternating voltage of constant amplitude but variable can be obtained by using VSIs. Another feature of VSIs is that, they can be operated in both voltage control mode and current control mode.

2.6. Active and Reactive Powers and DC-Link Voltage Controller

The controller tasks are achieved mainly by two cascaded loops [18]:

1. Fast internal current loop to control the grid current in order to get a high-quality power with low harmonics.
2. External voltage loop to control the DC-link voltage, which controls the power flow in the system.

2.6.1. Clarke's and Park's Transformation

2.6.1.1. Clarke's Transformation

The transformation of stationary circuit to a stationary reference frame was developed by E. Clarke. The stationary two-phase variables of Clarke's transformation are denoted as α and β [19]. As shown in figure below, α-axis and β-axis are orthogonal.

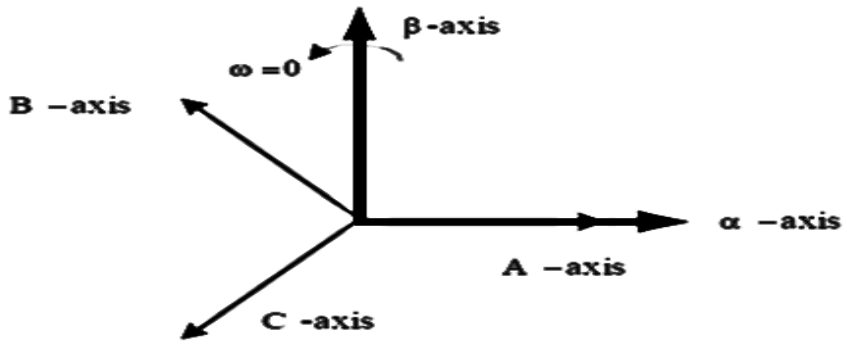

Figure 2.6 Clarke's Transformation

2.6.1.2. Park's Transformation

It is used to transform the three phase quantities to the two phase quantities in some system for the aim of controlling. The changes of variables are employed in the analysis of various static and constant parameters in power system components. All known real transformations for these

components are also contained in the transformation to the arbitrary reference frame. This transformation is a well-known three-phase to two-phase transformation in synchronous system analysis [19]. It is presented in the figure below.

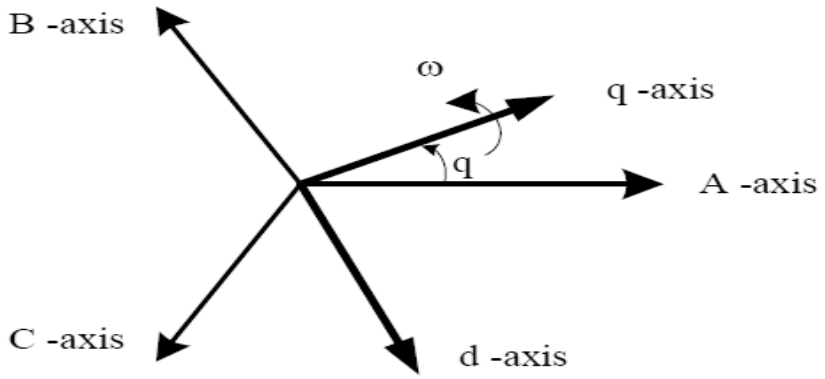

Figure 2.7 Park's Transformation

2.7. Grid Synchronization

To achieve power flow between the renewable resource generator and the utility network, the injected inverter current needs to be synchronized with the grid voltage. Different algorithms are used for grid synchronization. The main purpose of these algorithms is to obtain the phase information of grid voltage. Transformation from natural reference frame to stationary or synchronous reference frame may be required to make this possible **[**18]. Zero crossing method, Filtering of grid voltages and PLL are the methods that are used for grid synchronization. Among these three, PLL is the most widely used method. A brief explanation of PLL is presented below.

2.7.1. Phase Locked Loop (PLL)

PLL provides good rejection of harmonics and other disturbances. It is implemented in synchronous reference frame [20]. Figure 2.8 shows the basic structure of PLL. The phase lock is achieved by setting the reference d axis voltage U_d* to zero. A PI regulator is usually used to control U_d and the output of the controller is the grid frequency, which can be integrated to find the grid voltage phase angle.

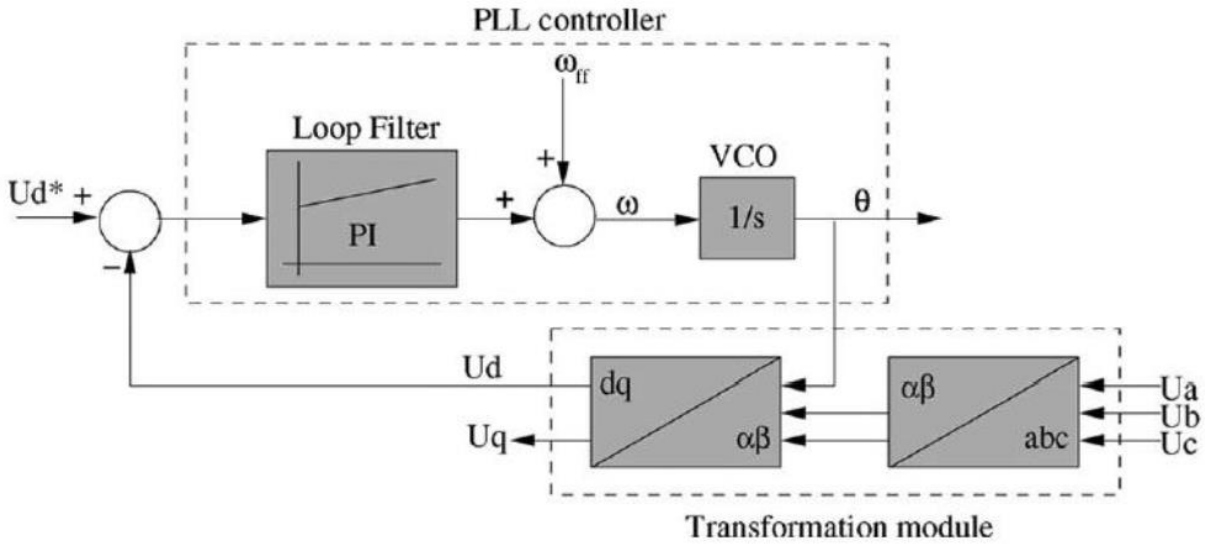

Figure 2.8 PLL loop [22]

- The Phase Detector: the phase detector outputs a signal that is proportional to the phase difference between the reference signal and the signal generated by the transformation block (abc→ dq).
- The Loop Filter: This block presents a low-pass filter, usually PI controller, to attenuate the high-frequency AC components from the phase detector output. The output of this block is the grid frequency.
- VCO Controller: This block integrates the grid frequency to obtain the phase shift of the grid voltage (Θ).

2.8. Power Decoupling

Power decoupling in a PV system is usually achieved by using a capacitor. In case of a single stage system, decoupling capacitor is placed between the inverter and PV panels. For a multistage system, it is placed between the output of DC-DC converter and inverter input. Decoupling capacitor is used to reduce the oscillatory nature of power obtained from PV modules [21].

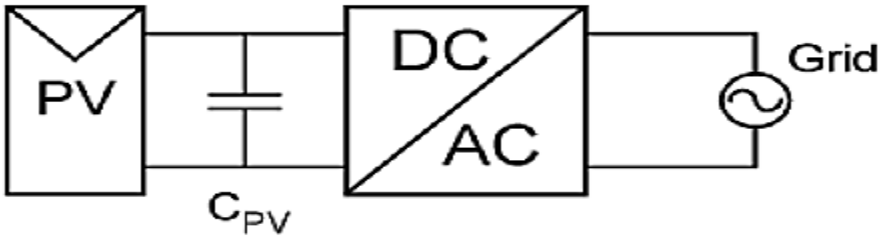

Figure 2.9 Capacitor location in single stage

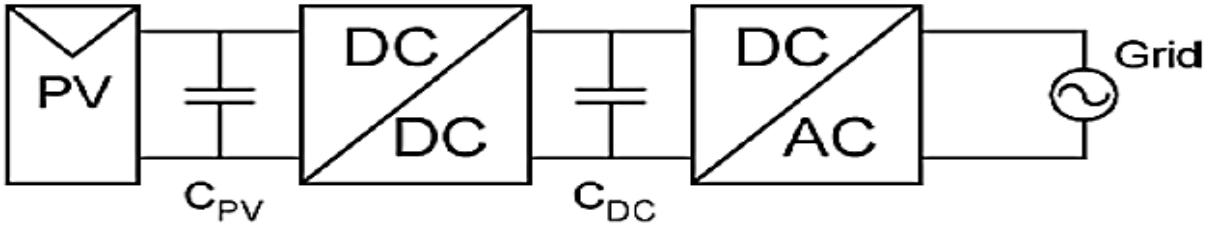

Figure 2.10 Capacitor location in multistage system

2.9. Modulation Techniques for Inverter

To convert the DC voltage into an AC voltage signal, the switches present in an inverter need to be switched on and off by providing pulses at their gates. There are a number of techniques that can be used to generate pulses. The most commonly used are the space vector pulse width modulation (SVPWM) and sinusoidal pulse width modulation (SPWM) [18]. In this thesis work, the space-vector pulse width modulation is going to be applied due to its simplicity for digital implementation and maximum utilization of DC bus voltage.

2.10. Filter as Grid Interface

Inverters, as being switching devices cannot be directly connected to the grid. This is because the inverter produces harmonics which degrades power quality. There are different standards in which put a limitation on the harmonics that can be injected into the grid [22-24]. A transformer may be used to connect the system to the grid [25]. The windings of the transformer serve as inductance which reduces the harmonics present in the current wave. Transformers are expensive and bulky which leads to the system being costly. Therefore, a transformer-less topology to connect inverter to the grid has come into existence, and that is by using a filter circuit as the interface. There are three types of passive filters that are generally used; they are an L, LC and LCL-filter. These filters are shown in figure 2.11.

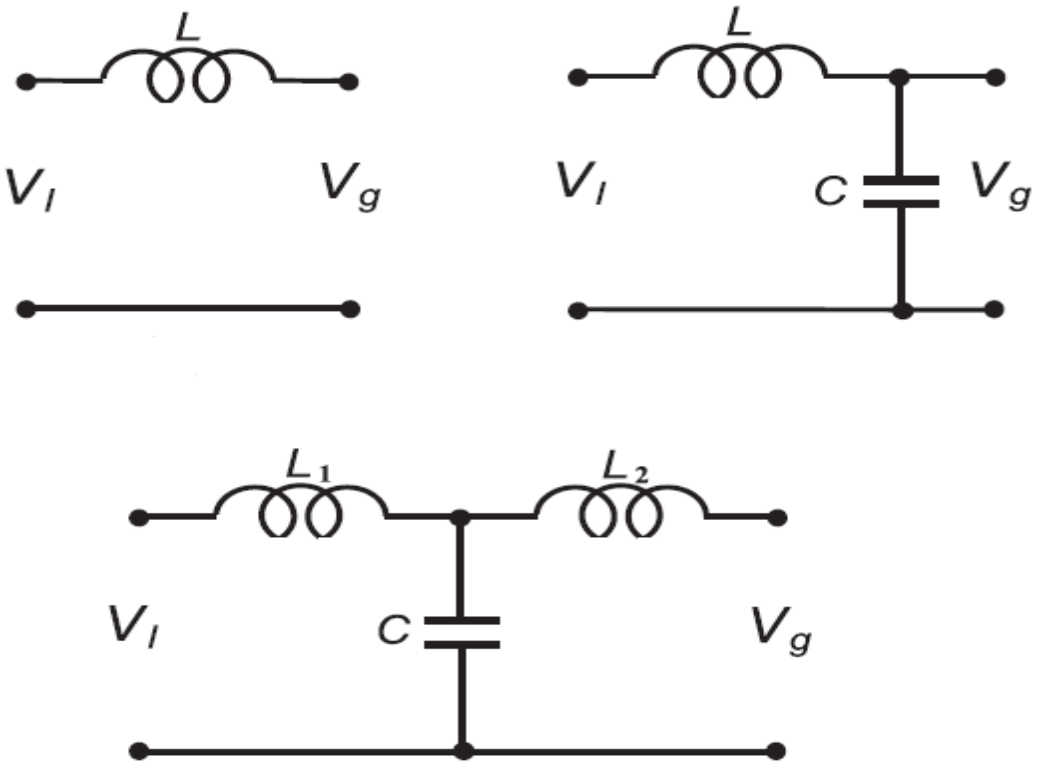

Figure 2.11 L, LC and LCL filters [26]

Chapter Three

System Modeling of Photovoltaic Inverter

3.1. Photovoltaic Cell

The Photovoltaic (PV) cell is a PN junction device made from semiconductor materials. It is commonly made up of doped silicon [26]. The energy conversion in a PV cell may be described in three steps. First, the absorption of solar (photons') energy generates electron-hole pairs. Then, the electrons and holes are separated by the structure of the device. Finally, electric charges are collected at the terminal of PV cell. The rate of generation of electric charge depends on the solar irradiance, the temperature of the cell and the semiconductor material type. The output power from a single PV cell is very low. A large number of PV cells are connected in series and parallel, making a PV module, to produce higher power levels [27]. Then, several modules are connected in series and parallel to make a PV array as shown in figure below.

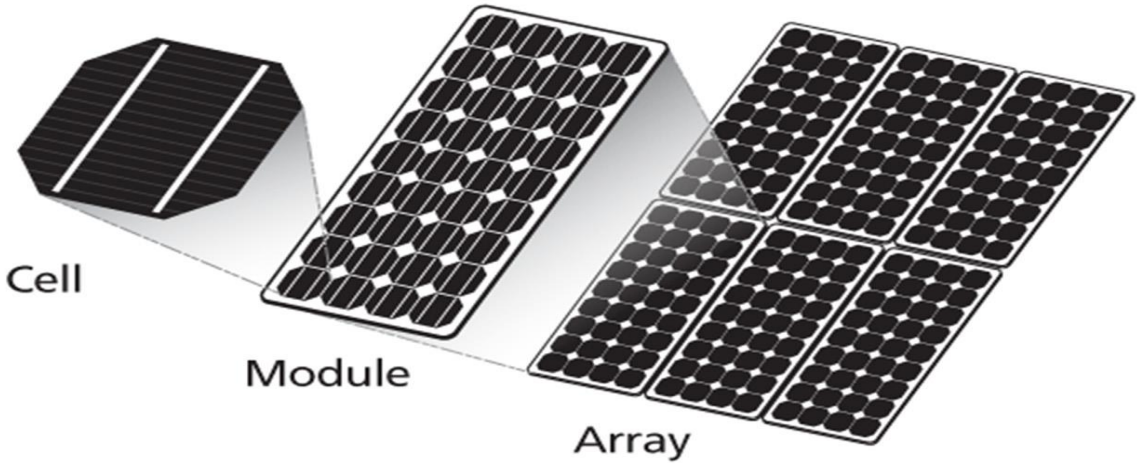

Figure 3.1 PV Cell, Module and Array [27]

3.2. Modelling of PV Modules

The goal of PV model is to find the equivalent circuit parameters (I_{ph}, I_o, I_{rs}, I_{sh} and I_{pv}) using the information provided in the PV module datasheet in table 3.1. The parameters that are normally provided by the datasheets of the PV module are the short-circuit current (I_{sc}), the open-circuit voltage (V_{oc}), and the operating voltage and current at the given standard values. All these values are given at STC, which are a temperature of 25^{o}C and an irradiance of 1000 Watt/m^2.

A solar cell is basically a p-n junction which is fabricated in a thin wafer of semiconductor. The electromagnetic radiation of solar energy can be directly converted to electricity through the photo voltaic effect. When it is being exposed to the sunlight, the photons with energy can be greater than the band-gap energy of the semiconductor creates some electron-hole pairs proportional to the incident irradiation [28]. The equivalent circuit of the photovoltaic cell is as shown below in figure 3.2.

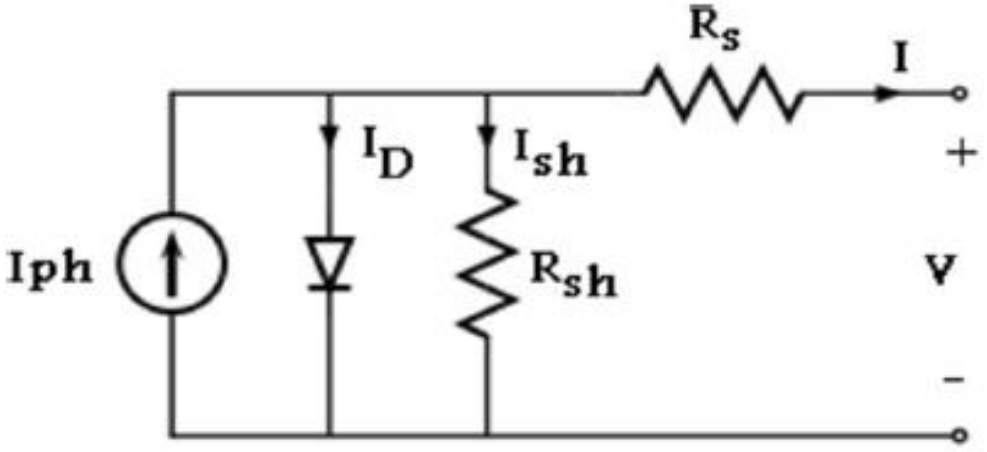

Figure 3.2 The Equivalent Circuit of Photovoltaic cell [29]

From the above circuit diagram, the current source (I_{ph}) represents the cell photo current. R_{sh} and R_s represent the shunt and series resistance of the cell respectively. Most of the time, the value of shunt resistance is too large and that of series is very small. Hence they may be neglected for analysis purpose. PV cells are grouped in larger units called PV modules which are further interconnected in parallel-series configuration to form PV arrays [29].

According to the equivalent circuit, the photo current depends on the solar radiation and temperature of the environment condition is calculated as follows:

$$I_{Ph} = \frac{G}{1000}\left[I_{SC} + K_i(T - T_{ref})\right] \quad (3.1)$$

Where G is solar radiation, I_{sc} is short circuit current of the PV cell, T_{ref} is the nominal temperature and K_i is the temperature coefficient of short circuit current of the cell at 25^{o}C and 1000w/m^2.

From equivalent-circuit, the diode current of the cell can be expressed as:

$$I_D = I_O\left[e^{\frac{V+IR}{V_T}} - 1\right] \quad (3.2)$$

The thermal voltage is given by:

$$V_T = \frac{KT}{q} \tag{3.3}$$

Where V is the external voltage and I is the external current of the photovoltaic cell.

V_T is thermal voltage and I_o is the dark saturation current of the diode.

The dark saturation current of the diode is mathematically expressed as:

$$I_O = I_{rs}\left(\frac{T}{T_{ref}}\right)^3\left[e^{\left(\frac{qE_{go}\left(\frac{1}{T_{ref}}-\frac{1}{T}\right)}{AK}\right)}\right] \tag{3.4}$$

Where, A is the ideality factor of the diode.

K is the Boltzmann constant.

q is electron charge.

E_{go} is the band-gap energy of the semiconductor.

The reverse saturation current of the photovoltaic cell is obtained as,

$$I_{rs} = \frac{I_{SC}}{\left[e^{\left(\frac{qV_{OC}}{ANsKT}\right)}-1\right]} \tag{3.5}$$

Where V_{oc} is open-circuit voltage.

N_s is the number of PV modules connected in series.

T is the temperature effect on the solar PV module.

According to Ohm's law, the current through shunt resistance is equal to:

$$I_{Sh} = \frac{V+IR_S}{R_{Sh}} \tag{3.6}$$

By applying all the above equations, the external current can be found as:

$$I_{PV} = I_{Ph} - I_O\left[e^{\left(\frac{qV_{PV}}{NsAKT}\right)}-1\right] - I_{Sh} \tag{3.7}$$

Table 3.1. Design parameters for PV array [30]

Parameter name	Specification values
Rated power	305.226W
Open-circuit voltage(V_{oc})	64.2V
Short-circuit current(I_{sc})	5.96A
Temperature coefficient of I_{sc} (K_i) at 25°C and 1000W/m^2	0.061745
Number of PV cells connected in series(N_s)	96
Electron charge(q)	1.6*10^-19C
Ideality factor(A)	0.94504
Boltzmann's constant(K)	1.3805*10^-23J/k
Band-gap energy of semiconductor(Ego)	1.1eV
Shunt resistance(R_{sh})	269.593Ω
Series resistance(R_s)	0.37152Ω
Nominal temperature(T_{ref})	298k
Operating temperature(T)	25°C
Solar irradiation(G)	1000W/m^2

The Simulink modeling is done using the above equations in the following manner.

The conversion of temperature from degree Celsius to kelvin is shown in figure 3.3.

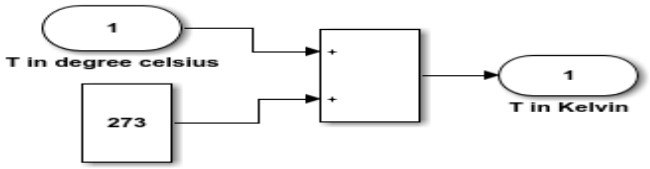

Figure 3.3 Block diagram of temperature conversion

Figure 3.4 shows the simulink block diagram which is used to find the photo current (I_{ph}). The converted values of temperature and irradiance level together with the value of current temperature coefficient from PV module datasheet are used to calculate the photo current (I_{ph}) using eq. (3.1).

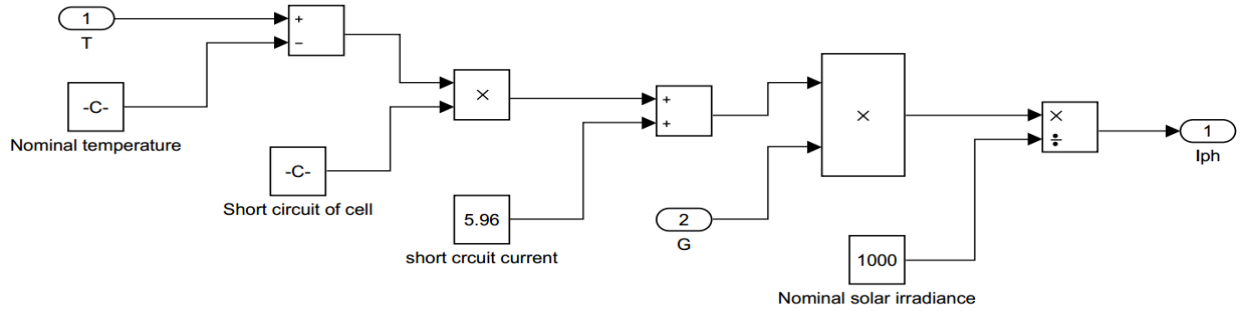

Figure 3.4 Block diagram of photo current

The diode saturation current (I_o) which is calculated using the eq. (3.4) is presented by the simulink block diagram shown in figure 3.5.

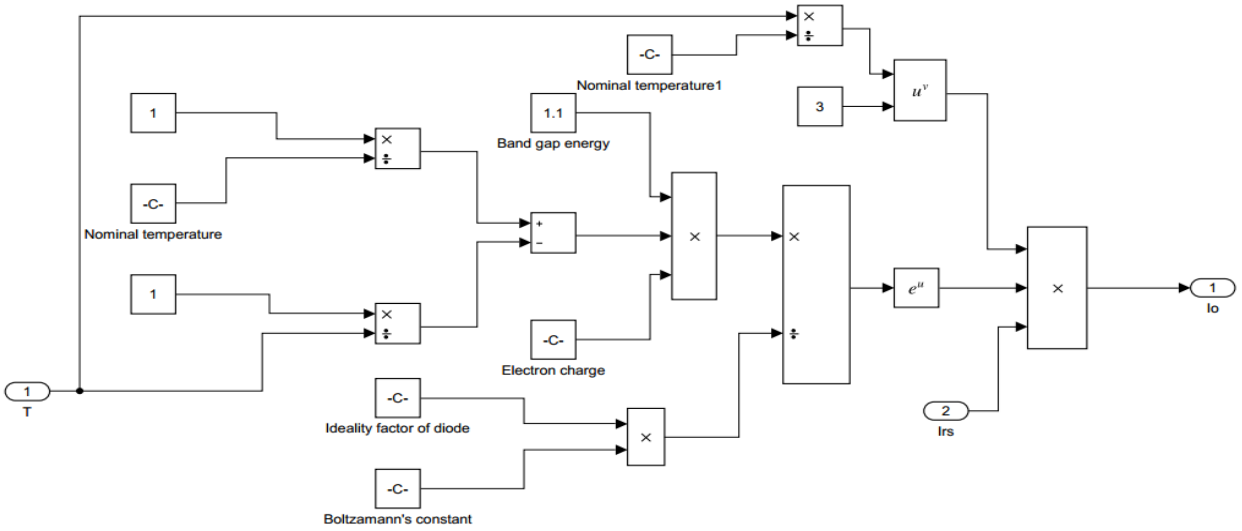

Figure 3.5 Block diagram of diode saturation current

The block diagram which is used to determine the reverse saturation current (I_{rs}) at STC using eq. (3.5) is shown in figure 3.6.

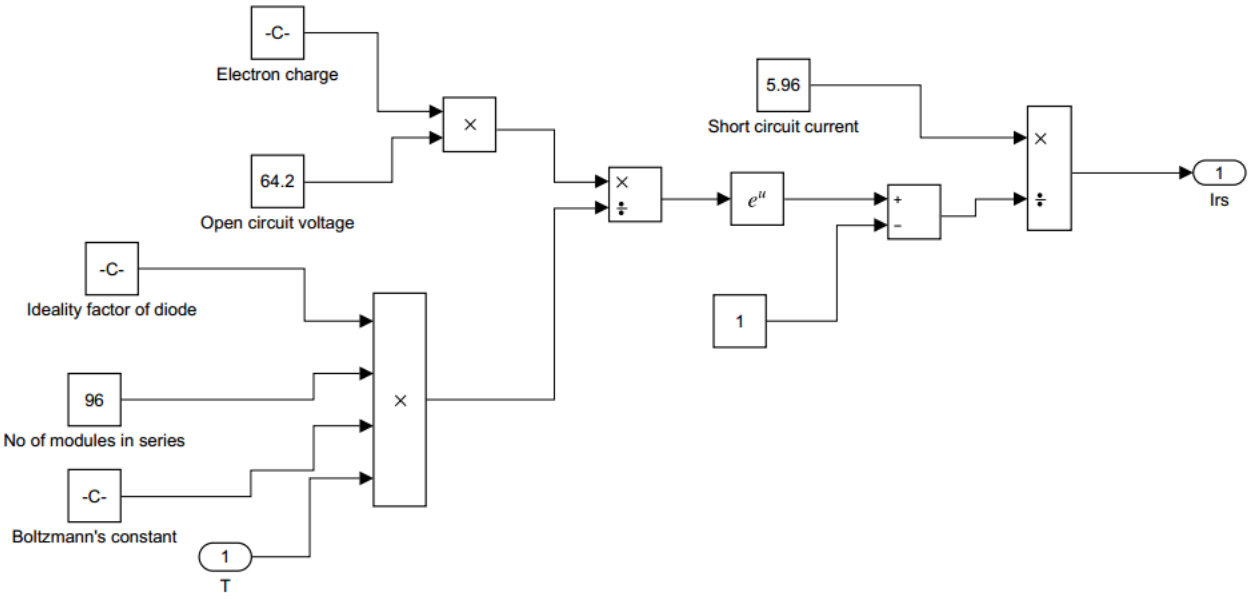

Figure 3.6 Block diagram of reverse saturation current

The Simulink block diagram of shunt current(I_{sh}) shown in figure 3.7 can be used to obtain the shunt current using eq. (3.6).

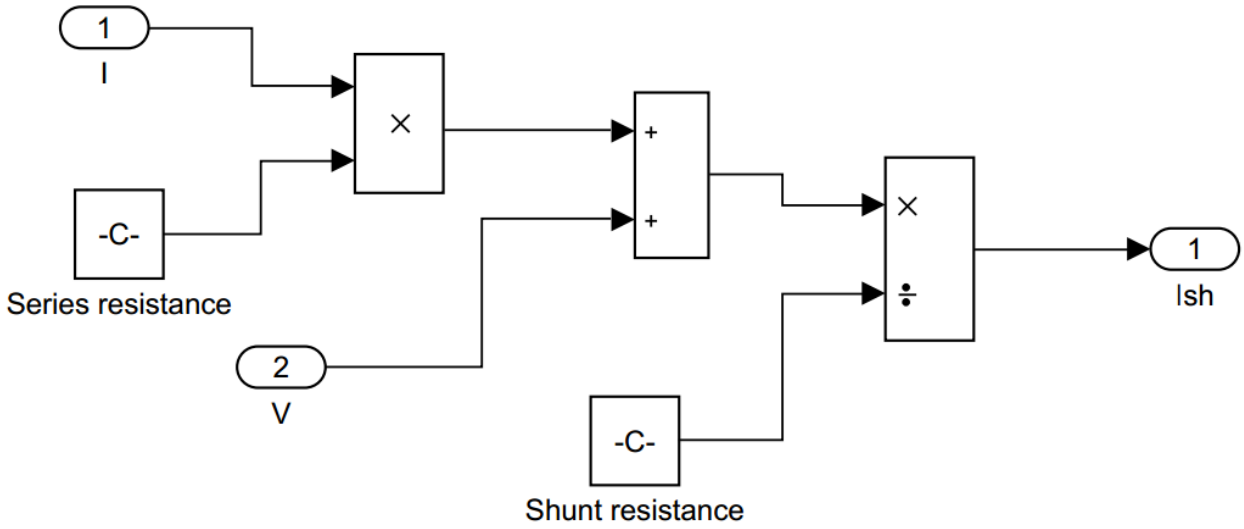

Figure 3.7 Block diagram of shunt current

After the values of the photo current (I_{ph}), the diode saturation current (I_o), the reverse saturation current (I_{rs}) and the shunt current (I_{sh}) are being calculated, all these values are substituted in eq. (3.7) to calculate the output current of the solar PV system. The Simulink block diagram shown in figure 3.8 represents eq. (3.7).

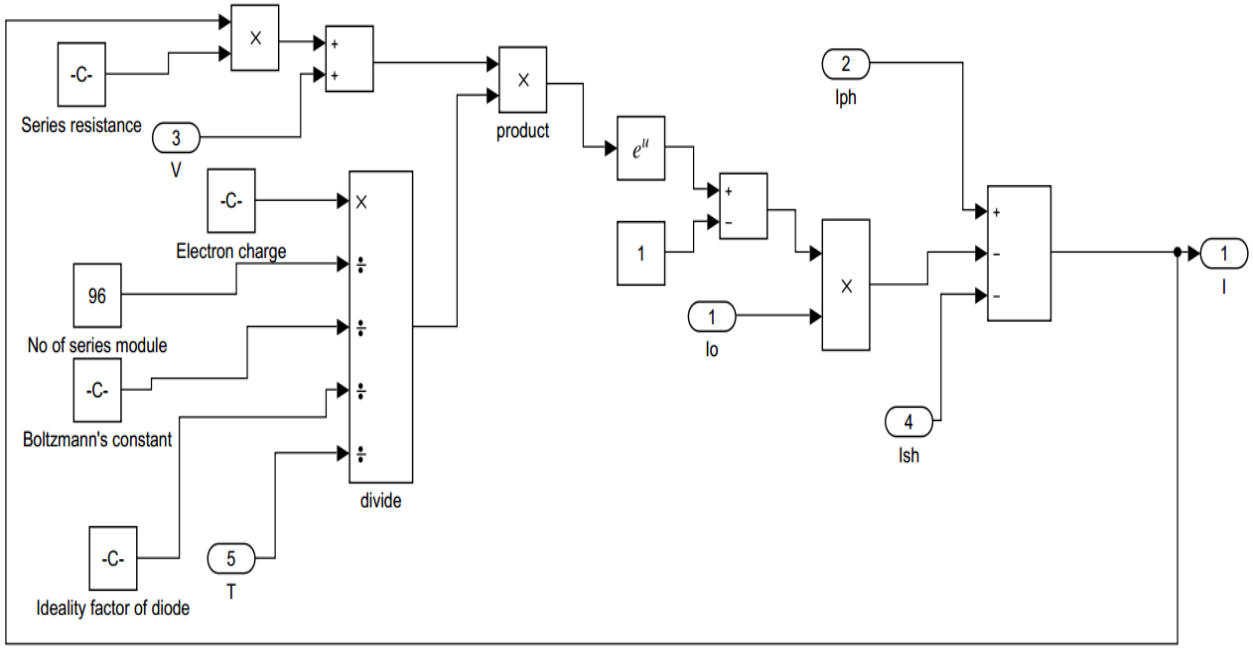

Figure 3.8 Block diagram of output current

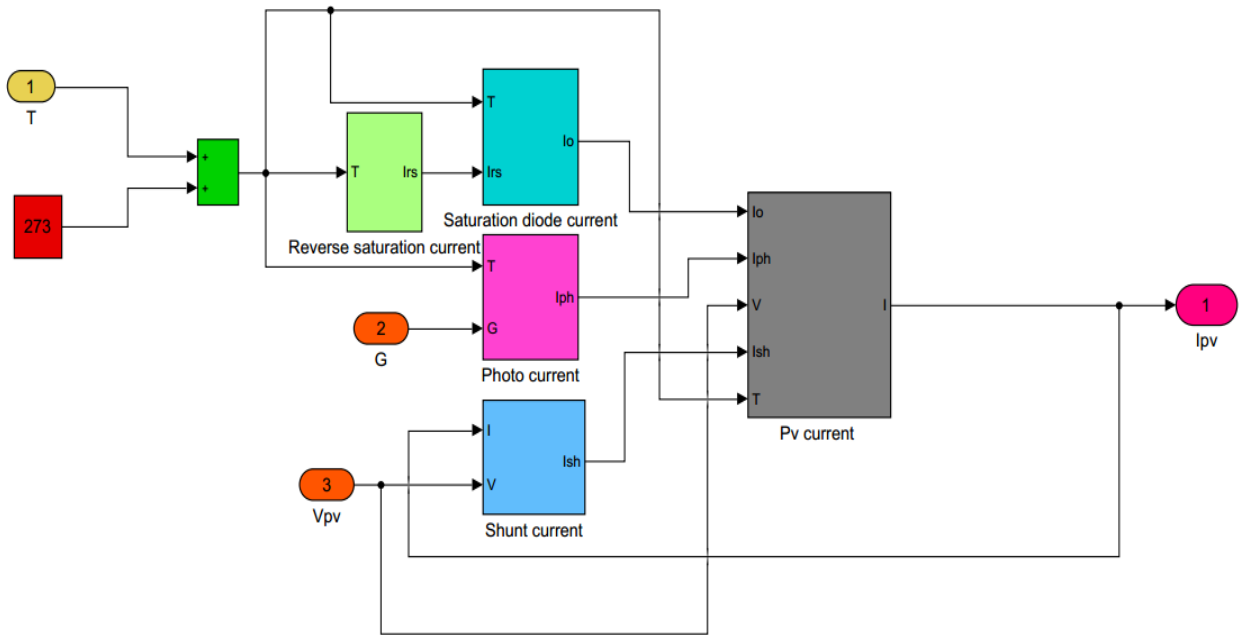

Figure 3.9 Block diagram of Solar PV System for a single PV module

The following PV array model is formed by integrating of five a single PV module which is connected in series to generate a power about 1.5KW. A single PV module produces only a power of 305W.

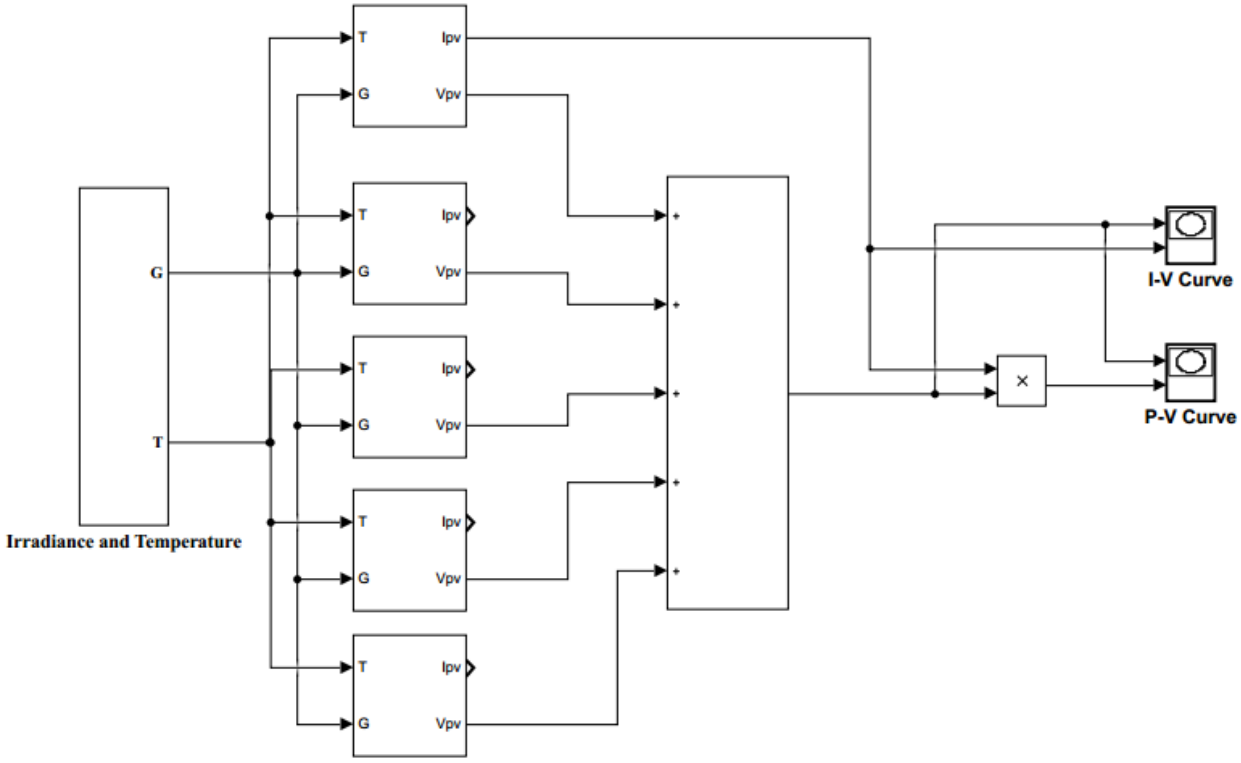

Figure 3.10 Block diagram of Solar PV System for a PV array

3.3. Modeling of Boost converter

DC/DC power converters are employed in PV systems to change the output voltage. Normally, a DC/DC converter is sequentially inserted between the load and the PV panel to gain the power available from the solar panel. It is useful for a PV system with unstable and fluctuating output. If the PV system uses both AC and DC converters, a DC-link capacitor can enhance the DC output voltage stability, and therefore, reduce the effect of fluctuation on the AC output [31]. DC converters may be boost converters (step-up), buck converters (step-down), or a combination of both, like CUK converters and buck-boost converters. Converter type may be selected based on the desired capacity or size of the output voltage to provide the appropriate input voltage for the inverter with the dc voltage stabilization and regulation capability [32]. This is important for hybrid energy systems, grid connected systems and standalone systems. DC/DC converter in such systems works with a maximum power operating algorithm so that the PV system generates more power. Figure 3.11 shows the basic circuit diagram of boost converter used in this work.

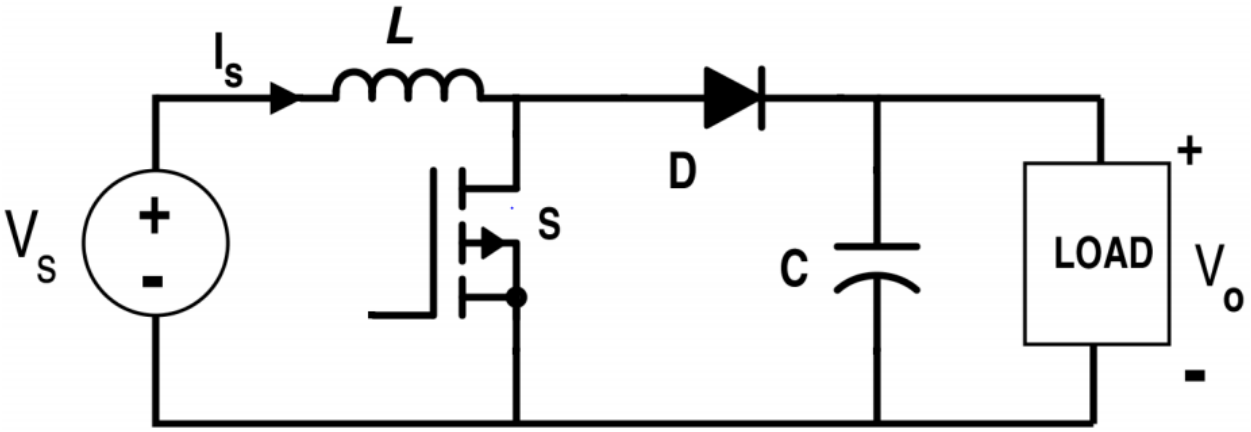

Figure 3.11 Circuit diagram of Boost converter

3.3.1. Design of DC-DC converter

Two stage topology is chosen for grid connected solar PV system. In this model, DC-DC converter is used to boost the output voltage of PV array to the required voltage level which is fed into the inverter as an input from the converter side. The switching device is an important part of DC/DC conversion. The switching device is selected based on the specific design of the system, for instance, switching speed and power capacity. Generally, MOSFET is chosen for supplying lower power capacity with fast switching speed whereas IGBT is used for higher power capacity with medium switching speed [33].

The input voltage available from the PV array to the boost converter is 273.5V and the desired output voltage is 700V. The selected switching frequency is 5 kHz for the switching device IGBT.

The duty cycle of the boost converter is calculated using the formula,

$$D = 1 - \frac{V_{PV}}{V_{DC-link}} \tag{3.8}$$

The boost inductor can be calculated using the formula,

$$L > \frac{D(1-D)^2 R}{2f_s} \tag{3.9}$$

Where, V_{pv} is the input voltage to the converter, Vpv=273.5V

V_o is the desired output voltage, Vo=700V

f_s is the switching frequency in the boost converter which is chosen to be 5KHz

The Photovoltaic capacitor can be calculated using the formula [34],

$$C_{PV} = \frac{V_{PV} D}{4\Delta V_{PV} {f_s}^2 L} \tag{3.10}$$

The DC-link capacitor can be obtained using the following formula [21],

$$C_{DC-Link} = \frac{P_{PV}}{4\pi f_s V_o \Delta V_o} \quad (3.11)$$

Where, P_{PV} *is* the nominal power of PV module

f_s *is* the switching frequency ,V_o *is* the voltage across the capacitor

ΔV_o *is* the amplitude of the ripple voltage which is chosen to be 3%

Table 3.2. Design parameters for boost converter

Parameter name	Value
output voltage of PV array at 1000W/m^2 and 25^{o}C	273.5V
output current of PV array at 1000W/m^2 and 25^{o}C	5.58A
Desired output voltage(V_o)	700V
output power of PV array at 1000W/m^2 and 25^{o}C	1.5KW
Switching frequency(f_{sw})	5000Hz

The calculated values of each component used for this design are provided below.

Table 3.3. Boost converter calculated parameters

Parameter name	Value
Duty cycle(D)	60.93%
PV capacitor(C_{pv})	75uF
Inductance(L)	3.2mH
DC-link capacitor($C_{DC\text{-}Link}$)	220uF
Resistance(R)	321ohm

3.3.2. Incremental Conductance MPPT

The main function of the MPPT in a PV energy conversion system is to setting continuously the system so that it extracts maximum power from the solar array in any case of weather or load conditions. Since the solar array has a non-ideal voltage-current characteristics and the conditions such as irradiance, ambient temperature, and wind that affect the output of the solar array are unpredictable, the tracker should deal with a nonlinear and time-varying system.

The conventional MPPT algorithms are using $\frac{dP}{dV} = 0$ to obtain the maximum power point. Several algorithms can be used in order to implement the MPPT as follows: perturb & observe, incremental conductance, parasitic capacitance and constant voltage, but only the first two are the most frequently used.

The incremental conductance algorithm has been chosen as a MPPT control strategy in this thesis work. This algorithm has advantages compared to perturb and observe as it can determine when the MPPT has reached the MPP, where perturb and observe oscillates around the MPP. The incremental conductance can track rapidly the increase and decrease of irradiance conditions with higher accuracy than perturb and observe. One disadvantage of this algorithm is the increased complexity when compared to perturb & observe [35].

Using the P-V curve described in figure 2.5 under chapter 2, the following equation can be analyzed:

$$\begin{aligned} \frac{dP}{dV} &= 0 \text{ at MPP,} \\ \frac{dP}{dV} &> 0 \text{ at the left side of MPP,} \\ \frac{dP}{dV} &< 0 \text{ at the right side of MPP.} \end{aligned} \tag{3.12}$$

In addition, the following equations can be obtained using eq. (3.12) by applying chain rule for the derivative of product yields,

$$\frac{dP}{dV} = \frac{d(IV)}{dV} = I + V\frac{dI}{dV} = I + V\frac{\Delta I}{\Delta V} \tag{3.13}$$

The DC-DC converter is controlled by incremental conductance technique in order to achieve the maximum power point (MPP). The incremental conductance method is based on the observation, the slope of the PV array curve is zero at MPP. In addition to this, the curve is increasing from left of MPP and decreasing from the right of MPP.

$$\frac{\Delta I}{\Delta V} = -\frac{I}{V} \text{ at MPP,}$$
$$\frac{\Delta I}{\Delta V} > -\frac{I}{V} \text{ at the left side of MPP,} \quad (3.14)$$
$$\frac{\Delta I}{\Delta V} < -\frac{I}{V} \text{ at the right side of MPP.}$$

Here is the block diagram of the incremental conductance method used to extract the maximum power from the PV array.

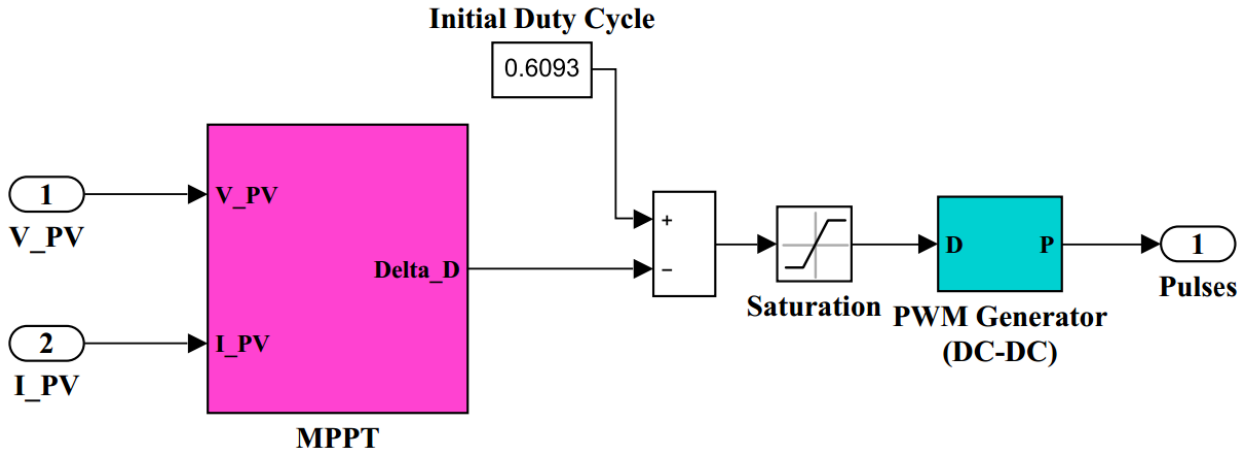

Figure 3.12 Block Diagram of Incremental Conductance

3.4. DC-AC Inverter

The PV array outputs are DC source energy, but the output of the grid side energy is AC source to transfer the generated energy to the grid, it should be converted into AC energy with controllable magnitude, phase and frequency. To achieve this, the three phase voltage source inverter is being used. The voltage source inverter (VSI) switches are controlled using space-vector pulse width modulation (SVPWM) [36]. The SVPWM technique is widely used to control the voltage source inverter, compared to sinusoidal pulse width modulation (SPWM), the SVPWM is more suitable for digital implementation and it has better DC-link voltage utilization. Moreover, it is capable of reducing the total harmonic distortion (THD) [37].Three phase two level VSI is going to be used in this work.

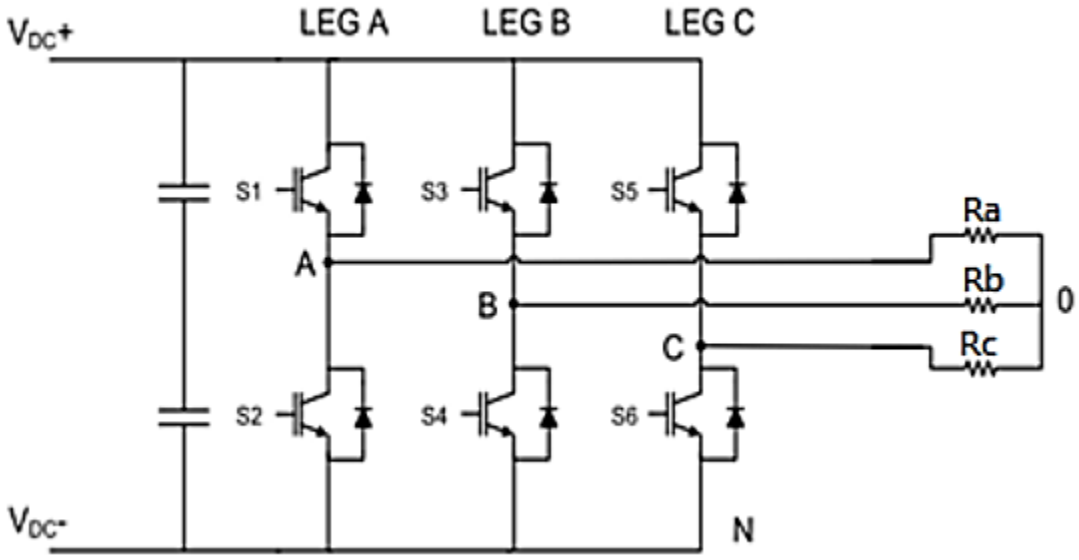

Figure 3.13 Three phase two-level inverter

The relationship between the DC input and the AC output line to line voltage is given by:

$$V_{LL}(rms) = 1.15m\frac{V_{dc}}{2}\frac{\sqrt{3}}{\sqrt{2}} \quad (3.15)$$

Where, m is the modulation index, V_{DC} is the DC-link voltage and V_{LL}(rms) is the line to line voltage which is chosen for this design.

3.4.1. Design of LCL-Filter

The LCL-filter is used to attenuate the high-frequency harmonics of the output current. The circuit diagram of LCL-filter is shown in figure 3.14.

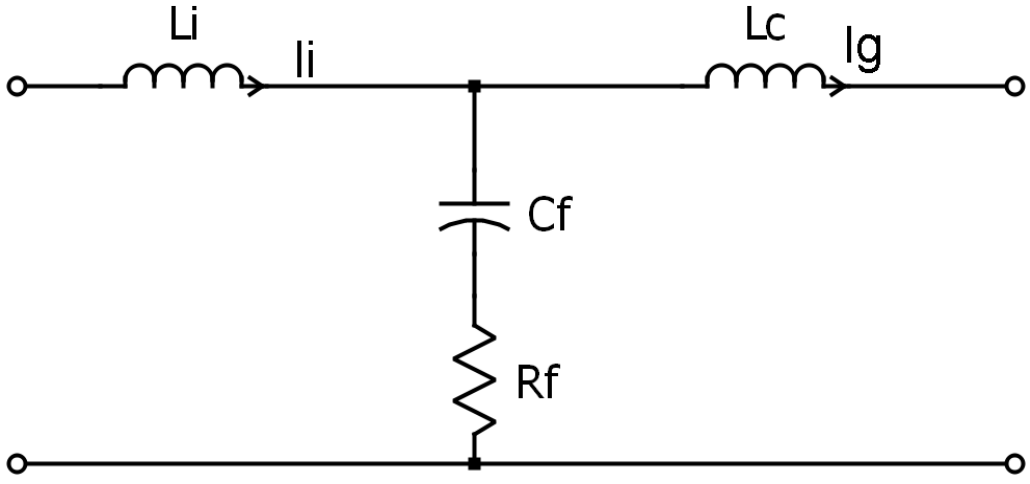

Figure 3.14 Circuit diagram of LCL-filter [38]

The design procedure for the LCL-filter can be described by the following steps [38-41]:

Step 1: the filter capacitance is selected based on the limit of the reactive power absorbed by the capacitor. Generally, it should be less than 5% of the rated power. The value of capacitance is given by [39]:

$$C_f = XC_b \tag{3.16}$$

Where, C_b is the base capacitance and x is the percentage of reactive power absorbed at rated condition.

The base capacitance of the system can be calculated using the following formula:

$$Z_b = \frac{V^2_{LLrms}}{P_{rated}} \tag{3.17}$$

$$C_b = \frac{1}{2\pi f_g Z_b} \tag{3.18}$$

Where, V_{LLrms} is the rms value of line to line voltage, P_{rated} is the rated power of the system, Z_b is the base impedance and f_g is the grid frequency.

Step 2: the inverter side inductor is used to reduce the ripple of the inverter current and it is calculated using the relationship between the ripple current and inverter inductor [39]:

$$\Delta I = \frac{V_{DC}}{8L_i f_s} \tag{3.19}$$

Where, ΔI is the ripple current, usually limited from 10% to 20% of rated current, f_s is switching frequency.

The ripple current of the inverter (ΔI) can be selected as 20% of base current. The base current (I_b) of the system is given by:

$$I_b = \frac{P_{rated}}{\sqrt{3}V_{LLrms}} \tag{3.20}$$

The value of the inverter inductor can be found as:

$$L_i = \frac{V_{DC}}{8f_s(20\%)I_b} \tag{3.21}$$

Step 3: the grid side inductor can be found based on the required ripple attenuation factor (RAF) at switching frequency. RAF is the ratio of the grid current to the inverter output current as follows:

$$RAF = \left|\frac{I_g(s)}{I_i(s)}\right| = \frac{\frac{1}{(L_g C_f)}}{s^2 + \frac{1}{(L_g C_f)}} \tag{3.22}$$

RAF at switching frequency is given by eq. (3.22) which can be rewritten as eq. (3.23) to calculate the grid inductor.

$$RAF_s = \left|\frac{I_g(s)}{I_i(s)}\right| = \frac{1}{1-\omega^2{}_s L_g C_f} \tag{3.23}$$

$$L_g = \left|\frac{I_g(s)}{I_i(s)}\right| = \frac{RAF_s+1}{RAF_s\omega^2{}_s C_f} \tag{3.24}$$

Step 4: the resonance frequency should be far away from the grid frequency and switching frequency. A suitable range of f_{res} is given by the following equations [38]:

$$f_{res} = \frac{1}{2\pi}\sqrt{\frac{L_g+L_i}{L_i L_g C_f}} \tag{3.25}$$

$$10f_g < f_{res} < \frac{f_s}{2} \tag{3.26}$$

Step 5: to avoid the resonance phenomenon, a damping resistor (R_f) is usually connected in series with filter capacitor. The value of the damping resistor can be calculated using the following formula [42]:

$$R_f = \frac{1}{3(2\pi f_{res} C_f)} \tag{3.27}$$

Figure 3.15 depicts the effect of the damping resistor on the transfer function of the LCL-filter which illustrates the bode plot of the filter transfer function without using damping resistor and the performance of damping resistor how it prevents the resonance frequency in the filter.

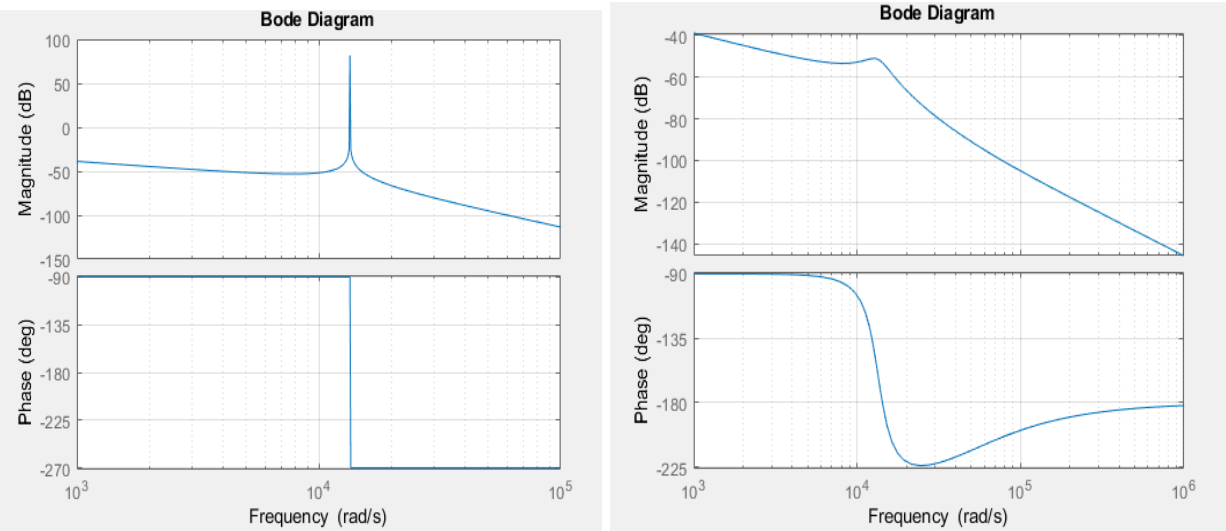

(a) (b)

Figure 3.15 Bode Plot of LCL filter: (a) without Damping Resistor (b) with Damping Resistor

After calculating the required parameter values of the inverter filter design, it is provided in the following table.

Table 3.4. Inverter and grid parameters

Parameter name	Value
Inverter inductor(L_i)	39.7mH
Grid inductor(L_g)	8mH
Filter capacitor(C_f)	0.76uF
Damping resistor(R_f)	31ohm's

The MATLAB code used to obtain the inverter and grid parameters are available in appendix B.

3.5. Space Vector PWM Strategy Control

Space-vector modulation (SVM) is one of the preferred real-time modulation techniques and is widely used for voltage source inverters control. The SVPWM is accomplished by rotating the reference vector around the state diagram which is composed of six basic non-zero vectors forming a hexagon shown in figure 3.16.

3.5.1. Principle of Space Vector PWM

For the simplicity of analysis on PWM techniques, the values on three phase (a-b-c) coordinate system are usually transferred to that on $\alpha\ \beta -$ plane. In the SVPWM technique, the reference voltage vector is V_{ref} that rotates in the space with an angular frequency of ω is selected as the control instruction. The principle of SVPWM requires the determination of a sector, calculation of vector segments and calculation of switching time durations [43].

The procedure for implementing a two level space vector PWM can be summarized as follows.

1. Calculate the angle (α) and reference voltage vector (V_{ref}) based on the input voltage components.
2. Find the sector in which V_{ref} lies, and the adjacent space vectors based on the sector angle α.
3. Find the time intervals T_1, T_2 and T_0 based on switching time and the angle.

Angle (α) and Reference Voltage Vector (V_{ref})

In the SVPWM, the three phase output voltage vector is represented by a reference vector that rotates at an angular speed of $\omega=2\pi f$. The SVPWM uses the combinations of switching states to approximate the reference vector. A reference voltage vector (V_{ref}) that rotates with angular speed in the α-β plane represents three sinusoidal waveforms with angular frequency ω in the coordinate system. The space vector with magnitude (V_{ref}) rotates in a circular direction at an

angular velocity of where the direction of rotation depends on the phase sequence of the voltages. If it has a positive phase sequence, then it rotates in the counter clockwise direction. Otherwise, it rotates in the clockwise direction with a negative phase sequence. The three phase voltages could be described with only two components, α and β, in a two dimensional plane. The magnitude of each active vector is $2\frac{Vdc}{3}$. The active vectors are apart and describe a hexagon boundary. The locus of the circle projected by the space reference vector depends on V_0, V_1, V_2, V_3, V_4, V_5, V_6 and V_7. According to the principle of space-vector PWM, the alpha-beta (αβ)–coordinate system can be realized by Clarke transformation using eq. (3.28).

$$\begin{bmatrix} v_\alpha \\ v_\beta \end{bmatrix} = \frac{2}{3}\begin{bmatrix} 1 & -\frac{1}{2} & -\frac{1}{2} \\ 0 & \frac{\sqrt{3}}{2} & -\frac{\sqrt{3}}{2} \end{bmatrix} X \begin{bmatrix} v_a \\ v_b \\ v_c \end{bmatrix} \tag{3.28}$$

The 3-phase quantities are reduced to two phase quantities, the first one is direct axis (real axis) and other one is quadrature axis (imaginary axis). These two quantities are represented as the magnitude (V_{ref}) and angle (α). V_{ref} rotates with the speed of angular velocity ($\omega=2\pi f$). The SVPWM is the combination of the reference voltage and 6 switching states of the inverter. The basic switching vector and sector diagram is shown in figure 3.16, forms a hexagon which can be seen as consisting of six sectors spanning 60°each. The reference vector which represents three-phase sinusoidal voltage is generated using SVPWM by switching between two nearest active vectors and zero vectors [44].

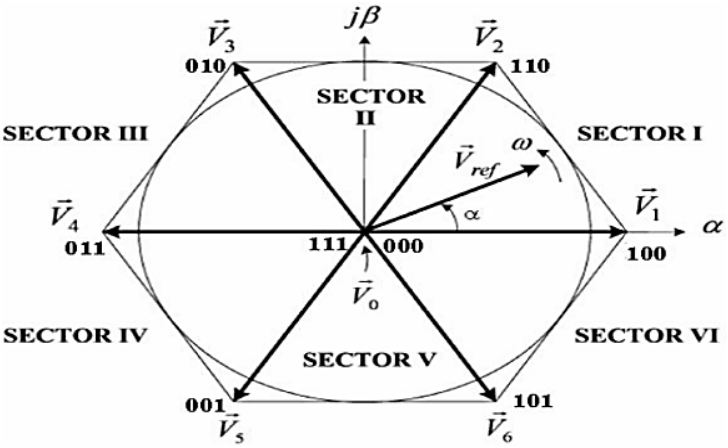

Figure 3.16 Representation of space vector in complex plane [44]

The magnitude of the reference voltage and angle (α) of the above equation used to implement the SVPWM are calculated as follows,

$$|V_{ref}| = \sqrt{{V_\alpha}^2 + {V_\beta}^2} \tag{3.29}$$

$$\alpha = \tan^{-1}\left(\frac{V_\beta}{V_\alpha}\right) \tag{3.30}$$

Determination of Sector

It is very necessary to understand in which sector the reference output voltage lies in order to determine the switching time and sequence. The phase voltages corresponding to eight switching states, six nonzero vectors and two zero vectors at the origin. Depending on the reference voltage V_α and V_β , the angle of the reference vector can be used to determine the sector as shown in Table 3.5.

Table 3.5. Sector Identification

Sector	Degrees
1	$0 < \alpha \leq 60^o$
2	$60^o < \alpha \leq 120^o$
3	$120^o < \alpha \leq 180^o$
4	$180^o < \alpha \leq 240^o$
5	$240^o < \alpha \leq 300^o$
6	$300^o < \alpha \leq 360^o$

Determination of the Switching Times for each transistor

It is necessary to arrange the switching sequence so that the switching frequency of each inverter leg is minimized. There are many switching patterns that can be used to implement SVPWM. To minimize the switching losses, only two adjacent active vectors and two zero vectors are used in a sector. To meet this optimal condition, each switching period starts with one zero vectors and end with another zero vector during the sampling time. This rule applies normally to three phase inverters as a switching sequence. Therefore, the switching cycle of the output voltage is double the sampling time and the two output voltage waveforms become symmetrical. Table 3.6 shows a symmetric switching sequence [43]. Referring to this table, the binary representations of two

adjacent basic vectors differ in only one bit, so that only one of the upper transistors switches is closed when the switching pattern moves from one vector to an adjacent one. The two vectors are time weighted in a sample period to produce the desired output voltage.

To calculate the time of application of different vectors, consider figure 3.17 which is depicting the position of different available space vectors and the reference vector in the first sector.

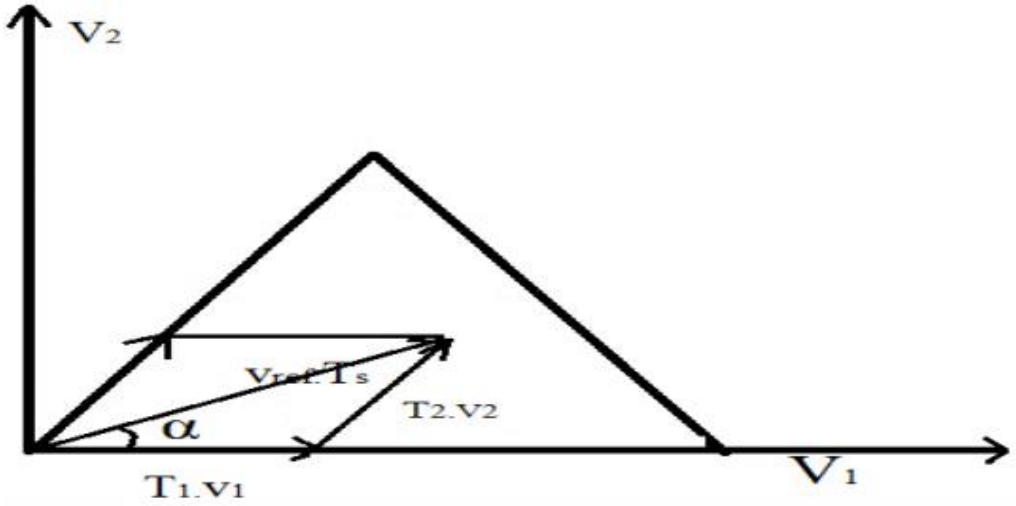

Figure 3.17 Principle of space vector time calculation

The time of each active phase vector can be calculated in the following manner,

$$T_1 = \sqrt{3}\frac{V_{ref}}{V_{dc}} T_S \sin\left(\frac{n\pi}{3} - \alpha\right)$$
$$T_2 = \sqrt{3}\frac{V_{ref}}{V_{dc}} T_S \sin\left(\alpha - \frac{(n-1)\pi}{3}\right) \quad (3.31)$$
$$T_0 = T_S - T_1 - T_2$$

Where n denotes the number of sector.

Table 3.6. Seven segment switching sequence [43]

Space vector	Switching state	On state switch	Off state switch	Vector definition
V_0	000	S_4, S_6, S_2	S_1, S_3, S_5	$V_0 = 0$
V_1	100	S_1, S_6, S_2	S_4, S_3, S_5	$V_1 = \frac{2}{3}V_{dc}$
V_2	110	S_1, S_3, S_2	S_4, S_6, S_5	$V_2 = \frac{2}{3}V_{dc}e^{-j\frac{\pi}{3}}$
V_3	010	S_4, S_3, S_2	S_1, S_6, S_5	$V_3 = \frac{2}{3}V_{dc}e^{-j\frac{2\pi}{3}}$
V_4	011	S_4, S_3, S_5	S_1, S_6, S_2	$V_4 = \frac{2}{3}V_{dc}e^{-j\frac{3\pi}{3}}$
V_5	001	S_4, S_6, S_5	S_1, S_3, S_2	$V_5 = \frac{2}{3}V_{dc}e^{-j\frac{4\pi}{3}}$
V_6	101	S_1, S_6, S_5	S_4, S_3, S_2	$V_6 = \frac{2}{3}V_{dc}e^{-j\frac{5\pi}{3}}$
V_7	111	S_1, S_3, S_5	S_4, S_6, S_2	$V_7 = \frac{2}{3}V_{dc}$

Chapter Four

Grid Connected PV System

The Distributed power generation systems (DPGS) can be broadly classified into two categories which are standalone and grid connected PV systems. In standalone PV systems, storage batteries are used which stores the energy obtained from these intermittent sources. These batteries serve as input to the inverter which converts DC power into AC power.

In the grid connected PV systems, energy storage devices may not be required as the energy obtained from the sun light directly. In the case of a solar PV system, the sun light can be directly converted to AC and transferred to the grid. To achieve this, the inverter must be controlled in advanced way using control loops so that the expected power can be transferred to the grid and also the inverter's output terminals cannot directly be connected to the grid because of the harmonics that are available in the current due to the switching nature of the inverter. A filter is used to reduce the total harmonic distortions (THD) from the inverter and grid current.

4.1. Control Structure of Grid Connected Inverter

Control system of a grid connected inverter is responsible for managing the power injection into the grid, which is obtained from a distributed generator. Mostly, control structures based on two cascaded loops are employed for this work. A number of combinations of cascaded loops can be used, which include outer power and inner current loop [45] and outer voltage and inner power loop [46]. But the most widely used strategy as mentioned in [18] is the one which uses a slower outer dc-link voltage control loop and a faster inner current control loop.

Voltage control loop is responsible for balancing the power flow of the system. If there is more power available from the dc side, the controller present in this loop changes the reference current so that more ac power can be delivered to the grid. The current control loop deals with maintenance of power quality and reduction of harmonics available in the inverter current, so that it can be injected into the grid.

The control system can be designed in one of the three reference frames which are natural reference frame, stationary reference frame and synchronous reference frame. In natural reference frame, there needs to be a controller for each phase current [18]. As the currents are sinusoidal, non-linear controllers like dead beat and hysteresis are used in natural reference frame. Fig. 4.1 shows control structure in natural reference frame.

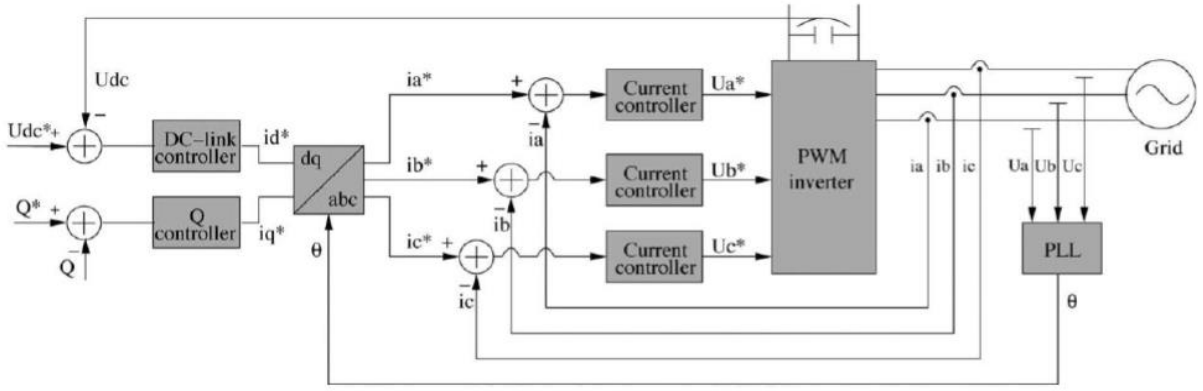

Figure 4.1 Control Structure in Natural reference Frame [18]

In stationary reference frame control implementation, abc variables are transformed into $\alpha\beta$ axis variables. In this case, the variables are also sinusoidal. Proportional-Resonant controllers are normally used in stationary reference frame structure as PI controllers cannot remove steady state error in case of sinusoidal signals [18]. One possible implementation of control structure in stationary reference frame is depicted in fig. 4.2.

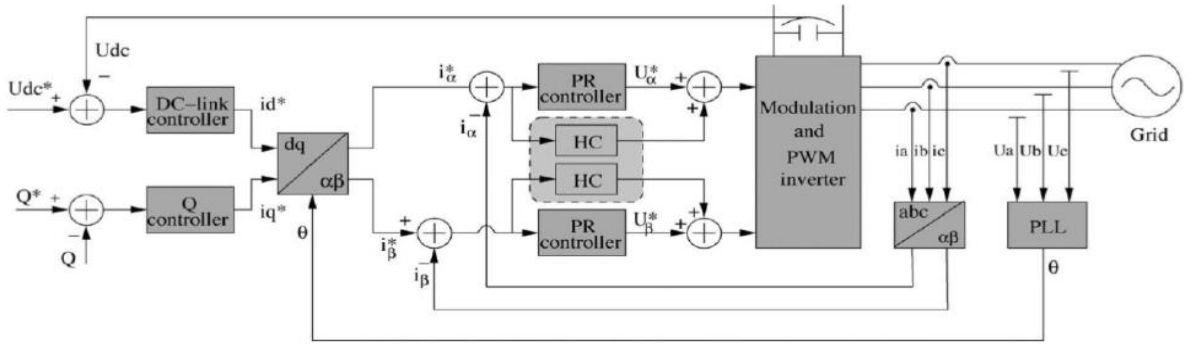

Figure 4.2 General Structure for Implementation of Control in Stationary RF [18]

In Synchronous reference frame, the sinusoidal variables are transformed into a frame that rotates at synchronous speed with sinusoidal variables, which makes these quantities appear as DC values. This means that PI controllers can be used as they provide satisfactory results when dealing with DC quantities [18]. Fig. 4.3 shows general control structure in synchronous reference frame (SRF).

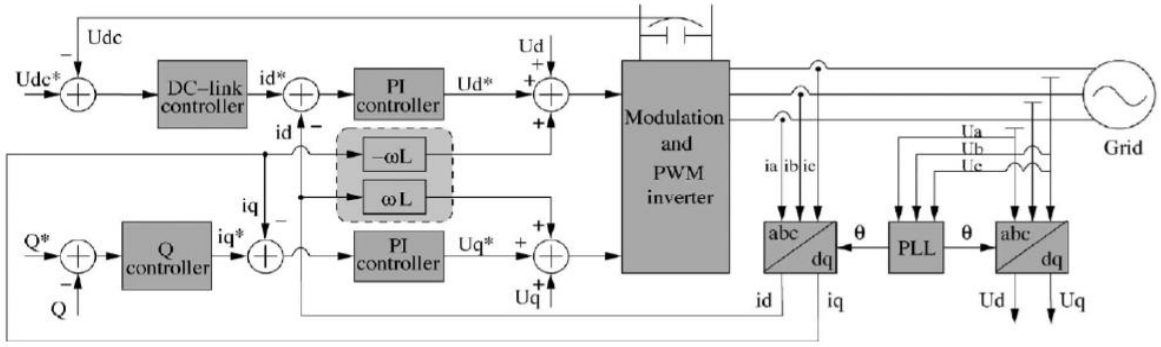

Figure 4.3 General Control Structure in Synchronous Reference Frame [18]

As can be seen in figure 4.4, the cross coupling terms and voltage is fed forward in the control loop so that active and reactive power injection into the grid can be independently controlled [47]. Synchronous reference frame (SRF) control structure is the most widely used.

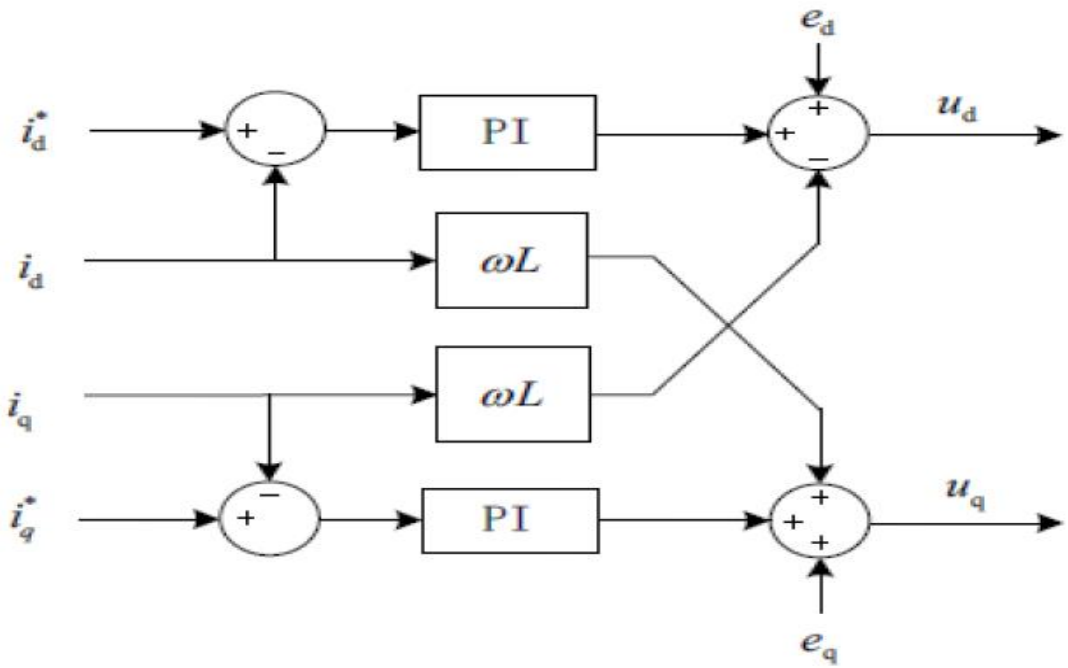

Figure 4.4 Current Control Loop; Cross coupling [47]

4.2. Control Structure of the Inverter

The most important part of the system rather than obtaining maximum power from the PV array is the control of the inverter so as to control the active and reactive power flow. From the grid

synchronization to power flow management and pulse width modulation of the inverter is taken care by the control structure of the inverter.

In this model, the control going to be used is synchronously rotating reference frame which is used to transform voltage and current quantities from natural reference frame (abc-frame) to synchronously rotating reference frame (dq-frame).

4.2.1. Representation of Three Phase Variables in Stationary RF

It transforms a three phase abc signals into a two phase orthogonal system in stationary reference frame which is called as α-β frame where both α and β axes are locked in position by the transformation. This transformation is widely used in electrical machine analysis and in the control of power electronic converters due to the advantage of working with reduced number of signals than the actual. The transformation from natural reference frame (abc-frame) to stationary reference frame (αβ-frame) is given in matrix form as follows [48],

$$\begin{bmatrix} i_\alpha \\ i_\beta \\ i_0 \end{bmatrix} = \frac{2}{3}\begin{bmatrix} 1 & -\frac{1}{2} & -\frac{1}{2} \\ 0 & \frac{\sqrt{3}}{2} & -\frac{\sqrt{3}}{2} \\ \frac{1}{2} & \frac{1}{2} & \frac{1}{2} \end{bmatrix} X \begin{bmatrix} i_a \\ i_b \\ i_c \end{bmatrix} \tag{4.1}$$

$$\begin{bmatrix} v_\alpha \\ v_\beta \\ v_0 \end{bmatrix} = \frac{2}{3}\begin{bmatrix} 1 & -\frac{1}{2} & -\frac{1}{2} \\ 0 & \frac{\sqrt{3}}{2} & -\frac{\sqrt{3}}{2} \\ \frac{1}{2} & \frac{1}{2} & \frac{1}{2} \end{bmatrix} X \begin{bmatrix} v_a \\ v_b \\ v_c \end{bmatrix} \tag{4.2}$$

The scaling factor 2/3 is being considered for amplitude invariant transformations. In a balanced three phase systems, $I_a+I_b+I_c=0$ and I_0 can be neglected, which is resulting in simplified transformation form as follows,

$$\begin{bmatrix} i_\alpha \\ i_\beta \end{bmatrix} = \frac{2}{3}\begin{bmatrix} 1 & -\frac{1}{2} & -\frac{1}{2} \\ 0 & \frac{\sqrt{3}}{2} & -\frac{\sqrt{3}}{2} \end{bmatrix} X \begin{bmatrix} i_a \\ i_b \\ i_c \end{bmatrix} \tag{4.3}$$

From the three phase currents, the α-β current components can be calculated as can be seen in eq. (4.3). The α-β components of the voltages can be calculated from line to line voltages using eq. (4.4).

$$\begin{bmatrix} v_\alpha \\ v_\beta \end{bmatrix} = \frac{2}{3}\begin{bmatrix} 1 & -\frac{1}{2} & -\frac{1}{2} \\ 0 & \frac{\sqrt{3}}{2} & -\frac{\sqrt{3}}{2} \end{bmatrix} X \begin{bmatrix} v_a \\ v_b \\ v_c \end{bmatrix} \quad (4.4)$$

The simplified inverse Clarke transformation for converting the quantities back to natural reference frame (abc-frame) is given as

$$\begin{bmatrix} i_a \\ i_b \\ i_c \end{bmatrix} = \frac{3}{2}\begin{bmatrix} \frac{2}{3} & 0 \\ -\frac{1}{3} & \frac{1}{\sqrt{3}} \\ -\frac{1}{3} & -\frac{1}{\sqrt{3}} \end{bmatrix} X \begin{bmatrix} i_\alpha \\ i_\beta \end{bmatrix} \quad (4.5)$$

$$\begin{bmatrix} v_a \\ v_b \\ v_c \end{bmatrix} = \frac{3}{2}\begin{bmatrix} \frac{2}{3} & 0 \\ -\frac{1}{3} & \frac{1}{\sqrt{3}} \\ -\frac{1}{3} & -\frac{1}{\sqrt{3}} \end{bmatrix} X \begin{bmatrix} v_\alpha \\ v_\beta \end{bmatrix} \quad (4.6)$$

4.2.2. Representation of Three Phase Variables in SRRF

The three phase signals represented in stationary reference frame are time-varying quantities as the frame is stationary. If the quantities need to look like time-invariant, then the observer or the frame of reference should also be rotating along with the rotating space vector, such frame of reference is called dq-synchronous reference frame, proposed by Park (1929) for the analysis of synchronous machines. The transformations from abc-frame to dq0-frame is given as [48]

$$\begin{bmatrix} i_d \\ i_q \\ i_0 \end{bmatrix} = \frac{2}{3}\begin{bmatrix} cos\omega t & cos\left(\omega t - \frac{2\pi}{3}\right) & cos\left(\omega t + \frac{2\pi}{3}\right) \\ -sin\omega t & -sin\left(\omega t - \frac{2\pi}{3}\right) & -sin\left(\omega t + \frac{2\pi}{3}\right) \\ \frac{1}{2} & \frac{1}{2} & \frac{1}{2} \end{bmatrix} X \begin{bmatrix} i_a \\ i_b \\ i_c \end{bmatrix} \quad (4.7)$$

$$\begin{bmatrix} v_d \\ v_q \\ v_0 \end{bmatrix} = \frac{2}{3}\begin{bmatrix} cos\omega t & cos\left(\omega t - \frac{2\pi}{3}\right) & cos\left(\omega t + \frac{2\pi}{3}\right) \\ -sin\omega t & -sin\left(\omega t - \frac{2\pi}{3}\right) & -sin\left(\omega t + \frac{2\pi}{3}\right) \\ \frac{1}{2} & \frac{1}{2} & \frac{1}{2} \end{bmatrix} X \begin{bmatrix} v_a \\ v_b \\ v_c \end{bmatrix} \quad (4.8)$$

Where θ=ωt is the reference phase angle. This transformation requires the information of the reference phase angle. The phase angle information can be obtained by using the phase locked loop (PLL).

Since the system is balanced, the above eq. (4.7) and eq. (4.8) are simplified in the following transformation matrix form as follows,

$$\begin{bmatrix} i_d \\ i_q \end{bmatrix} = \frac{2}{3}\begin{bmatrix} cos\omega t & cos\left(\omega t - \frac{2\pi}{3}\right) & cos\left(\omega t + \frac{2\pi}{3}\right) \\ -sin\omega t & -sin\left(\omega t - \frac{2\pi}{3}\right) & -sin\left(\omega t + \frac{2\pi}{3}\right) \end{bmatrix} X \begin{bmatrix} i_a \\ i_b \\ i_c \end{bmatrix} \quad (4.9)$$

$$\begin{bmatrix} v_d \\ v_q \end{bmatrix} = \frac{2}{3}\begin{bmatrix} cos\omega t & cos\left(\omega t - \frac{2\pi}{3}\right) & cos\left(\omega t + \frac{2\pi}{3}\right) \\ -sin\omega t & -sin\left(\omega t - \frac{2\pi}{3}\right) & -sin\left(\omega t + \frac{2\pi}{3}\right) \end{bmatrix} X \begin{bmatrix} v_a \\ v_b \\ v_c \end{bmatrix} \quad (4.10)$$

The inverse Park transformation from dq0-frame to abc-frame is provided as follows,

$$\begin{bmatrix} i_a \\ i_b \\ i_c \end{bmatrix} = \begin{bmatrix} cos\omega t & -sin\omega t \\ cos\left(\omega t - \frac{2\pi}{3}\right) & -sin\left(\omega t - \frac{2\pi}{3}\right) \\ cos\left(\omega t + \frac{2\pi}{3}\right) & -sin\left(\omega t + \frac{2\pi}{3}\right) \end{bmatrix} X \begin{bmatrix} i_d \\ i_q \end{bmatrix} \quad (4.11)$$

$$\begin{bmatrix} v_a \\ v_b \\ v_c \end{bmatrix} = \begin{bmatrix} cos\omega t & -sin\omega t \\ cos\left(\omega t - \frac{2\pi}{3}\right) & -sin\left(\omega t - \frac{2\pi}{3}\right) \\ cos\left(\omega t + \frac{2\pi}{3}\right) & -sin\left(\omega t + \frac{2\pi}{3}\right) \end{bmatrix} X \begin{bmatrix} v_d \\ v_q \end{bmatrix} \quad (4.12)$$

In this thesis work, the dq0 to abc transformation helps the space vector pulse width modulation (SVPWM) to generate the pulse gates for the switching nature of the inverter in order to control the voltage source inverter (VSI).

4.2.3. Grid Synchronization

The phase information of the grid voltage can be obtained by using phase locked loop (PLL). The necessary phase information which is required for synchronizing the three phase inverter current with the three phase grid voltage is being obtained. The phase angle that is used in dq transformation for both current and voltage quantities to make sure that the magnitude of the grid and inverter are same. Figure 4.5 shows the internal structure of the phase locked loop present in the Simulink.

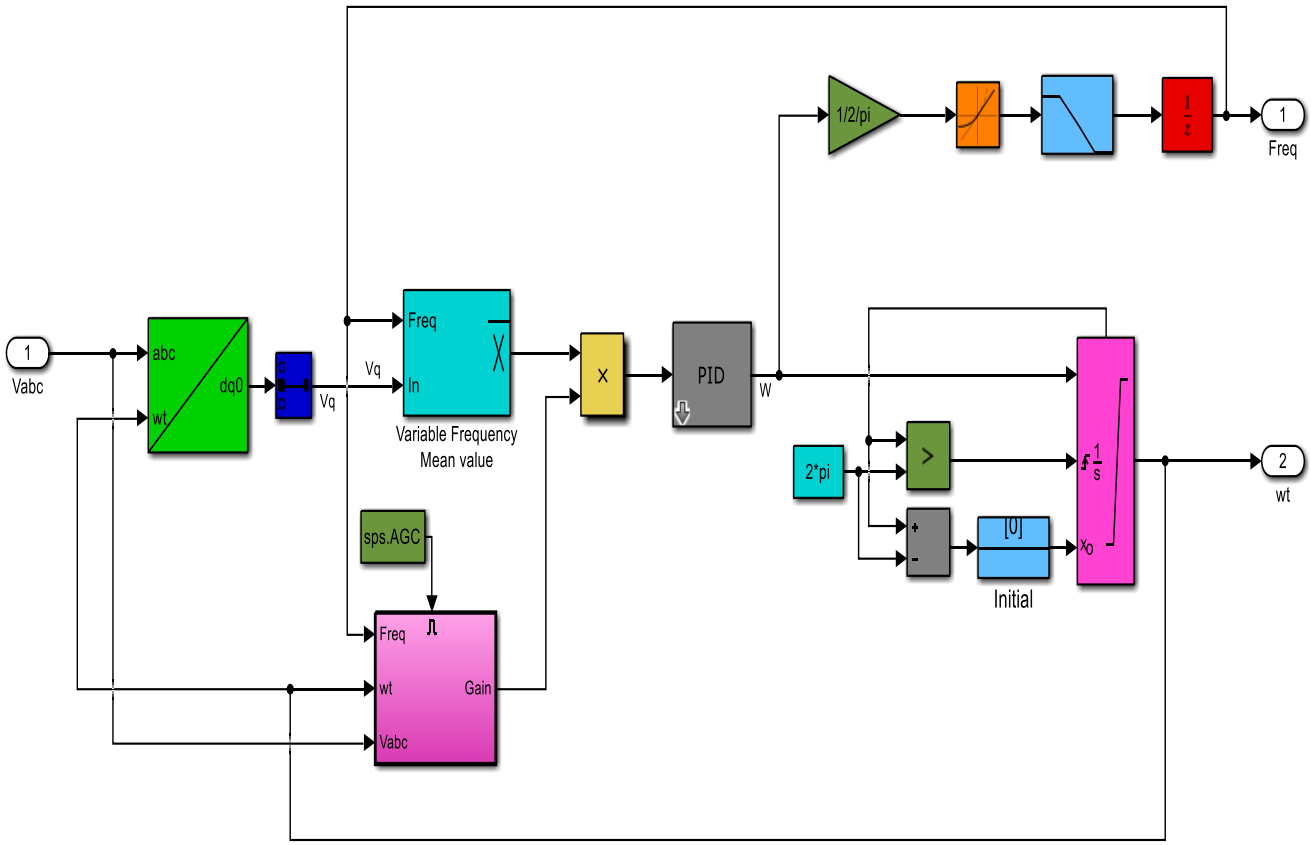

Figure 4.5 Internal Structure of Phase Locked Loop

4.2.4. Control Loops for Inverter Control

In this thesis work, there are two control loops that are used to balance the power flow on the side of DC and AC in order to increase the power quality which is fed into the grid and that are the external voltage loop controller and internal current loop controller [49].

PI Controller for Voltage and Current Control

Proportional-Integral (PI) controllers are one of the most commonly used types of controllers.

The measured DC voltage is compared with the reference voltage to feed the error signal to this controller to reduce the error. as well as, the measured direct and quadrature current are compared with the reference direct and quadrature current, then the error signal is fed to the PI controller.

DC-Link Voltage Control

This controller is used to regulate the DC voltage delivered from the boost at the input side of the inverter. The PI controller gains are selected using the formula [50]:

$$K_p = \frac{3C}{20T_s} \quad (4.13)$$

$$K_i = \frac{0.0769K_p}{T_s} \quad (4.14)$$

Where K_p and K_i are proportional gain, C is the boost converter capacitor and T_s is the switching period of the inverter switch.

Current Control Loop

This controller is used to regulate the injected current in synchronously dq-reference frame. The PI controller gain is selected using the formula,

$$K_p = \frac{0.004L}{T_s} \quad (4.15)$$

$$K_i = \frac{K_p}{\tau} \quad (4.16)$$

Where L is the filter inductor, R is the filter resistance which should be very minimum that is 1ohm's and τ is the time constant given by L/R.

The external voltage loop controller is used to keep the DC-link voltage constant. The output of the active current reference is generated by the DC-link voltage controller.

The reactive power controller sets the reactive current reference which is set to zero. The main function of the voltage loop controller is to change the active reference current so that the power available from the PV array can be matched with the power injected to the grid. Figure 4.6 shows the external voltage loop controller.

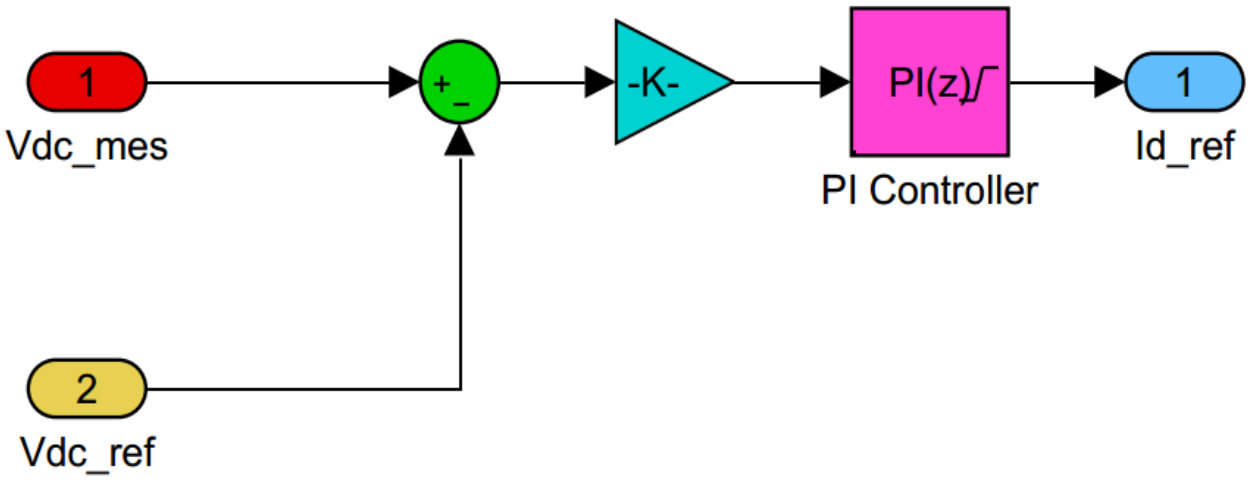

Figure 4.6 DC-Link Voltage Controller

The internal current controller loop is used to regulate the grid currents that are converted into direct current (I_d) and quadrature current (I_q). The internal current loop controller is worked based on the active current reference and reactive current reference. But, the reactive power current reference must be taken as zero in order to supply only active power to the grid by providing the desired voltage signal to achieve the unity power factor. Figure 4.7 shows the internal current loop controller.

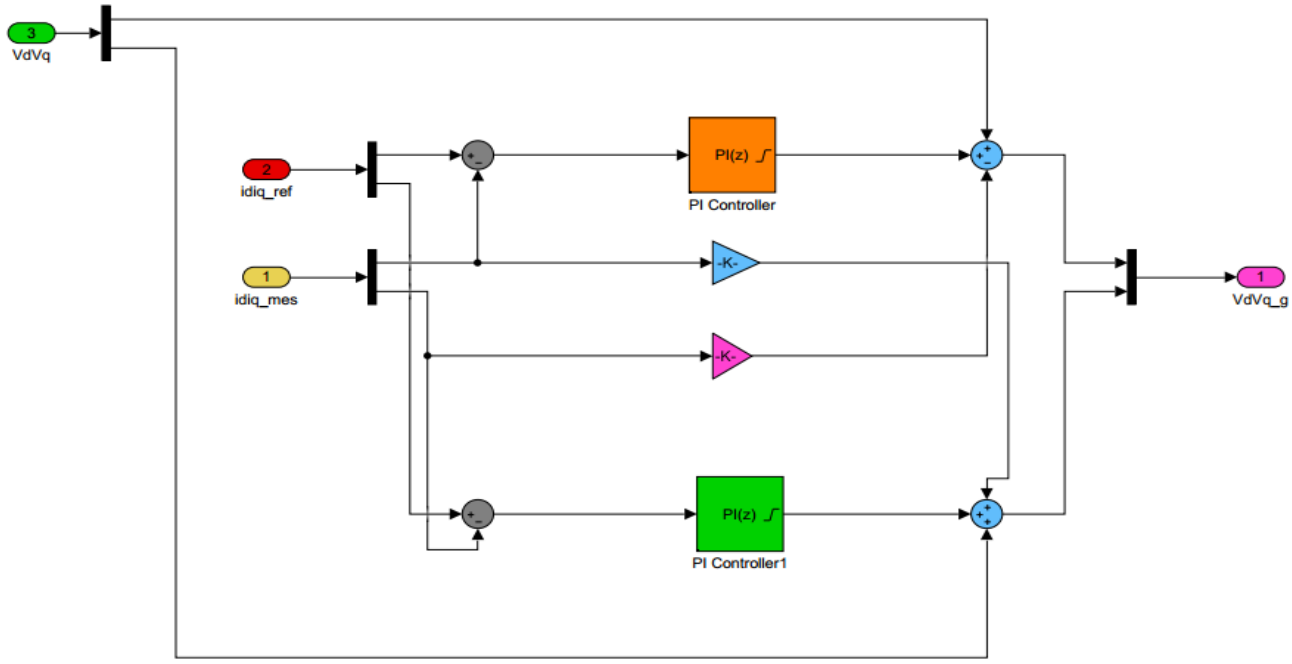

Figure 4.7 Internal Current Controller

The proposed method is done based on the controlling of current and voltage, active power and reactive power which are injected to the grid. Both current and voltage control scheme is mainly dependent on the dq-reference frame. The grid voltage and current can be converted into the direct voltage, quadrature voltage, direct current and quadrature current by using the natural reference frame (abc-frame) to synchronously rotating reference frame (dq-frame). The controller block performs the control action by comparing the measured direct and quadrature current with the reference direct and quadrature current, and then the error signals are being generated and fed to the PI controller. Figure 4.8 depicts the Simulink model of the current and voltage controller of grid connected PV inverter.

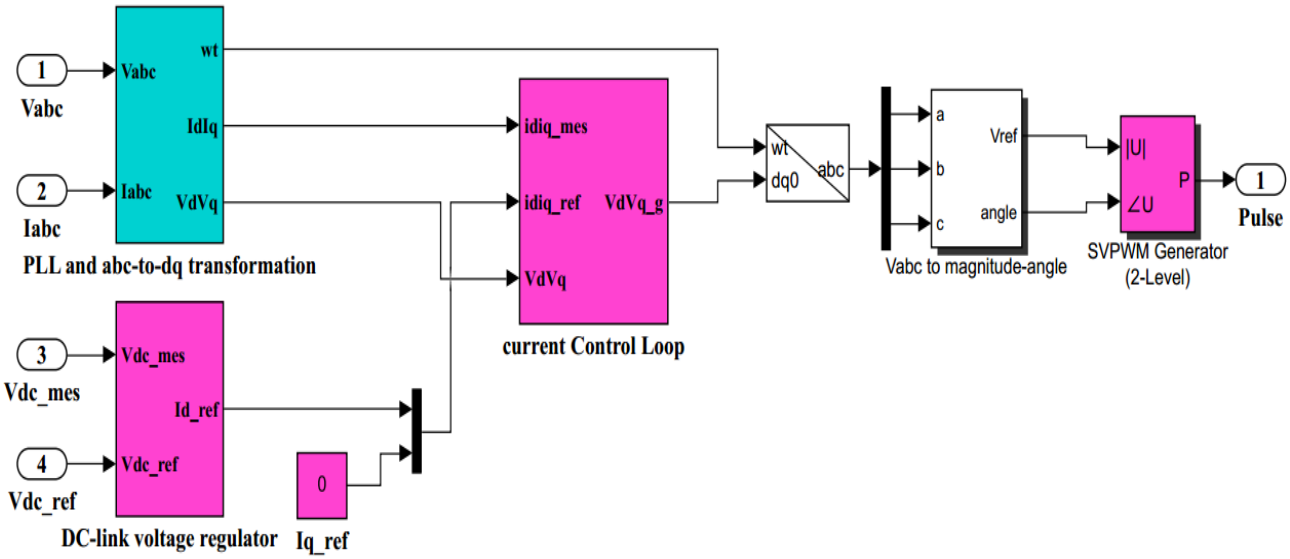

Figure 4.8 Overall Voltage and Current controller for Active and Reactive Power Control

4.3. Grid with Load

The grid can be modelled as three phase voltage source with the line-to-line voltage of rms value of 400V. The inverter connected with filter is used as input to the grid. Figure 4.8 shows a 1.5KW load is connected to the grid.

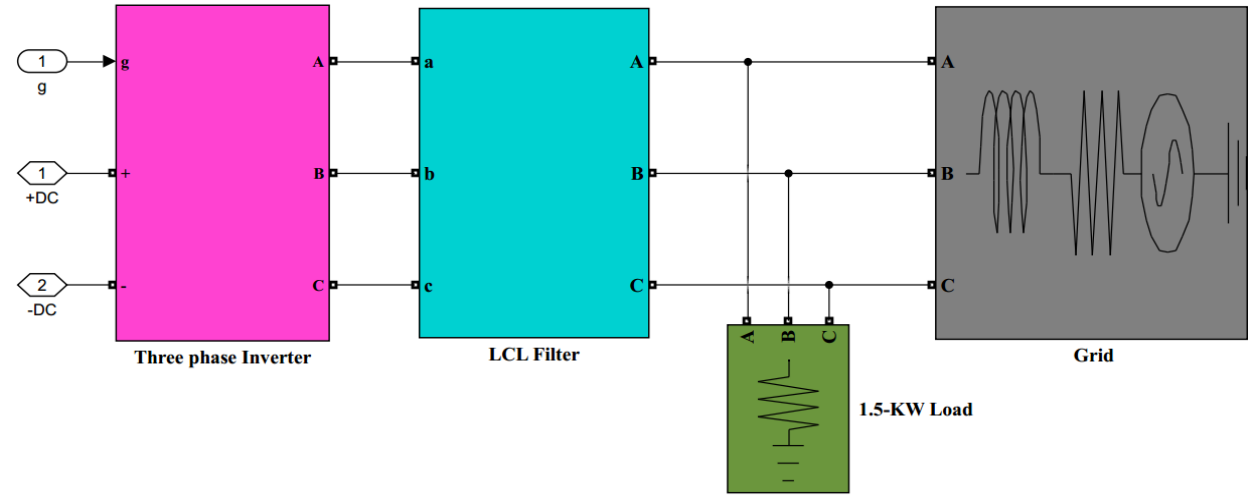

Figure 4.9 Model of Grid Connected Load

4.4. Block Diagram of Overall System

In the previous two chapters, the main basic components of the grid connected PV inverter system have been modeled. Those all components are the PV array, the DC-DC boost converter with MPPT controller using incremental conductance, the voltage source inverter (VSI) with the LCL filter, the phase locked loop (PLL), and the voltage source inverter controller. So, the entire grid connected PV system is built by using all components modeled in chapter 3 and chapter 4. The MATLAB/SIMULINK model for grid connected PV system which is shown in figure 4.10 consists of the following parts described below.

PV Array: the PV array consists of one parallel string and five series strings that each string consisting of 96 modules which are connected in series. The PV array can generate a maximum power of 1.5KW at a constant solar irradiance G=1000W/m^2 and temperature T=25^{o}C.

DC-DC Boost Converter: the boost converter is used to enhance the maximum voltage of the PV array from 273.5V to the appropriate voltage level that is 700V. The duty cycle of the boost converter is generated by MPPT using incremental conductance algorithm. The boost converter is operated at the switching frequency of 5 KHz.

MPPT Controller: uses the incremental conductance algorithm to generate the duty cycle of the boost converter. This controller automatically varies the duty cycle of the converter in order to extract the maximum power from the PV array.

Voltage Source Inverter: The two levels IGBT voltage source inverter is used to convert the 700V DC-link voltage to the line to line rms AC voltage of 400V. The inverter switches are controlled by using the space vector pulse width modulation (SVPWM) technique. So, the space vector pulse width modulation signals are generated by the inverter controller. The voltage source inverter controller is used to generate the appropriate gate signals for the voltage source inverter switch to generate the required AC voltage and current.

Inverter with SVPWM and Grid Filter: an LCL-filter is very important to reduce the total harmonics which is produced by the voltage source inverter.

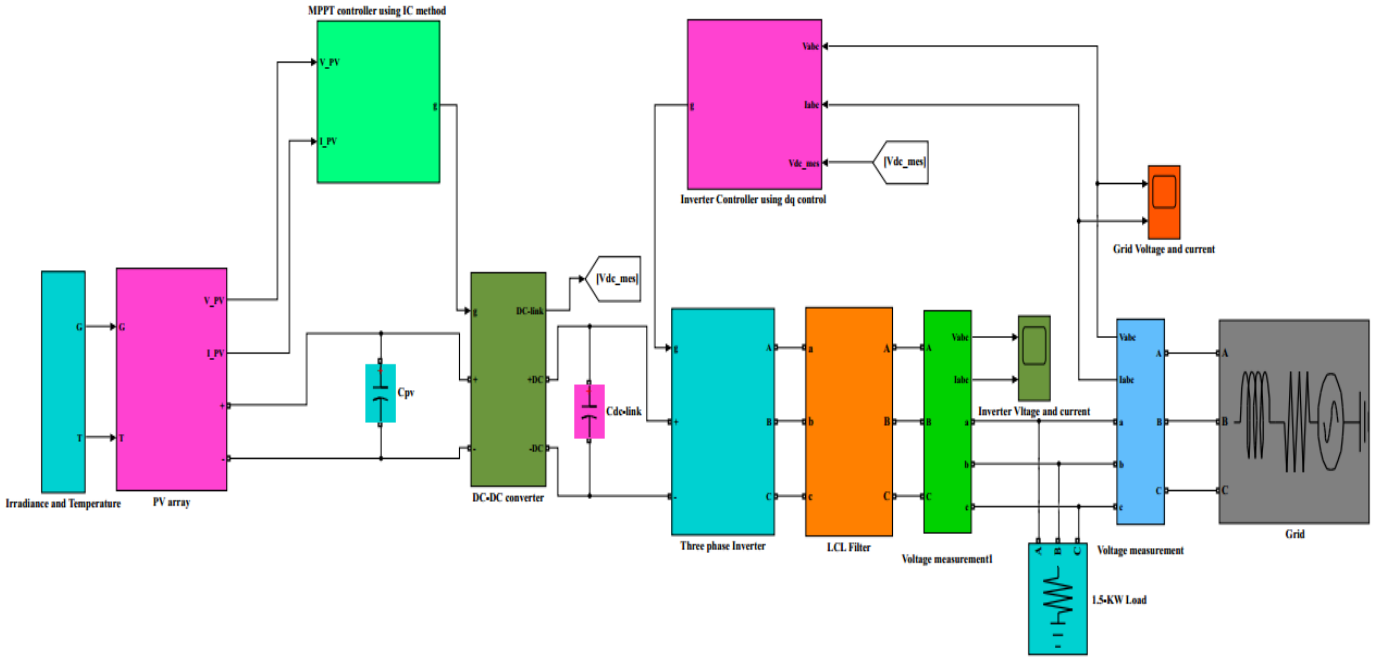

Figure 4.10 The Complete Model of the Grid Connected PV System

Table 4.1. Grid and controller parameters used for simulation

Parameter name	Value
Frequency of the system(f)	50Hz
Grid voltage(V_{LLrms})	400V
Current controller gains(K_p,Ki)	(0.79,20)
Voltage regulator gains(K_p,Ki)	(6.62,254)

Chapter Five

Simulation Results and Discussion

5.1. Introduction

In this chapter, the results obtained from the model which has been designed in chapter 3 and chapter 4 are presented. This shows all the simulations for the PV array with the characteristics curve, DC-DC boost converter with MPPT controller, reduction of THD of the inverter and the inverter control scheme and the results of the overall system under different atmospheric conditions. The complete grid connected PV model and simulation results were being done using MATLAB/SIMULINK.

5.2. PV Array

The results of the designed model have similarity with that of the results of the PV array which are provided in the datasheet in table 3.1. The graphs of I-V and P-V characteristics curve of the PV array are obtained which are quite similar to the actual behavior of a real PV array under the effect of various levels of irradiance and temperature which are depicted in figure 5.1 and figure 5.2. The MATLAB codes used to find the PV array characteristics are available in appendix A.

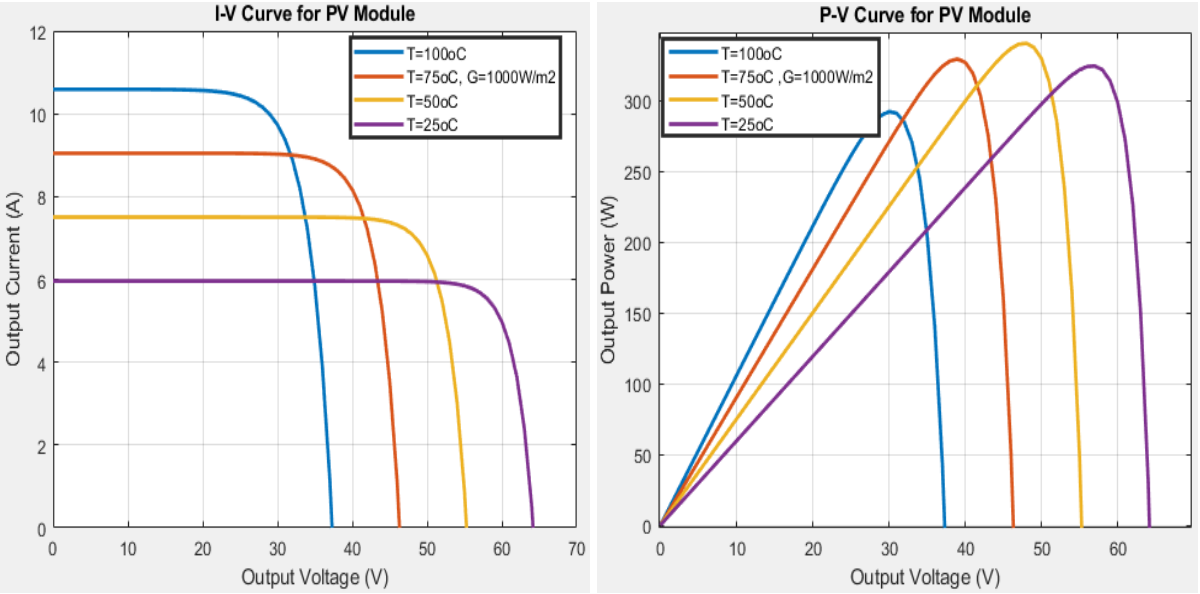

Figure 5.1 Effect of temperature changes on I-V and P-V Curve

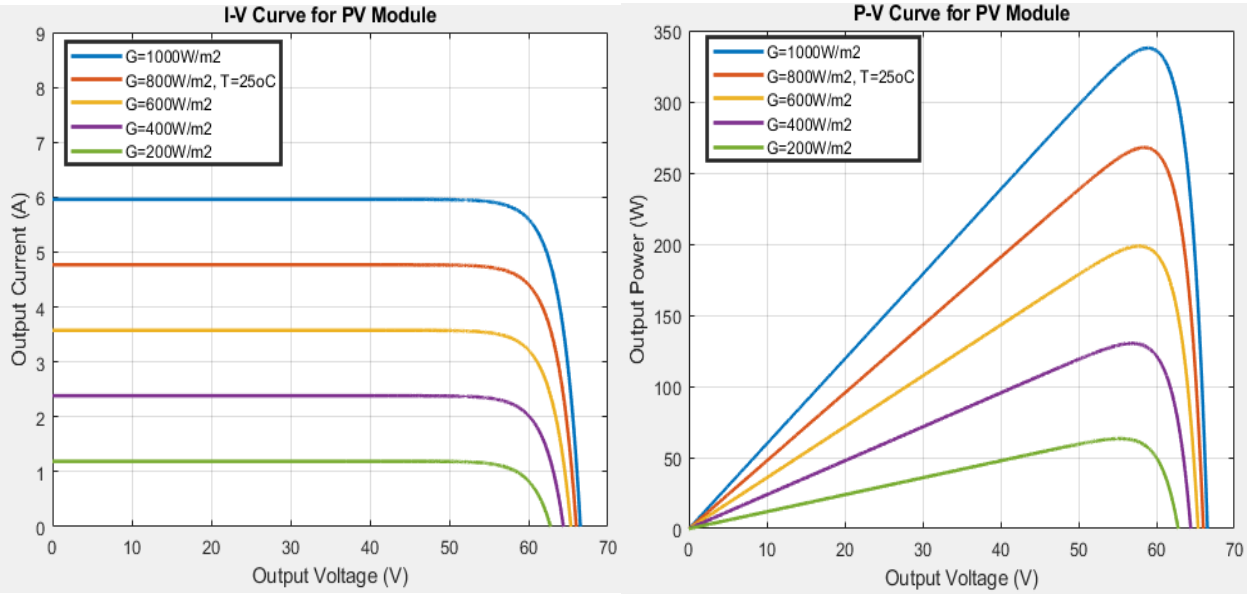

Figure 5.2 Effect of solar irradiance changes on I-V and P-V Curve

It is clear that the simulation results of the modeled PV module match with the PV module in the datasheet by comparing the designed model results with the datasheet results.

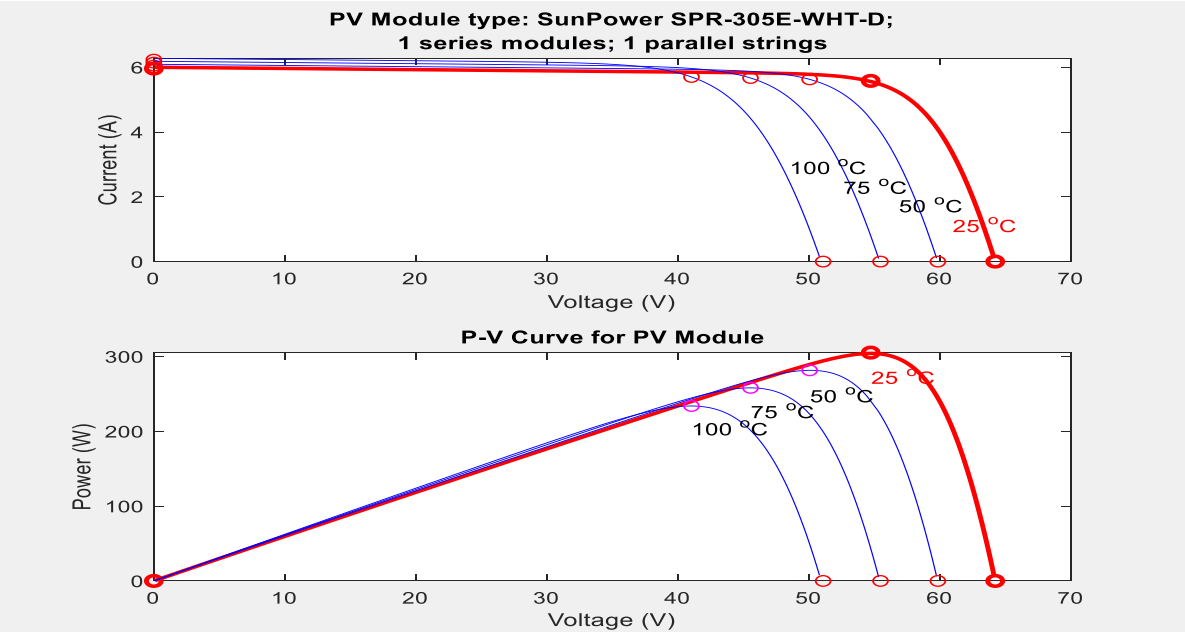

Figure 5.3 I-V and P-V Curve at different temperature found from datasheet

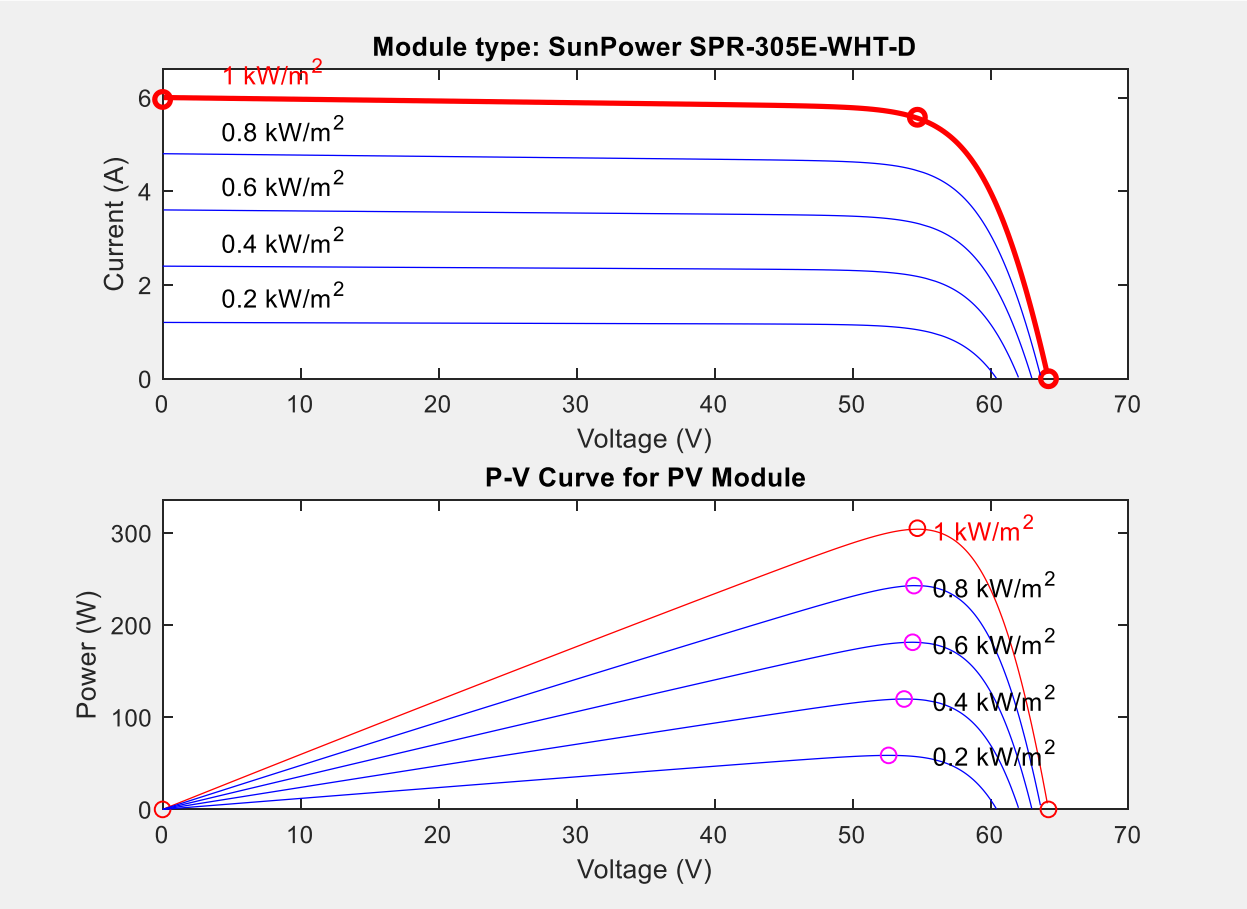

Figure 5.4 I-V and P-V Curve at different irradiance found from datasheet

The sun power SPR-305 module has a maximum power of 305W under standard test conditions. The PV array is constructed using a PV string which consists of five module connected in series in order to generate a power of around 1.5KW as shown in figure 5.5. The measured characteristics curves of I-V and P-V for PV array using MATLAB/Simulink under standard test conditions are shown in figure 5.6.

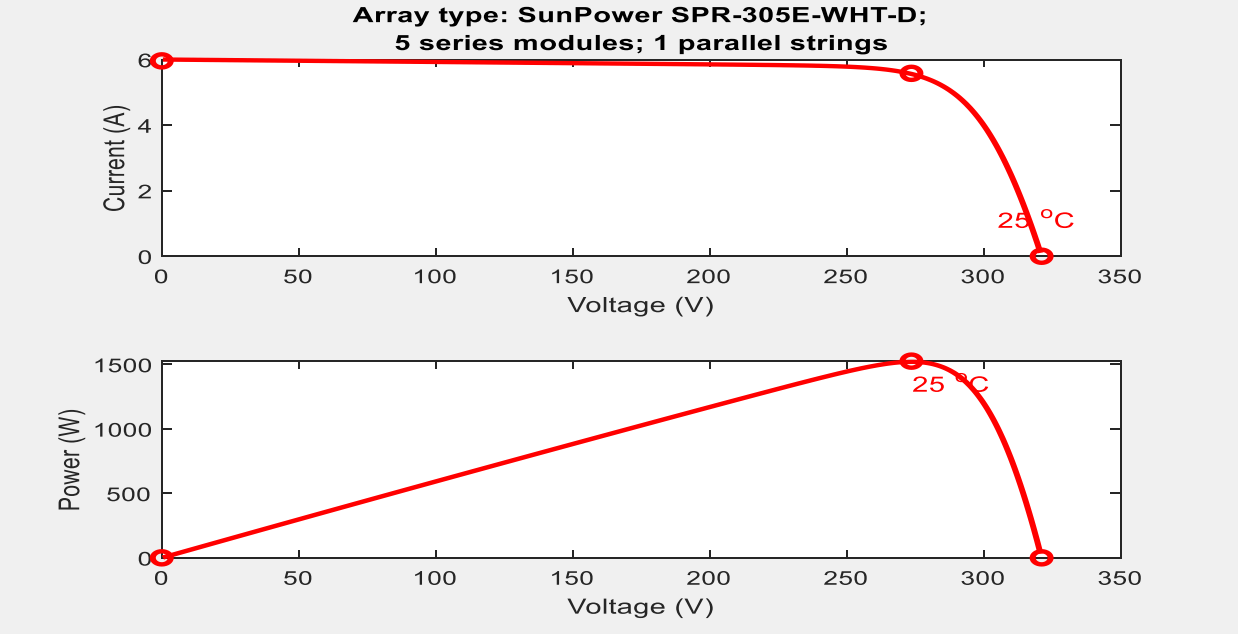

Figure 5.5 PV array characteristic curve for I-V and P-V under STC

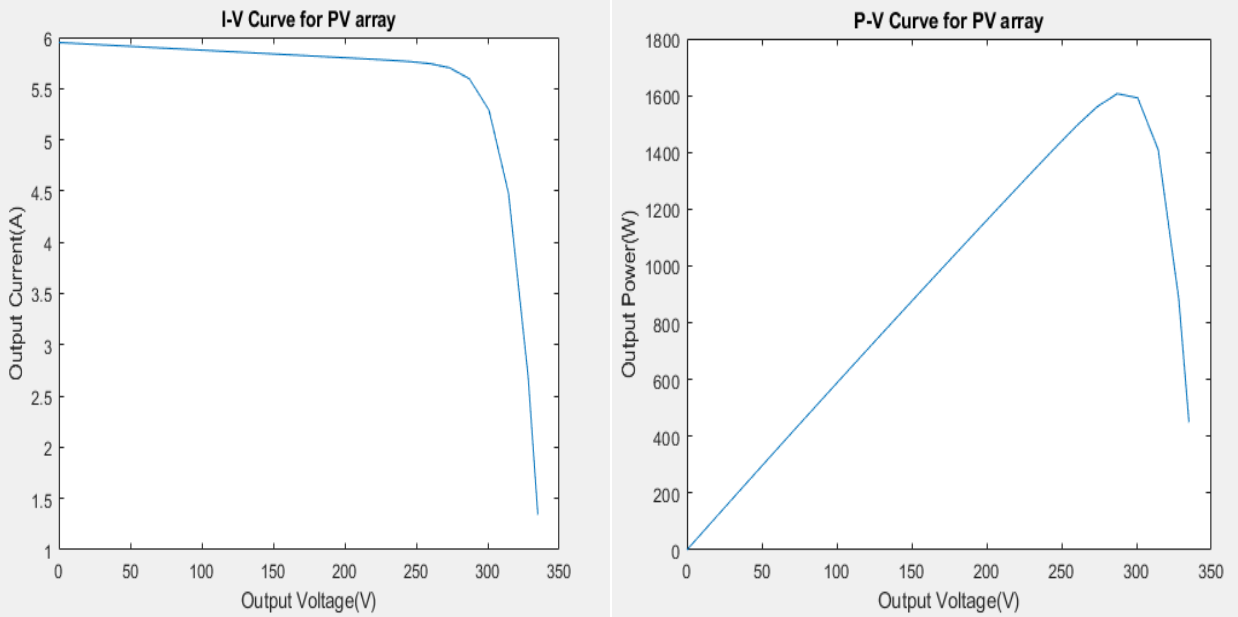

Figure 5.6 I-V and P-V Curve for PV Array Measured from MATLAB/Simulink

The simulation result of the system model in chapter 3 is implemented in Simulink environment. The simulation running time is 2.5 second. The input signals of the PV array can be either constant or time-varying irradiance and temperature which are illustrated in figure 5.7. However, the system is operated at different solar irradiance and temperature level.

The magenta color indicates the operating temperature that has a value of 25°C and 50°C respectively.

The red color shows the operating solar irradiation that has a value of 1000W/m^2, 250W/m^2 and again 1000W/m^2 respectively.

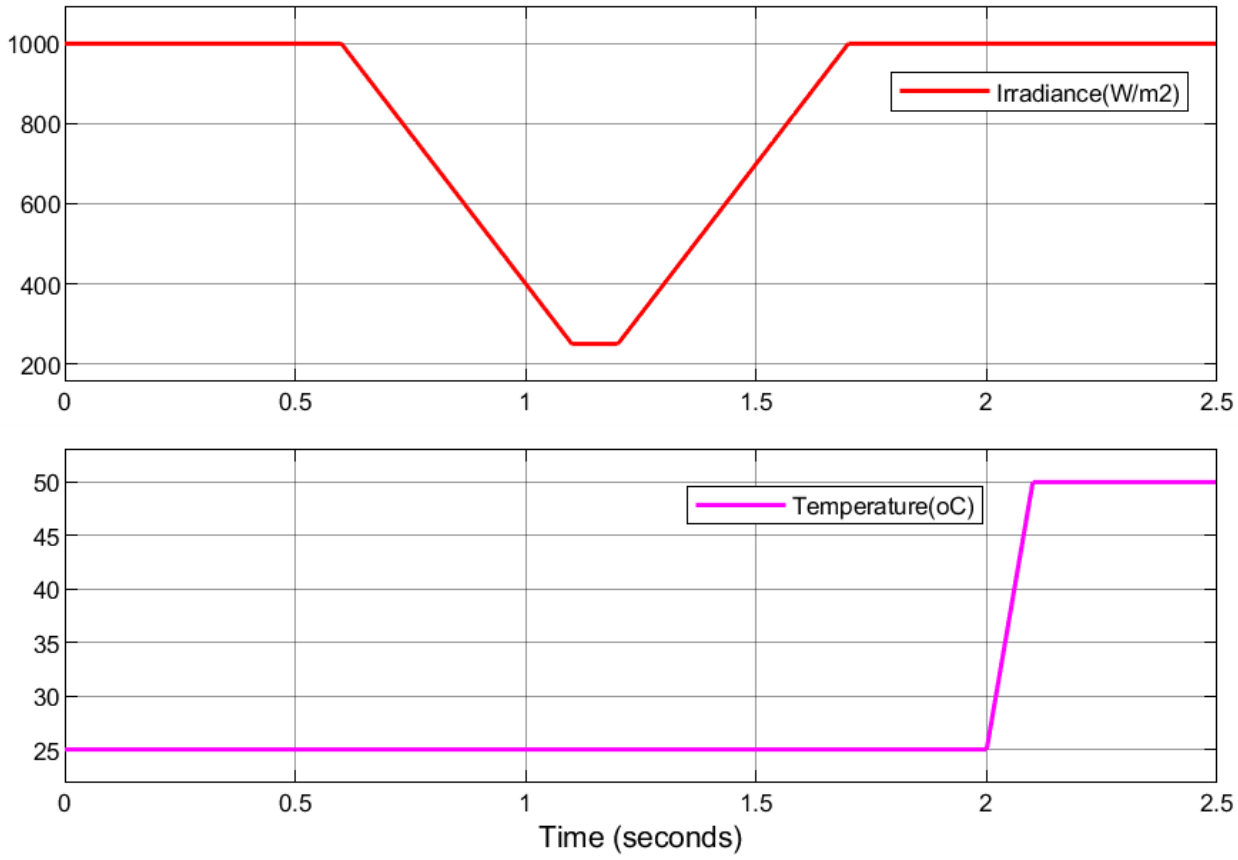

Figure 5.7 Temperature and Irradiance at different level

5.3. DC-DC Converter

In this thesis work, the boost converter is modelled to operate in continuous conduction mode using equations described in chapter 3. This converter boosts the output voltage of PV array to the required voltage level which is about 700V with applying the maximum power point tracking using incremental conductance algorithm around the boost converter side. Figure 5.8 shows the voltage and power which is extracted from the PV array and the system tracks the maximum output power and output voltage of PV array efficiently. Under standard test condition, the input power is 1.521KW and the voltage at maximum power point is around 273.2V.

At the temperature of 50 ^{O}C and irradiance of 1000W/m^2, the maximum available power is reduced to 1.33KW and voltage at maximum power point is 266V.

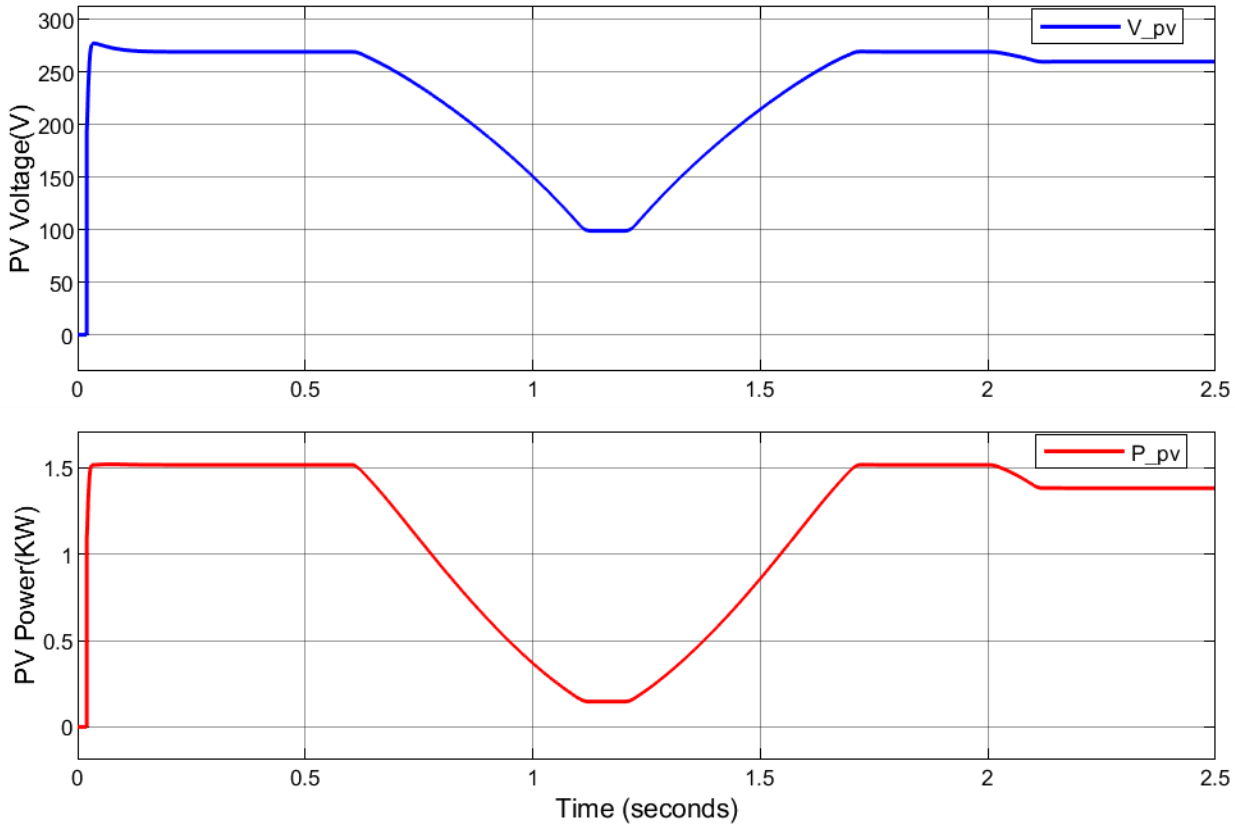

Figure 5.8 Output of PV array

5.4. DC-Link Voltage

The DC-link voltage is being controlled by the voltage regulator. Due to this, the maximum power obtained from PV array is approximately equal to the power injected to the grid. Figure 5.9 shows the results of DC-link voltage and reference voltage signal for the voltage controller. When the irradiance and temperature changes, the DC-link voltage also changes slightly but, the voltage controller returns it back to the desired level by keeping the voltage constant. The DC-link voltage tracks the reference voltage signal within the acceptable range. As can be seen in figure 5.10, the error signal between the DC-link voltage and the reference voltage signal is very closing to zero. So the DC-link voltage tracks the reference voltage signal with minimum error. This DC-link voltage can follow the reference voltage signal with the rise time of 0.001732 second and settling time of 0.215 second.

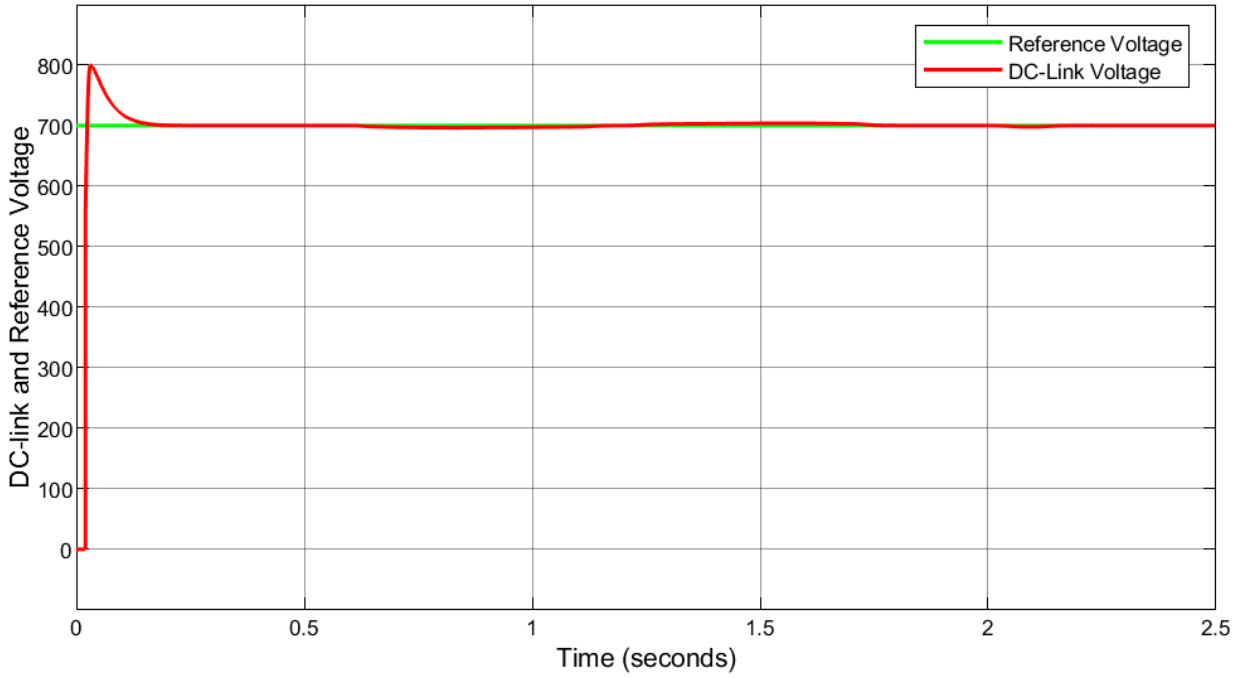

Figure 5.9 DC-link Voltage and Reference Voltage Signal

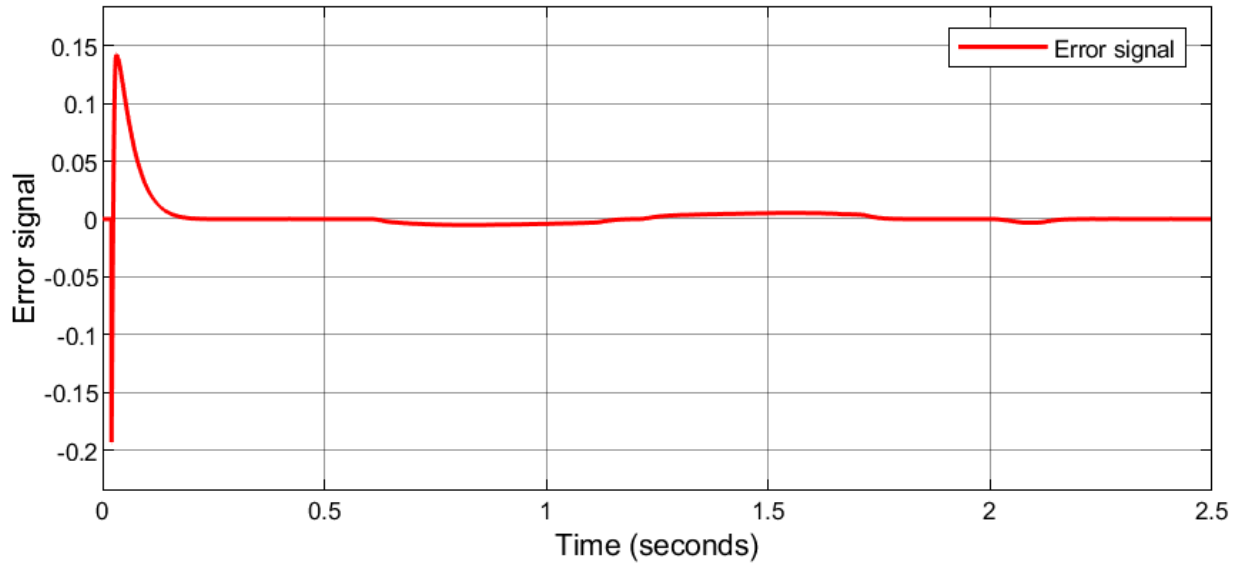

Figure 5.10 Error Signal Between DC-link Voltage and Reference Voltage

5.5. DC-AC Inverter

The inverter receives the DC voltage from the boost converter and it turns into AC signals. This AC signal is a two-level signal. The line-to-line voltage oscillates between the negative and positive of the DC-link voltage of the designed model as shown in figure 5.11.

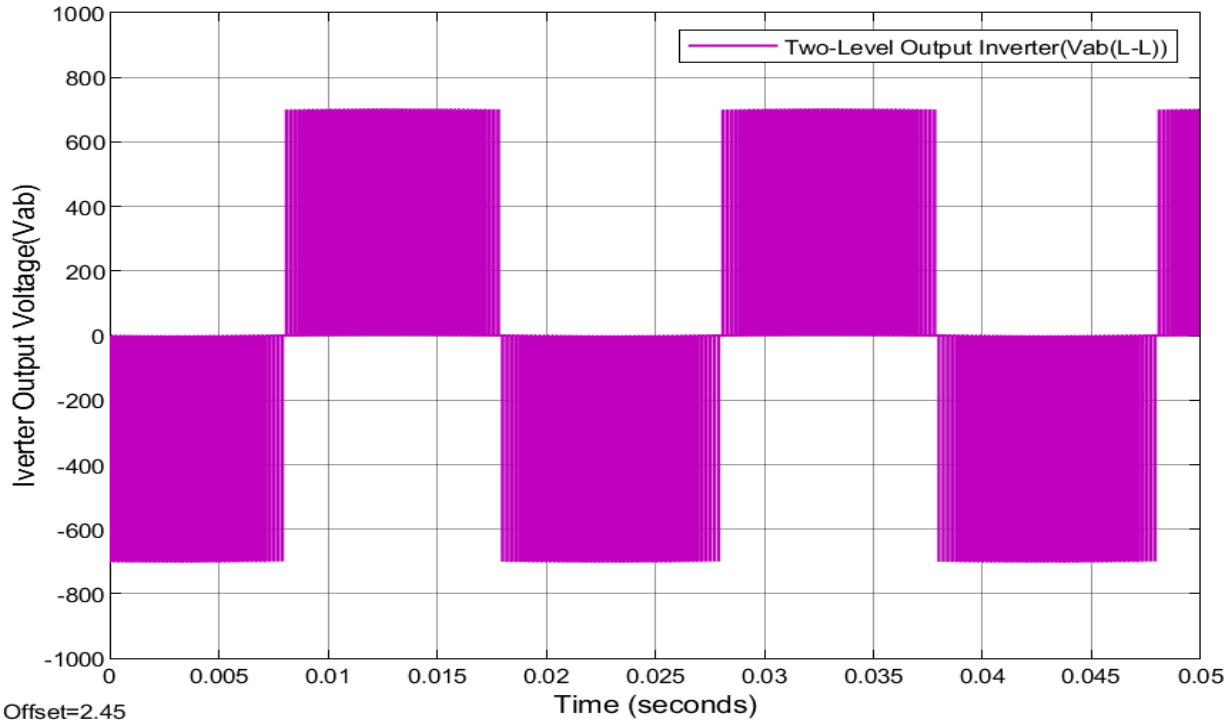

Figure 5.11 Inverter Output Voltage Vab

The voltage source inverter (VSI) output voltage and current with and without filter and FFT spectrum were evaluated.

Disturbances are highly available in the side of voltage source inverter which affects the whole grid connected PV system and reduces the power quality of the system. Due to this effect, an LCL-filter is used to attenuate the high frequency harmonics to fulfil the recommended standard. Figure 5.12 and figure 5.13 shows the effect of LCL filter on the reduction of disturbances of the inverter current and voltage.

The results of the output current and voltage of the inverter with FFT spectrum is shown in figure 5.14 and figure 5.15 respectively. The total harmonic distortion (THD) is less than 5% according to IEEE standard 929-2000 which is about 0.86%.

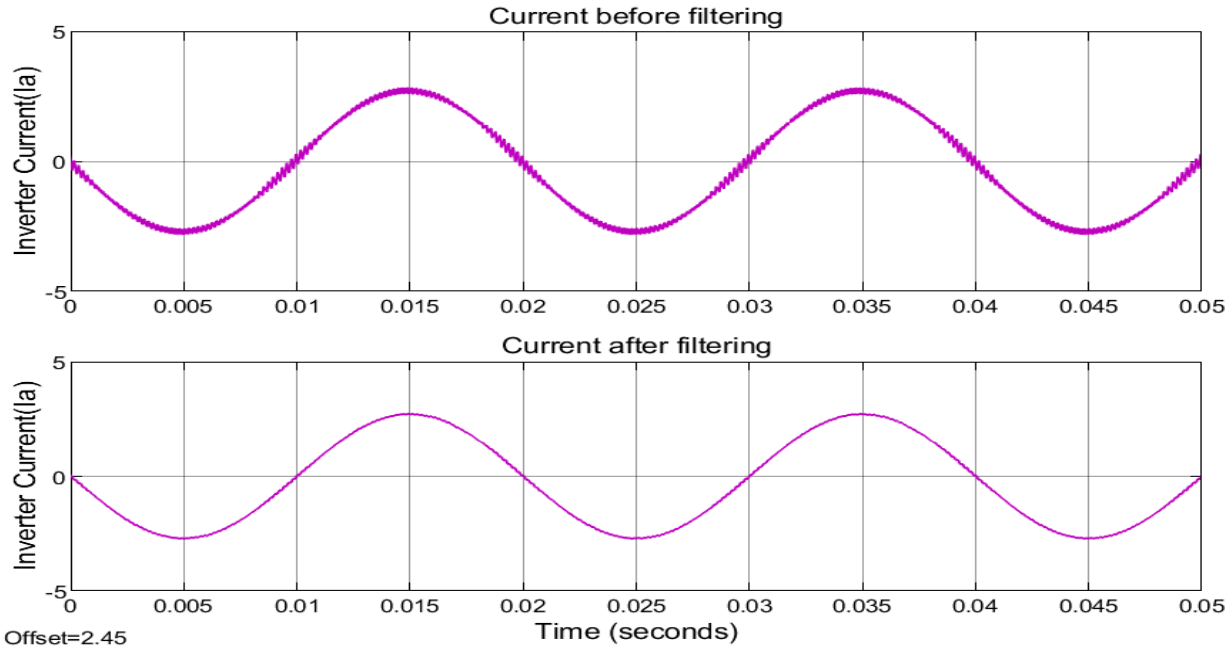

Figure 5.12 Output of Inverter before and after filter for Current waveform

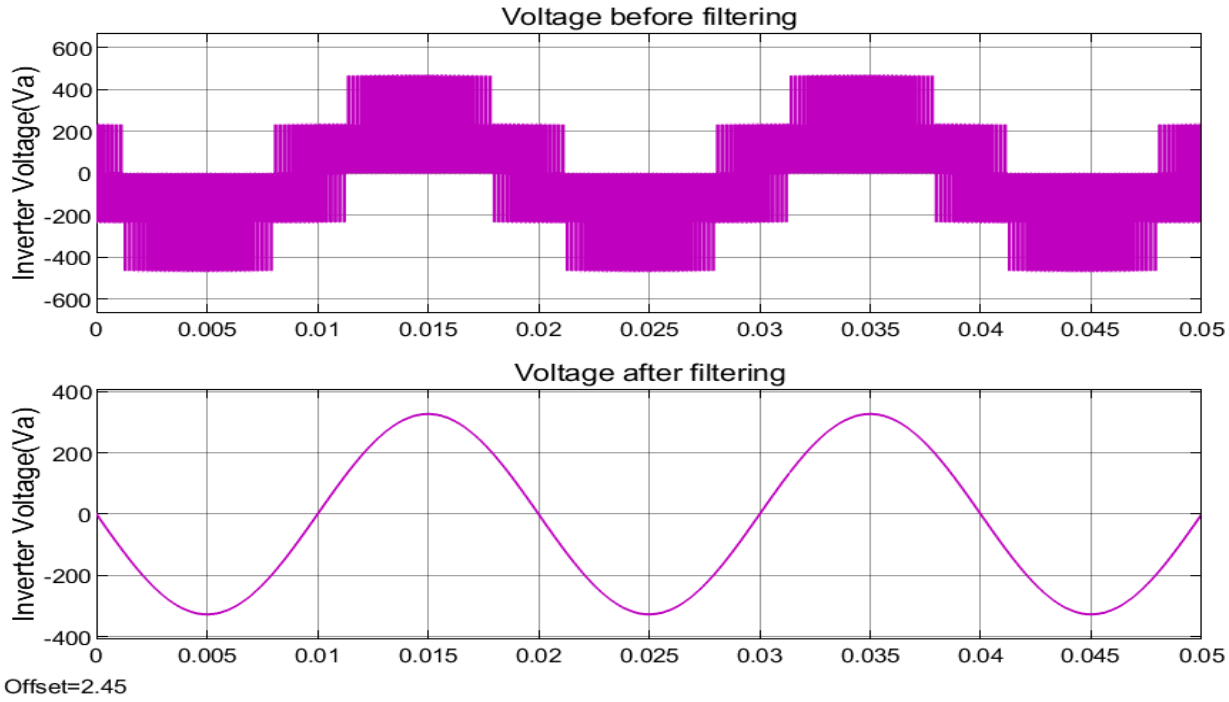

Figure 5.13 Output of Inverter before and after filter for Voltage waveform

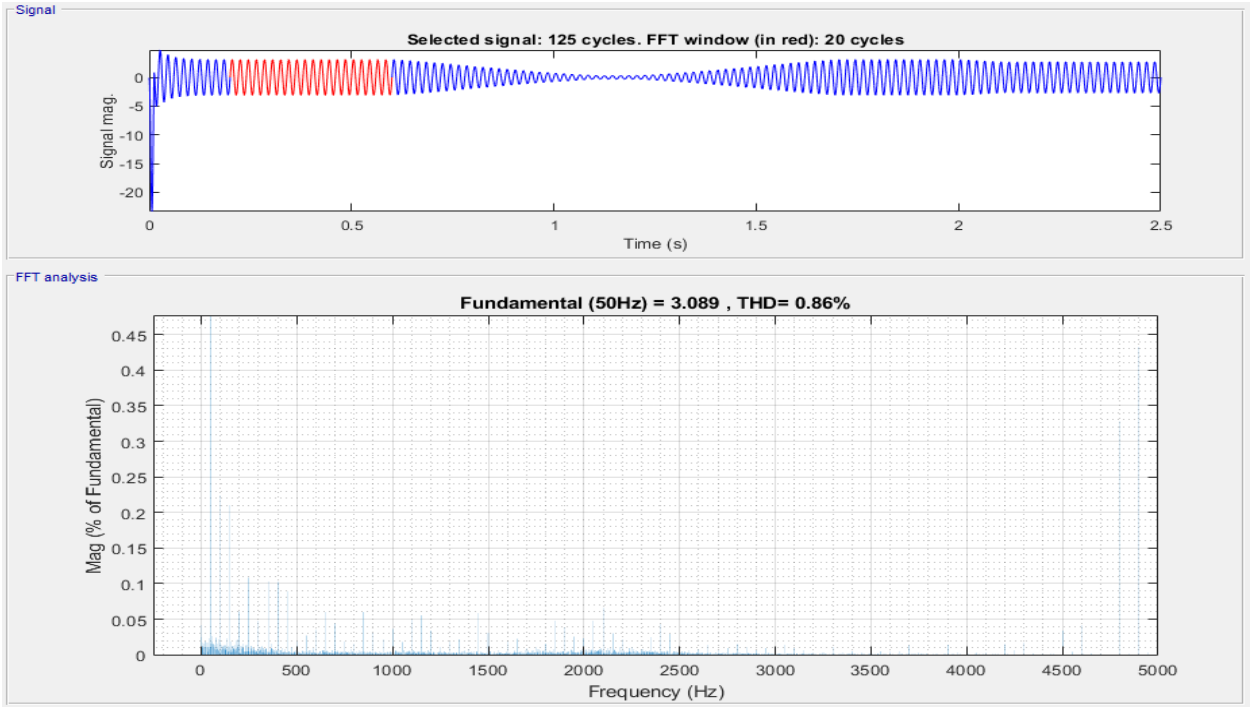

Figure 5.14 FFT Analysis of Inverter Output Current

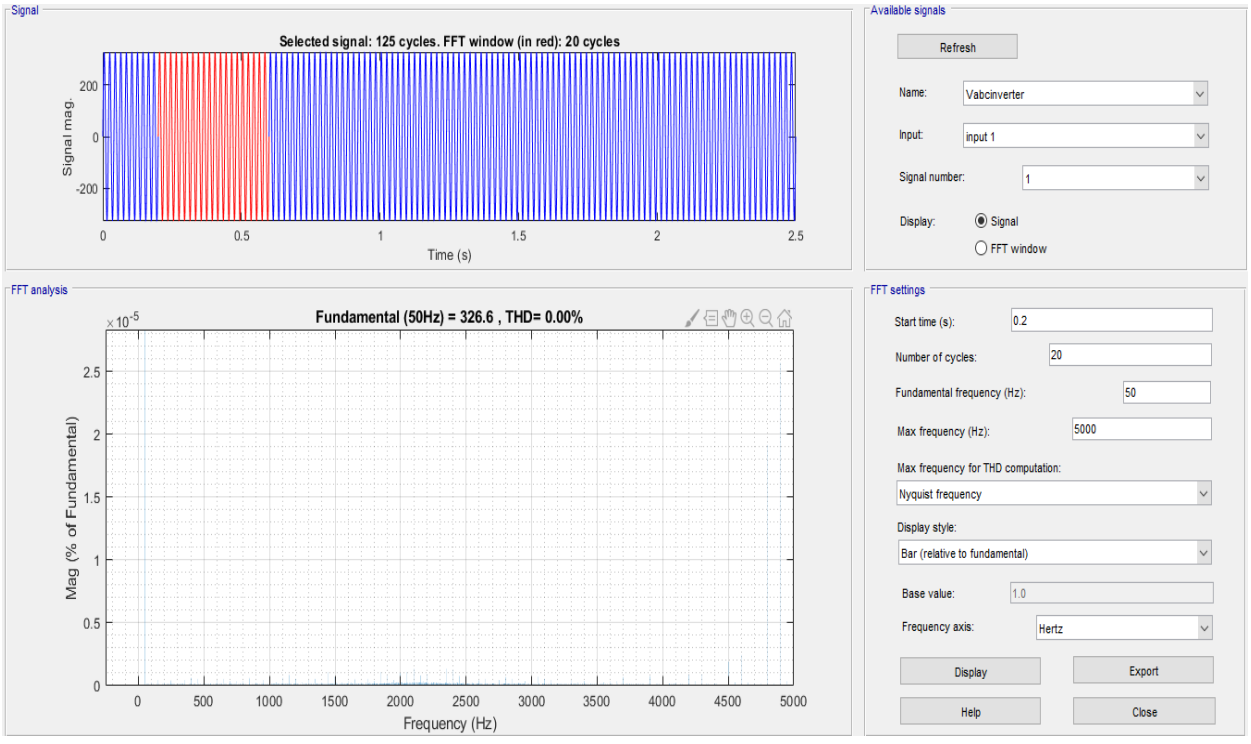

Figure 5.15 FFT Analysis of Inverter Output Voltage

5.6. Three Phase Voltage and Current Waveforms

After the completion of synchronization of the output of the inverter with that of output of the grid so that the magnitude, the phase angle and frequency of the inverter and grid are the same. The phase locked loop plays a vital role in generating phase angle from the grid voltage in order to synchronize the grid output with inverter output. Figure 5.16 shows the results of the output waveforms of three phase voltage of the inverter and grid by having a magnitude of rms value of 230V and frequency of 50Hz.

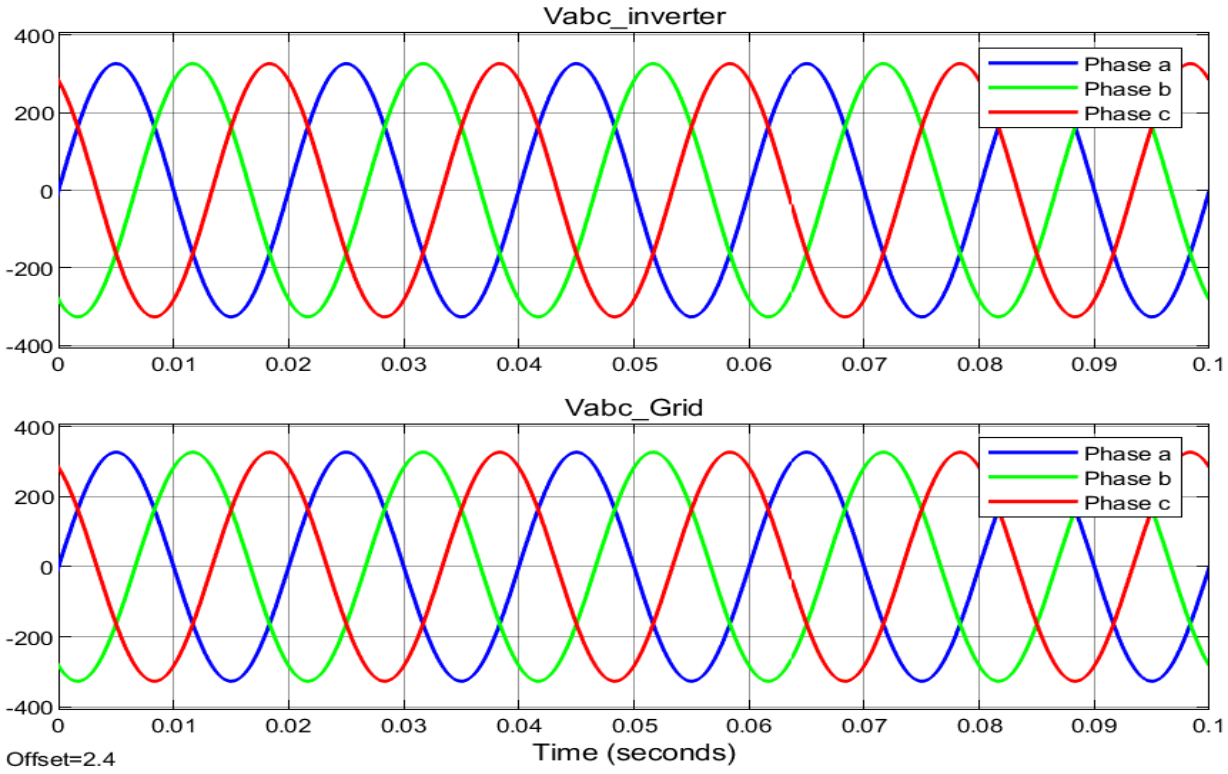

Figure 5.16 Output Waveform of Three Phase Voltage for Inverter and Grid

Figure 5.17 illustrates the results of the three phase current which are injected into the inverter and grid. As can be seen in the figure 5.17, the three phase grid voltage is in phase with that of the three phase inverter current. The magnitude of current of each phase is around 2.142A rms. The magnitudes of harmonics available in the injected current with respect to the fundamental frequency/harmonic order for phase A and the total harmonics distortion (THD) of the injected grid current and voltage, and Fast Fourier Transform (FFT) analysis of the grid current and volatge as frequency spectrum is shown in figure 5.18 and figure 5.19.

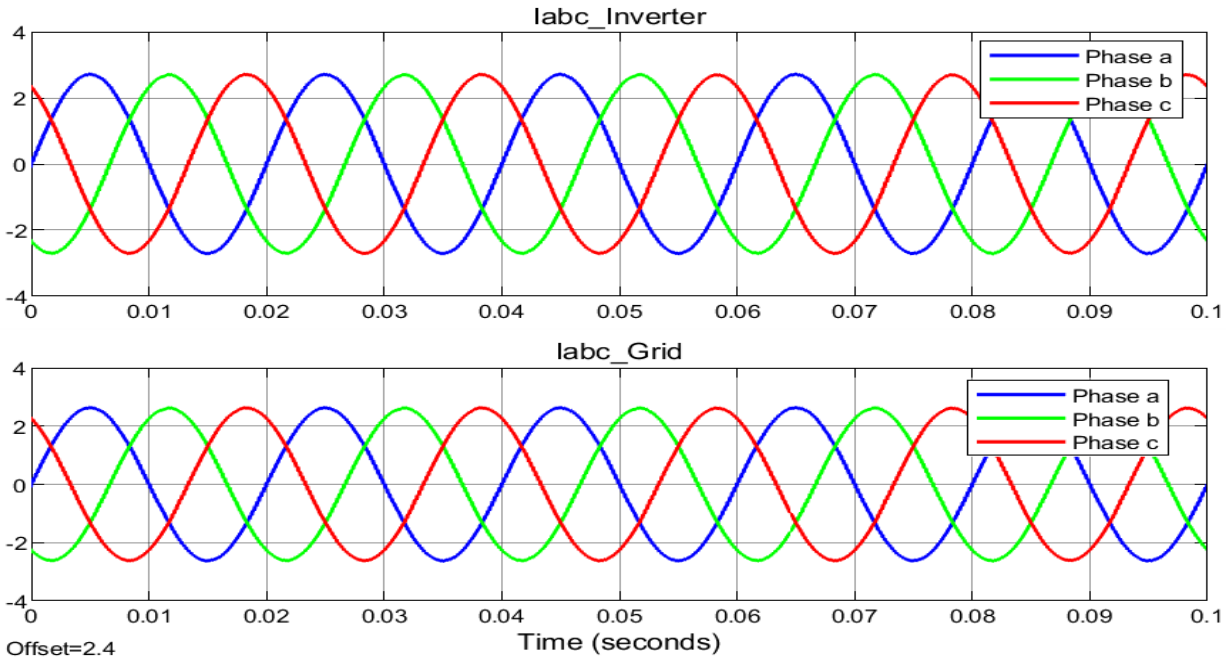

Figure 5.17 Output Waveform of Three Phase Current for Inverter and Grid

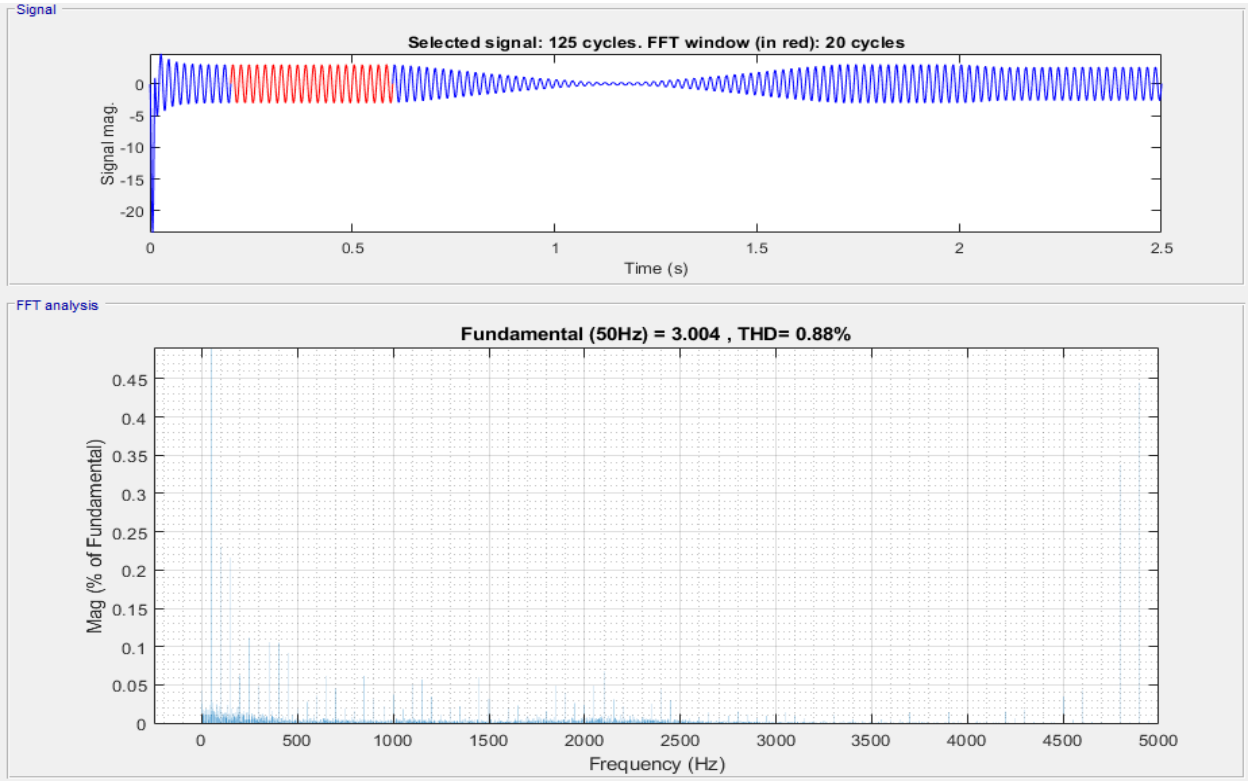

Figure 5.18 FFT Analysis of Grid Current

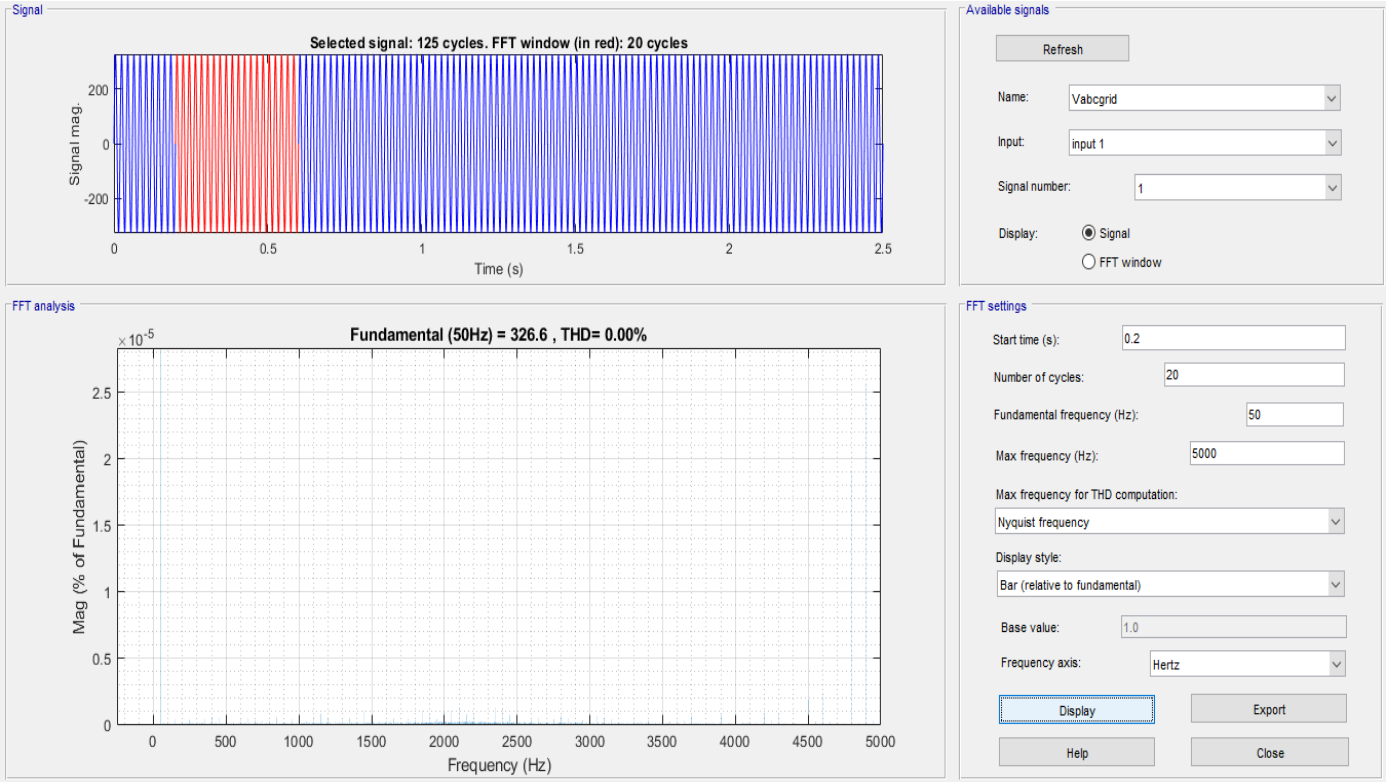

Figure 5.19 FFT Analysis of Grid Voltage

5.7. Active and Reactive Reference Currents

The active and reactive power of the system are highly dependent on the active and reactive reference current that are I_d^* and I_q^* respectively. The direct current component is responsible for controlling the active power from the inverter. The quadrature current component is responsible for controlling the reactive power output from the inverter that has to be forced to zero in order to achieve a unity power factor. The direct and quadrature current are tracked the active and reactive reference current effectively and efficiently.

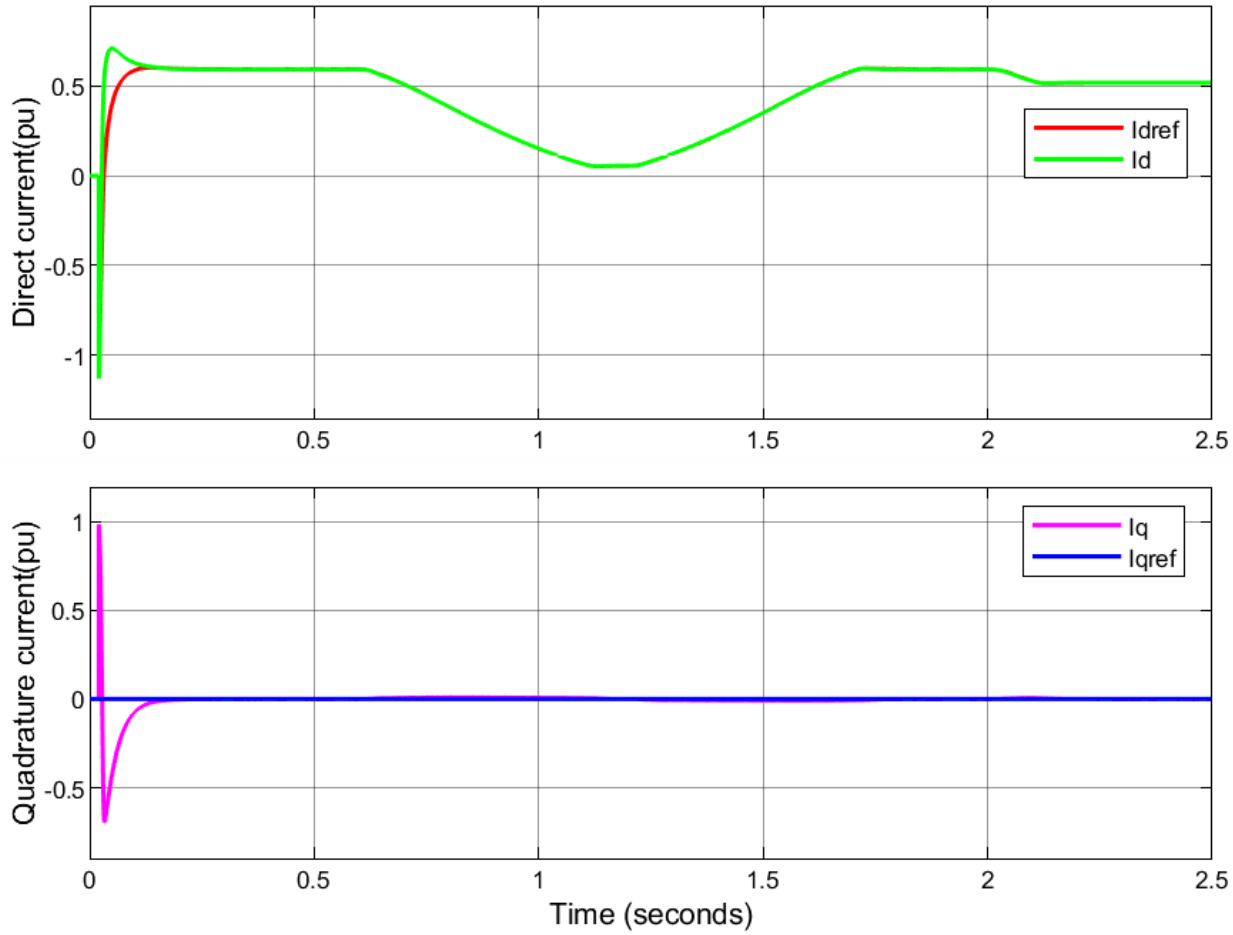

Figure 5.20 Direct and quadrature current component

5.8. Output Power of the System

The power delivered to the grid is 1474W so that the maximum power available from the PV array is 1521W depends on the constant solar irradiance and temperature. Only the active power is injected into the grid and the reactive power becomes zero. The active power and reactive power can be injected into the grid during the weather condition changes. The maximum power delivered to the grid is reduced to 1285W at 50^{o}C and 1000W/m^{2}. Figure 5.20 depicts the active power and reactive power injected to the grid.

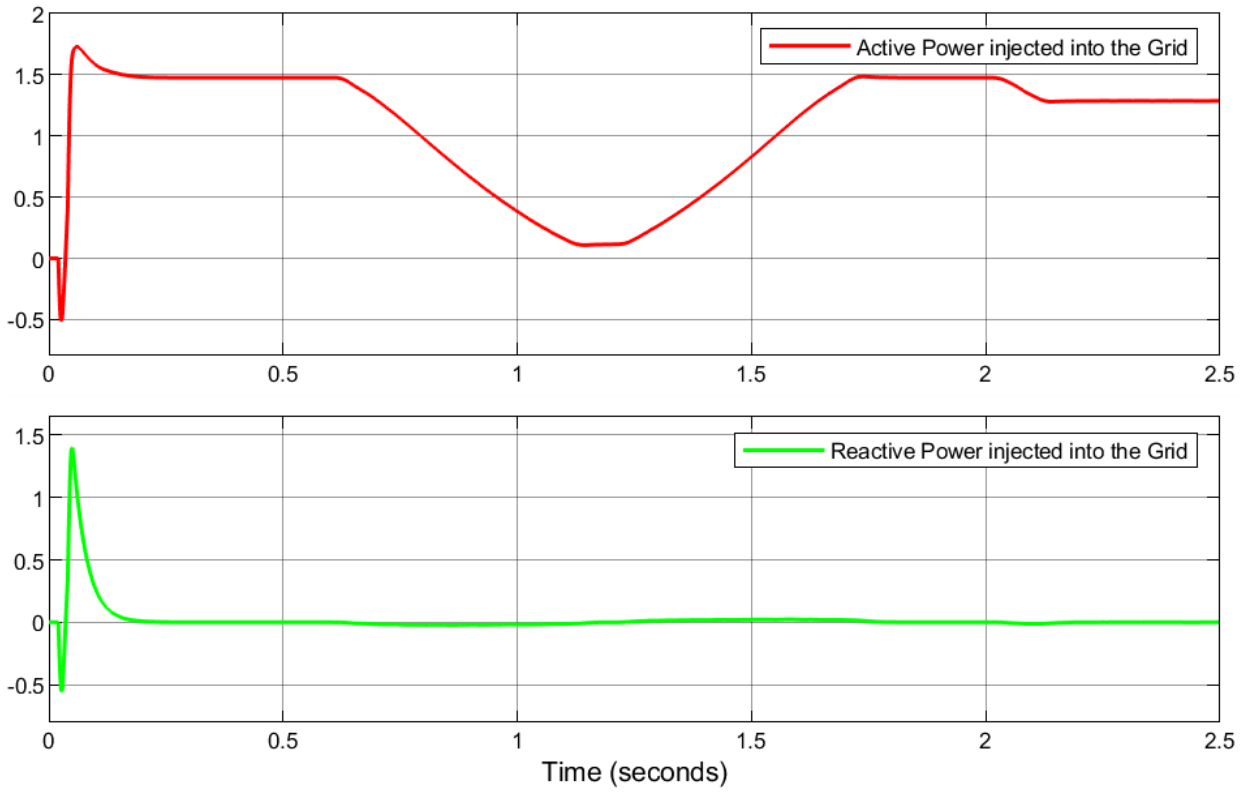

Figure 5.21 Active and Reactive Power injected into Grid

5.9. Effect of Resistive Load Change

The Simulation of the system shown in figure 4.10 were carried out for resistive and nonlinear loads using Matlab/Simulink environment. The complete model of grid connected PV system with local load connected to grid for a resistive load of 2.5kW and 3.5kW. The power flow of the system is decreased with the effect of load change. The DC-link voltage is kept constant at the given resistive load of 2.5kW and 3.5kW except the increasing of peak overshoot of the DC-link voltage. Figure 5.22 shows DC-link voltage at a given resistive load. The total harmonics distortion of the inverter and grid current with respect to the frequency was evaluated. When the resistive load increases, the total harmonic distortion of the grid current of the system increases. But the total harmonic distortion of the inverter is increased once, then it continues with the same value. The THD of the inverter and grid current can be considered constant due to the small variation in the harmonics. Figure 5.23 illustrates the THD of the inverter current at the load of 2.5kW and 3.5kW. Figure 5.24 shows the THD of the grid current at the load of 2.5kW. Figure 5.25 depicts the THD of the grid current at the load of 3.5kW.

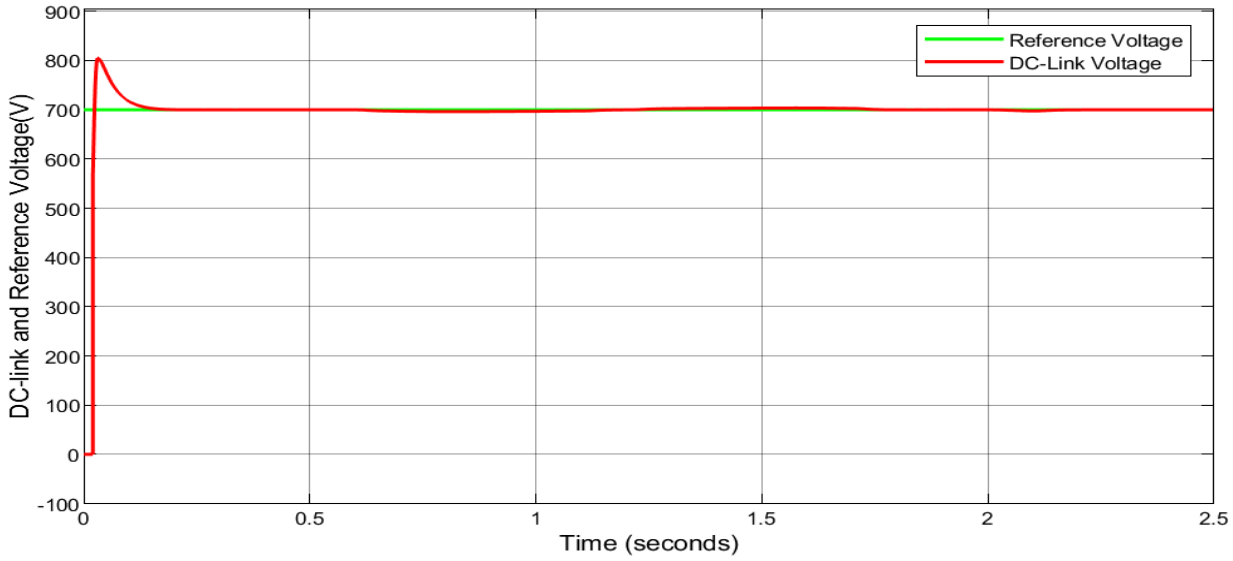

Figure 5.22 DC-Link voltage at resistive load of 2.5kW and 3.5kW

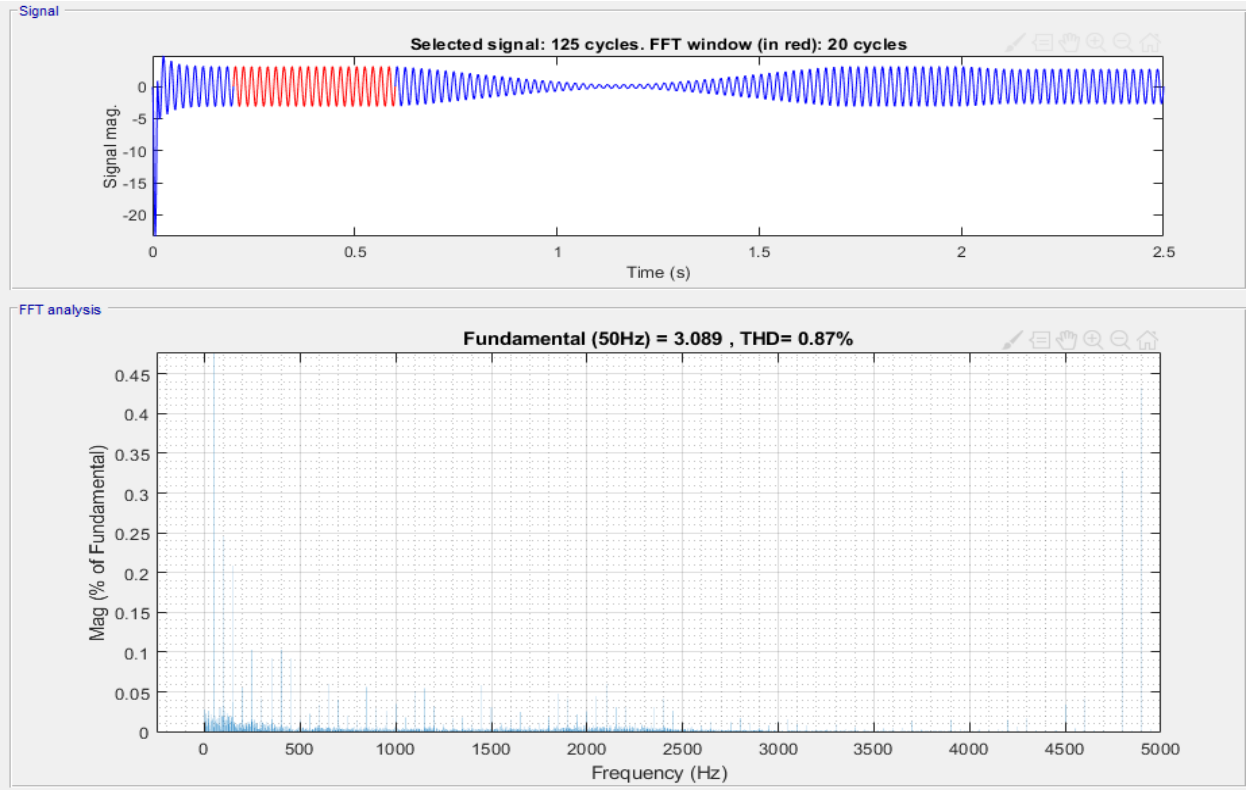

Figure 5.23 FFT Analysis of Inverter Current at load of 2.5kW and 3.5kW

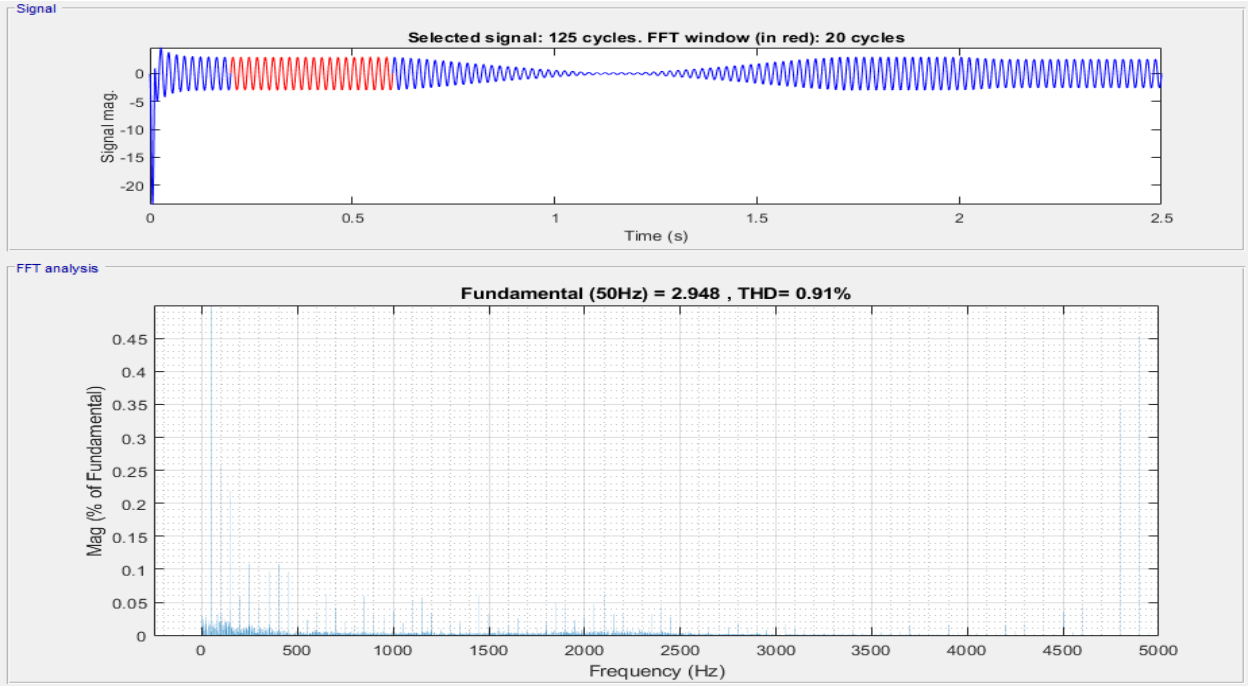

Figure 5.24 FFT Analysis of Grid Current at load of 2.5kW

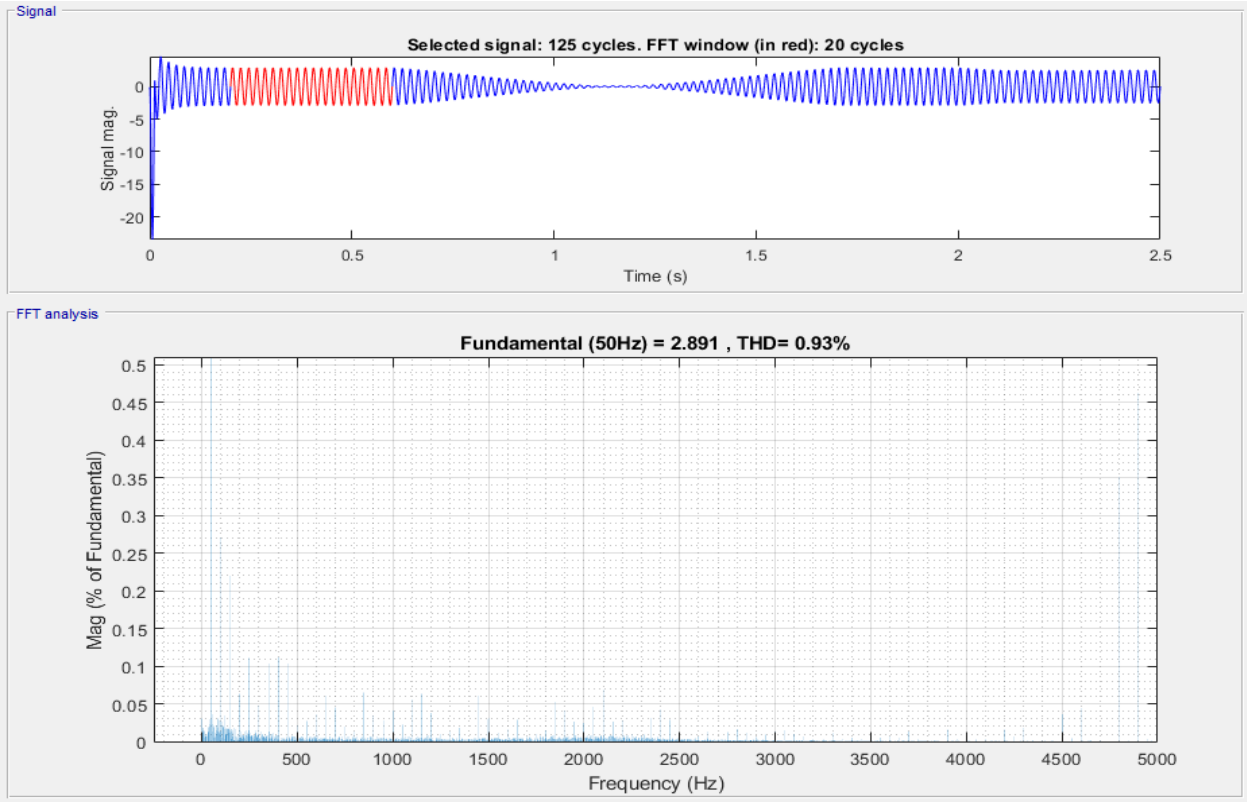

Figure 5.25 FFT Analysis of Grid Current at load of 3.5kW

Table 5.1. A summary for different values of resistive load

Resistive Load	THD of Inverter Current (%)	THD of Grid Current (%)
1.5kW	0.86	0.88
2.5kW	0.87	0.91
3.5kW	0.87	0.93

5.10. Effect of Non-Linear Load Change

The complete model of grid connected PV system with local load connected to grid for a nonlinear load of 125Ω and 320Ω. The types of nonlinear load was used in this work is the diode bridge rectifier as shown in figure 5.26. The power flow of the system is decreased with the increasing of nonlinear load values. The DC-link voltage is kept constant at the given nonlinear load except the decreasing of peak overshoot of the DC-link voltage. Figure 5.27 shows the DC-link voltage at a given nonlinear load. When the nonlinear load increases, the total harmonic distortion of the grid current is highly decreased. However, the total harmonic distortion of the inverter is decreased once and it continues with the same value. The THD of the inverter and grid current is very lower due to the effect of nonlinear load. Figure 5.28 illustrates the THD of the inverter current at the load of 125Ω and 320Ω. Figure 5.29 shows the THD of the grid current at the load of 100Ω. Figure 5.30 depicts the THD of the grid current at the load of 125Ω. Figure 5.31 illustrates the THD of the grid current at the load of 320Ω.

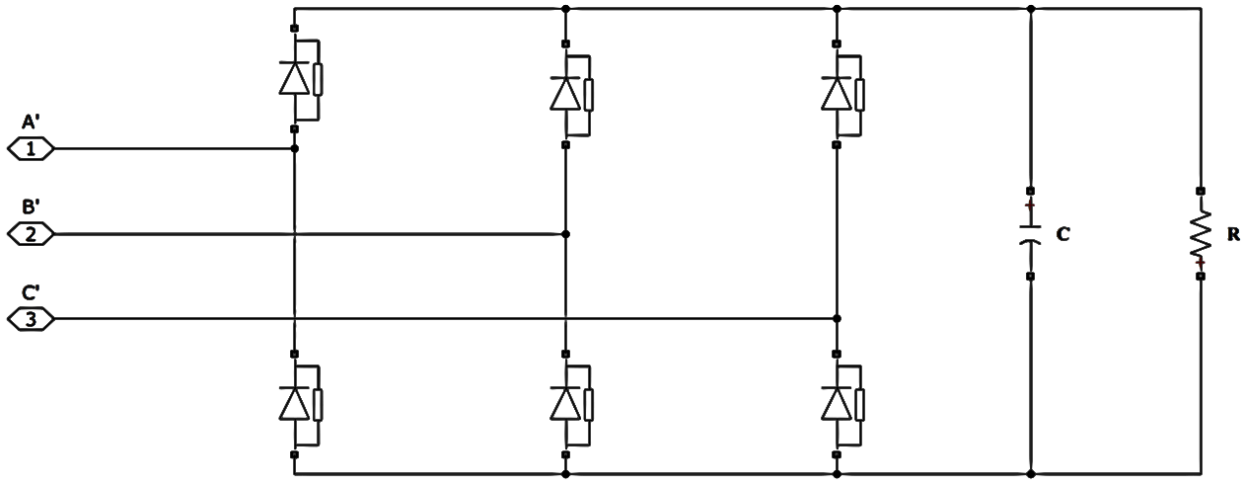

Figure 5.26 Non-linear Load

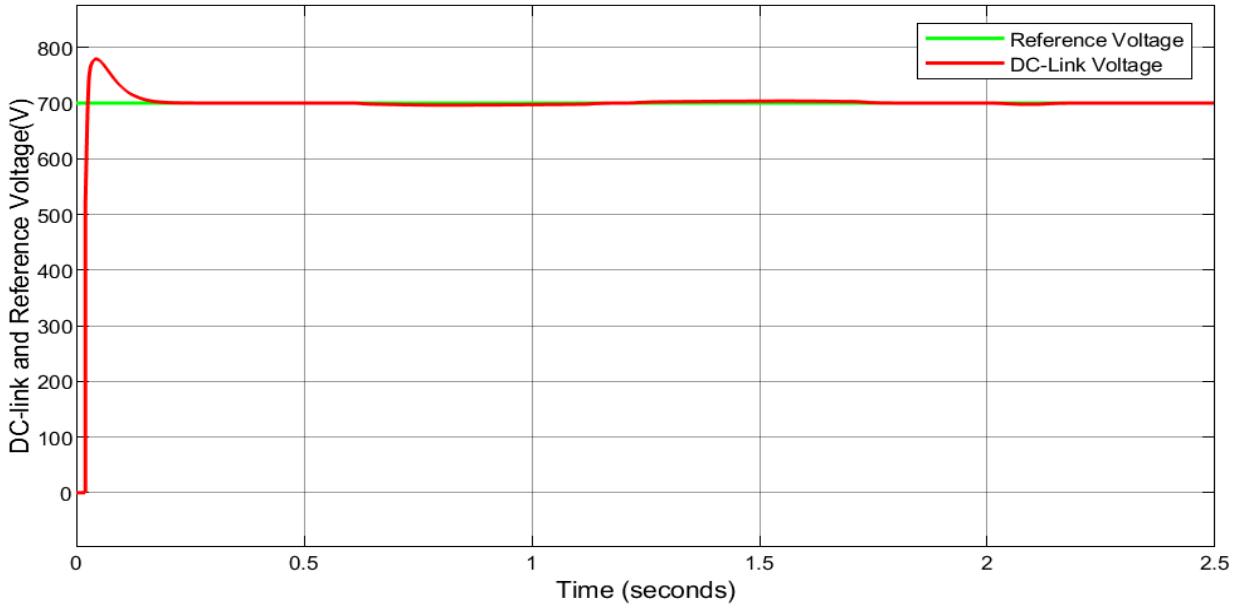

Figure 5.27 DC-Link voltage at non-linear load of 125Ω and 320Ω and *C* = 3000µF

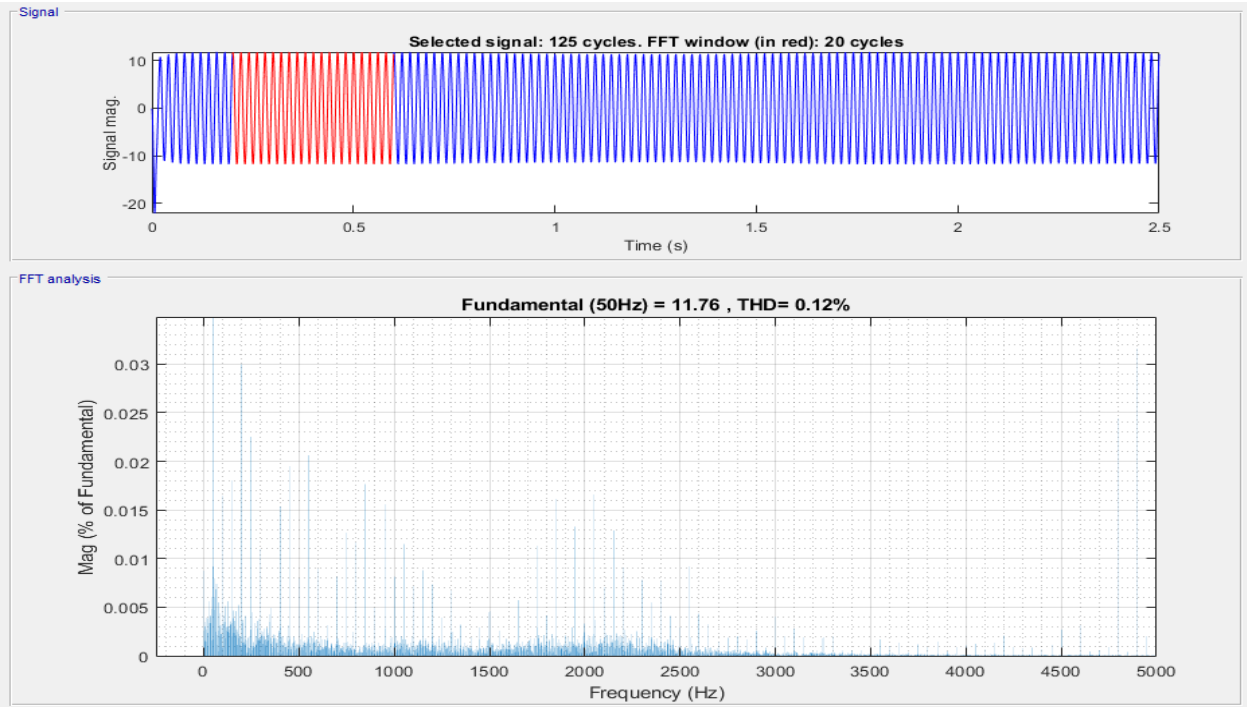

Figure 5.28 FFT Analysis of Inverter Current at non-linear load of 100Ω, 125Ω and 320Ω and *C* = 3000µF

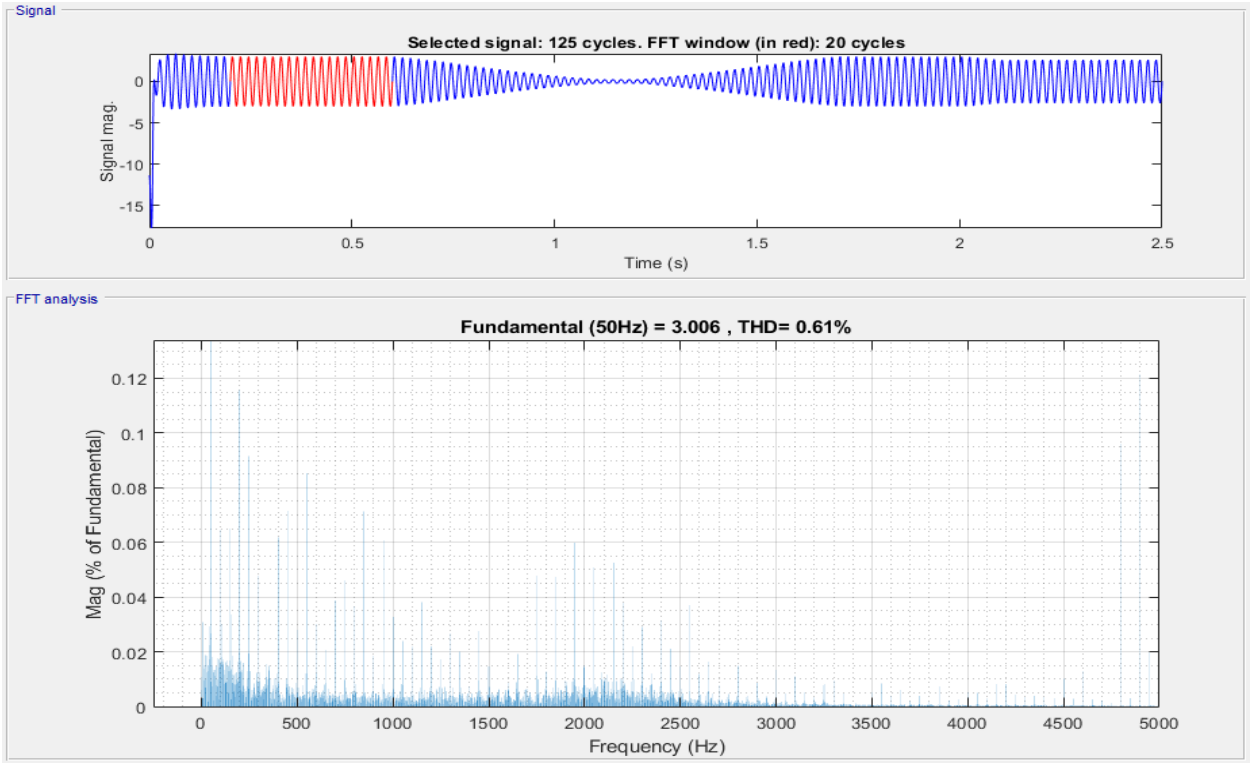

Figure 5.29 FFT Analysis of Grid Current at non-linear load of 100Ω and C = 3000µF

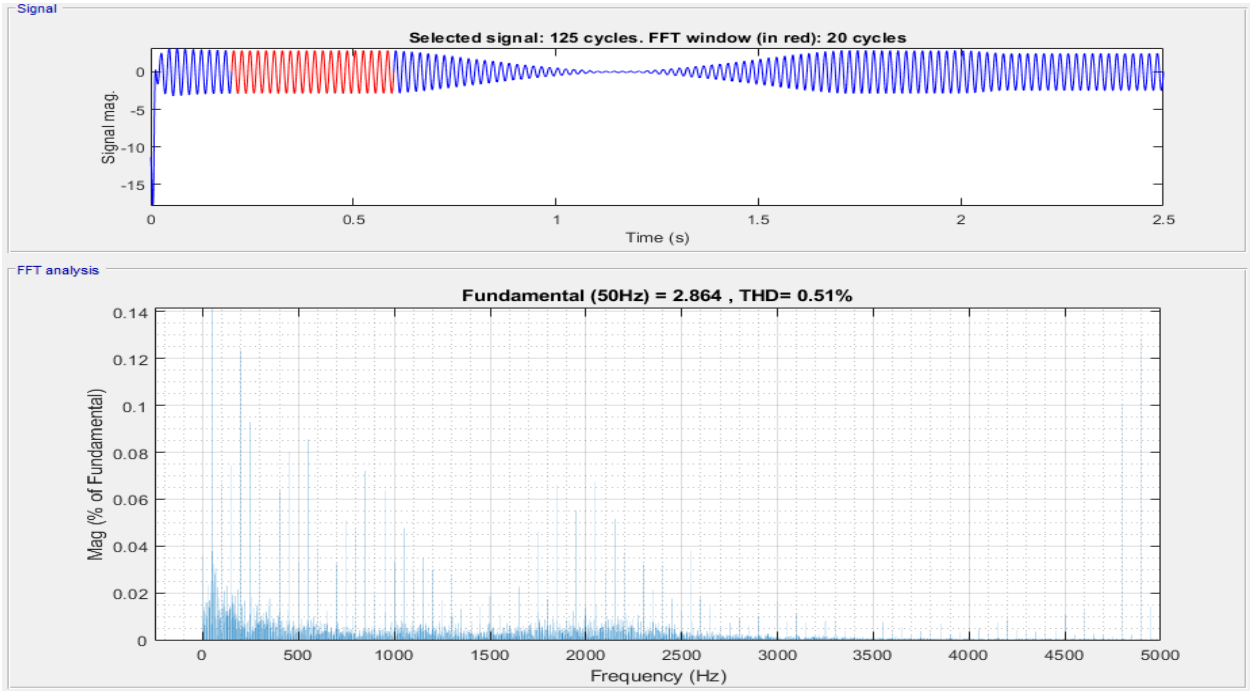

Figure 5.30 FFT Analysis of Grid Current at non-linear load of 125Ω and C = 3000µF

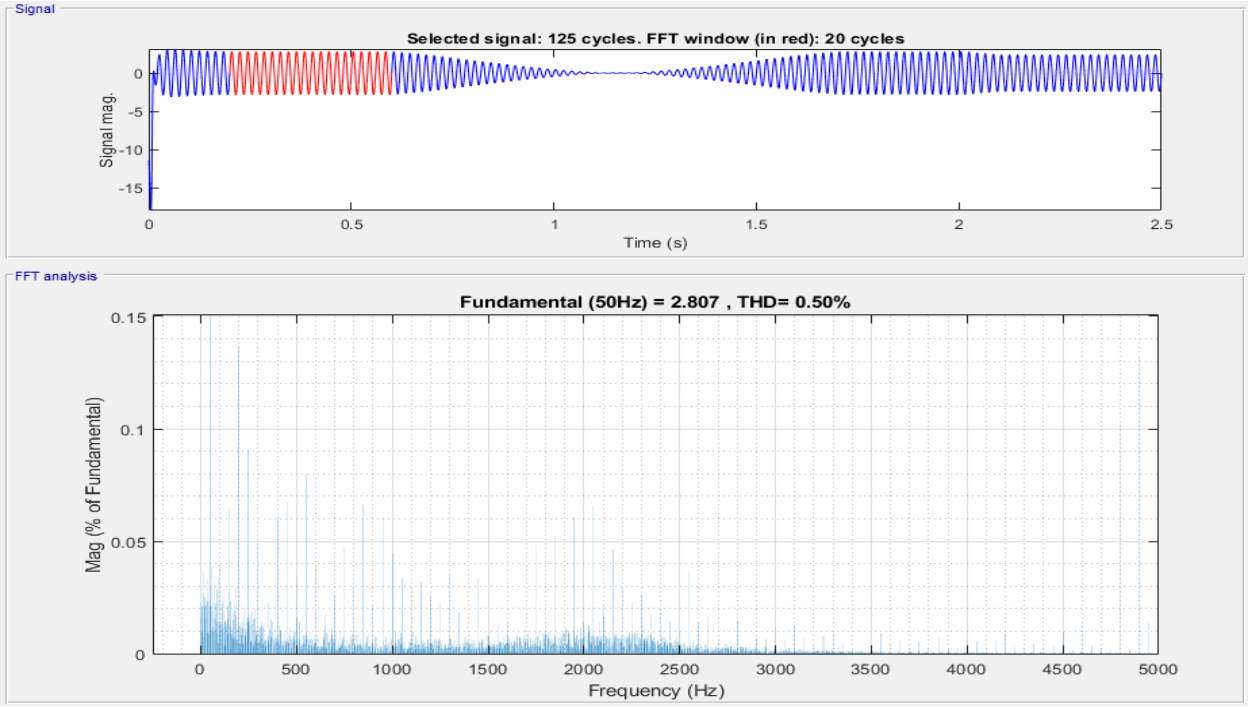

Figure 5.31 FFT Analysis of Grid Current at non-linear load of 320Ω and C = 3000µF

Table 5.2. A summary for different values of nonlinear load

Non-linear load and C = 3000µF	THD of Inverter Current (%)	THD of Grid Current (%)
100-Ω	0.12	0.61
125-Ω	0.12	0.51
320-Ω	0.12	0.50

Chapter Six

Conclusion and Future Work

6.1. Conclusion

In this thesis work, the task of designing and modelling of the three phase grid connected solar PV system using synchronously rotating reference frame has been successfully carried out. The proposed system comprises of the PV array, DC-DC boost converter, Incremental conductance based MPPT, 3-ϕ VSI, LCL-filter.

The PV array was modelled accurately that was constructed using MATLAB/SIMULINK environment. The accuracy of the model for PV array was verified by comparing the results of the model with the datasheet information. The DC-DC boost converter was designed and used to boost the output voltage of the PV array to the desired level. The control algorithms have been proposed in order to maximize the output power of the PV array. The most important parts of the system are the MPPT, DC-link regulator, active and reactive power control, total harmonics eliminations and synchronization control. Simulation results show that the incremental conductance based MPPT method tracks the maximum power point of the PV array to extract maximum power for a given environmental condition. A three phase voltage source inverter was controlled using SRRF with SVPWM to convert the DC voltage to an AC voltage in which its output current is synchronized with the grid voltage. An LCL-filter was designed which used to reduce and attenuate the high frequency harmonics at the output side of the inverter. This filter is used to interconnect the inverter output with the grid which provides the filtering of harmonics available in the current due to the switching nature of the inverter.

The control structure of the inverter is done based on two loops such as external loop and internal loop which are used to perform as DC-link voltage control and current control loop in order to maintain the power flow in the system and power quality and harmonics present in the current respectively. The simulation results show that the proposed system operates efficiently and effectively under various weather conditions. The efficiency of the overall system is around 97% which is improved more than the previous related work whose efficiency is around 96%. The total harmonic distortion of the grid current is 0.88% which is less than the previous work that is 1.42%. For resistive load change, the THD of the grid current and inverter current are 0.88%, 0.91% and 0.93%, and 0.86%, 0.87% and 0.87% for a load of 1.5kW, 2.5kW and 3.5kW

respectively. For a nonlinear load change, the THD of the grid current and inverter current are 0.61%, 0.51% and 0.50%, and 0.12%, 0.12% and 0.12% for a load of 100Ω, 125Ω and 320Ω and C = 3000μF respectively.

6.2. Future Work

The future work can be carried on to make broad the scope of the thesis that can be summarized into the following points:

- Perform some practical experiments to verify the obtained simulation results.
- It is possible to compare the model developed based incremental conductance using different types of MPPT techniques.
- Perform fault analysis on the developed system model using the constructed model.
- In this thesis work, the two-level three phase inverter is used; multilevel inverters are able to minimize the switching losses occurring in the inverter because the switching losses are the main concern in two level inverters.

References

[1] V. Katinas, M. Marčiukaitis and M. Tamašauskienė, "Analysis of the wind turbine noise emissions and impact on the environment", *Renewable and Sustainable Energy Reviews*, vol. 58, pp. 825-831, 2016.

[2] I. Onakpoya, J. O'Sullivan, M. Thompson and Heneghan, "The effect of wind turbine noise on sleep and quality of life: A systematic review and meta-analysis of observational studies", *Environment International*, vol. 82, pp. 1-9, 2015.

[3] R. Fu *et al.*, "U.S. Solar Photovoltaic System Cost Benchmark: Q1 2016" ,National Renewable Energy Laboratory, 2016.

[4] Marcelo Gustavo Molina,"Modeling and Control of Grid-connected Solar Photovoltaic Systems", Institute of Electrical Energy, National University of San Juan−CONICET, Argentina.

[5] V. Jagadeesh Babu and J. Arun Venkatesh, "Control of Grid Connected Hybrid Energy System using Synchronous Reference Frame Technique", *International Journal of Advanced Research in Electrical, Electronics and Instrumentation Engineering, Vol. 3, Special Issue 4, May 2014.*

[6] A. Angela Sheril and M. Ramesh Babu,"Synchronization Control of Grid Connected Photovoltaic System", *Middle-East Journal of Scientific Research* 25 (4): 864-870, 2017.

[7] Manel Hammami, Rabeh Abbassi and Souad Chebbi, "Design and simulation of a grid-connected photovoltaic system" Conference Paper, January, 2014.

[8] Bhavesh M. Jesadia and Prof. Indrajit N.Trivedi,"Analysis Of PV System Embeded To Distribution Grid For Active & Reactive Power Supply To Grid", *International Journal of Advance Engineering and Research Development, Volume 2, Issue 5, May, 2015.*

[9] Tomas Markvart (2001, ''Solar Electricity'', John wiley & sons Baffin's Lane chichester west Sussex P019IUD, England,p-25.

[10] Green *et al.*, "Solar cell efficiency tables (version 49)," *Progress in Photovoltaics: Research and Applications*, vol. 25, no. 1. pp. 3–13, Jan. 2017.

[11] S. Sumathi, L. Ashok Kumar, and P. Surekha, ''Solar PV and Wind Energy Conversion Sytems''.

[12] M. A. Elgendy, B. Zahawi and D. J. Atkinson, "Evaluation of perturb and observe MPPT algorithm implementation techniques," *6th IET International Conference on Power Electronics, Machines and Drives (PEMD 2012)*, Bristol, pp. 1-6, 2012.

[13] M. Eltawil and Z. Zhao, "MPPT techniques for photovoltaic applications", *Renewable and Sustainable Energy Reviews*, vol. 25, pp. 793-813, 2013.

[14] M. G. G. Villalva *et al.*, "Comprehensive Approach to Modeling and Simulation of Photovoltaic Arrays," *IEEE Transactions on Power Electronics*, vol. 24, no. 5. pp. 1198–1208, May 2009.

[15] Rashid, *Power Electronics: Circuits, Devices, and Applications*, 3rd ed. Prentice Hall, 2003.

[16] Mohan *et al.*, *Power Electronics: Converters, Applications and Design*, 3rd ed. John Wiley & Sons, Ltd, 2003.

[17] J. Jana, H. Saha and Das Bhattacharya, "A review of inverter topologies for single-phase grid-connected photovoltaic systems", *Renewable and Sustainable Energy Reviews*, vol. 72, pp. 1256-1270, 2017.

[18] F. Blaabjerg *et al.*, "Overview of Control and Grid Synchronizations of DPG Systems," *IEEE Transactions on Industrial Electronics*, vol.53, no. 5. pp. 1398–1409, 2006.

[19] *Digital Signal Processing Based Electromechanical Motion Control, 2004.*

[20] L. N. Arruda, S. M. Silva "Phase Locked Loop structures for utility Grid connected systems," in *Proc. IEEE-IAS Annu. Meeting*, vol. 4, pp. 2655–2660, 2002.

[21] S. Kjaer, J. Pedersen and Blaabjerg, "A Review of Single-Phase Grid-Connected Inverters for Solar Photovoltaic Systems", *IEEE Transactions on Industry Applications*, vol. 41, no. 5, pp. 1292-1306, 2005.

[22] IEC 61727. Solar Photovoltaic systems – characteristics of the utility interface 2004.

[23] IEEE 1547. Standards for Interconnecting DRs with Electric Power Systems, 2003.

[24] IEEE Standard 929. IEEE Recommended Practice for Utility Interface of solar PV Systems, 2000.

[25] M. Prodanovic and T. Green, "Control and filter design of three-phase inverters for high power quality grid connection," in *IEEE Transactions on Power Electronics*, vol. 18, no. 1, pp. 373 380, 2003.

[26] M. Rashid, *Power electronics handbook*, 3rd ed. Elsevier, 2011.

[27] G. M. Masters, *Renewable and Efficient Electric Power Systems*. Hoboken, NJ, USA: John Wiley & Sons, Inc., 2004.

[28] Samlexsolar, "Solar PV Cell Module, array".

[29] Xuan H. Nguyen & Minh Ph. Nguyen, ''Mathematical Modeling of PV Cell, PV Module and PV Array'', 2015.

[30] Omar Mohammed Benaissa, Samir Hadjeri and Sid Ahmed Zidi,"Modeling and Simulation of Grid Connected PV Generation System using Matlab/Simulink'', 2017.

[31] Liu X, Wang P & Loh PC (2010), ''Optimal Coordination Control for Standalone PV System with Nonlinear Load'', Proceedings of 2010 9th international power and energy conference, Singapore, 27-29October 2010, 5pp.

[32] Grandi G, Rossi C, Ostojic D et al (2009) A new multilevel conversion structure for grid-connected PV applications. IEEE Trans Ind Electron 56(11):4416–4426.

[33] Mohan N, Under land TM (2007) Power electronics: converters, applications, and design. Wiley, New York.

[34] F. Gao, D. Li, P. C. Loh, Yi Tang and Peng Wang, "Indirect dc-link voltage control of two stage single-phase PV inverter," *2009 IEEE Energy Conversion Congress and Exposition*, San Jose, CA, pp. 1166-1172, 2009.

[35] A.A.Nouredine and A.A. Yacine," simulation and implementation of single-stage three phase grid connected PV system using SVM-controlled three-level inverter'', 2017.

[36] K. Zhou and Wang, "Relationship between space-vector modulation and three-phase carrier-based PWM: a comprehensive analysis [three-phase inverters]," *IEEE Transactions on Industrial Electronics*, vol. 49, no. 1. pp. 186–196, 2002.

[37] W.F.Zhang *et al.*, "Comparison of Three SVPWM Strategies," *Journal of Electronic Science and Technology*, vol. 5, no. 3. Editorial Board of Journal of University of Electronic Science and Technology, pp. 283–287, 2007.

[38] M.-Y.Park *et al.*, "an LCL filter design for grid-connected PCS using THD and RAF," *The 2010 International Power Electronics Conference - ECCE ASIA -*. IEEE, pp. 1688–1694, Jun. 2010.

[39] X. Wei *et al.*, "Design of LCL filter for wind power inverter," in *2010 World NonGrid-Connected Wind Power and Energy Conference*, 2010, pp. 1-6.

[40] T. C. T. C. Y. Wang *et al.*, "Output filter design for a grid-interconnected three-phase inverter," in *IEEE 34th Annual Conference on Power Electronics Specialist*, 2003, vol. 2, pp. 779–784.

[41] Lissere. M. *et al.*, "Design and control of an LCL filter based three-phase active rectifier," *IEEE Transactions on Industry Applications*, vol. 41, no. 5. pp. 1281–1291, Sep. 2005.

[42] H. Cha and Vu, "Comparative analysis of low-pass output filter for single-phase grid-connected Photovoltaic inverter," in *Twenty-Fifth Annual IEEE Applied Power Electronics Conference and Exposition (APEC)*, 2010 pp. 1659–1665.

[43] Workagegn Tatek, "Model reference adaptive control based sensorless speed control of induction motor", 2017.

[44] Suresh Lakhimsetty, "Simulation of space vector PWM for voltage source inverter using matlab/Simulink'', 2014.

[45] D. Candusso, L. Valero, A. Walter, S. Bacha, E. Rulliere and B. Raison, "Modeling, control and simulation of a fuel cell based on power supply system with energy management," *IEEE 2002 28th Annual Conference of the Industrial Electronics Society. IECON 02*, pp. 1294-1299 vol.2, 2002.

[46] C. Ramos, A. Martins, and Carvalho, "Current control in the grid connection of the double output induction generator linked to a variable speed wind turbine," in *Proc. IEEE IECON*, vol.2, pp. 979–984, 2002.

[47] T. Huang, X. Shi, Y. Sun and D. Wang, "Three-phase photovoltaic grid-connected inverter based on feed-forward decoupling control," *2013 International Conference on Materials for Renewable Energy and Environment*, Chengdu. pp. 476-480, 2013.

[48] Matlab/Simulink from mathwork for 2018b.

[49] A. Vijayakumari, A. Devarajan and N. Devarajan, "Decoupled control of grid connected inverter with dynamic online grid impedance measurements for micro-grid applications", *International Journal of Electrical Power & Energy Systems*, vol. 68, pp. 1-14, 2015.

[50] L. Ma, W. Ran and T. Q. Zheng, "Modeling and control of three phase grid-connected photovoltaic inverter," Control and Automation (ICCA), 2010 8th IEEE International Conference on, Xiamen, 2010, pp. 2240-2245.

Appendices

Appendix A: MATLAB CODES to obtain I-V and P-V Curve

MATLAB code to obtain the PV characteristics curves for I-V and P-V curve

```
%constant and variables
q=1.6*10^-19; %electron charge
Ego=1.1; %band-gap energy of semiconductor
K=1.380504*10^-23; %Boltzmann constant
Ki=0.061745; %Temperature coefficient of short-circuit current
A=0.94504; %ideality factor
Isc=5.96; %short-circuit current
Voc=64.2; %open-circuit voltage
Rs=0.37154; %series resistance
Rsh=269.5934; %shunt resistance
Ns=96; %number of cells connected in series
Np=1; %number of cells connected in parallel
Tref=298; %nominal temperature
Tk= [100 75 50 25]; % different temperatures
Top=273+Tk; %operating temperature
G=1000; %solar irradiance
Vpv= (0:70); %output voltage of PV system
for i=1:4
 Iph=(Isc+Ki*(Top(i)-Tref))*G/1000;
 Irs=Isc/(exp((q*Voc)/(A*Ns*K*Top(i))-1));
 Io=Irs*(Top(i)/Tref )^3*(exp((q*Ego*((1/Tref)-(1/Top(i))))/(A*K)));
 Ish=Vpv/Rsh;
 Ipv=Iph-Io*(exp((q*Vpv)/(A*Ns*K*Top(i))-1)-Ish);
 Ppv=Vpv.*Ipv;
figure(1)
plot(Vpv, Ppv,'linewidth',2)
title('P-V Curve for PV Module')
```

```
xlabel('Output Voltage (V)')
ylabel('Output Power (W)')
axis([0 70 0 350])
legend('T=100oC','T=75oC','T=50oC','T=25oC');
hold on
grid on
figure(2)
plot(Vpv, Ipv,'linewidth',2);
axis([0 70 0 12])
title('I-V Curve for PV Module')
xlabel('Output Voltage (V)')
ylabel('Output Current (A)')
legend('T=100oC','T=75oC','T=50oC','T=25oC')
hold on
grid on
end
%constant and variables
q=1.6*10^-19; %electron charge
Ego=1.1; %band-gap energy of semiconductor
K=1.380504*10^-23; %Boltzmann constant
Ki=0.061745; %Temperature coefficient of short-circuit current
A=0.94504; %ideality factor
Isc=5.96; %short-circuit current
Voc=64.2; %open-circuit voltage
Rs=0.37154; %series resistance
Rsh=269.5934; %shunt resistance
Ns=96; %number of cells connected in series
Np=1; %number of cells connected in parallel
Tref=298; %nominal temperature
Top=273+25; %operating temperature
G=[1000 800 600 400 200];%different solar irradiances
```

```
Vpv=(0:0.01:70);%output voltage of PV system
for i=1:5
 Iph=(Isc+Ki*(Top-Tref))*G(i)/1000;
 Irs=Isc/(exp((q*Voc)/(A*Ns*K*Top))-1);
 Io=Irs*(Top/Tref)^3*(exp((q*Ego*((1/Tref)-(1/Top)))/(A*K)));
 Ish=Vpv/Rsh;
 Ipv=Iph-Io*(exp((q*Vpv)/(A*Ns*K*Top)-1)-Ish);
 Ppv=Vpv.*Ipv;
figure(1)
plot(Vpv,Ppv,'linewidth',2)
title('P-V Curve for PV Module')
xlabel('Output Voltage (V)')
ylabel('Output Power (W)')
legend('G=1000w/m2','G=800w/m2','G=600w/m2','G=400w/m2','G=200w/m2')
axis([0 70 0 350])
hold on
grid on
figure(2)
plot(Vpv,Ipv,'linewidth',2);
axis([0 70 0 12])
title('I-V Curve for PV Module')
xlabel('Output Voltage (V)')
ylabel('Output Current (A)')
legend('G=1000w/m2','G=800w/m2','G=600w/m2','G=400w/m2','G=200w/m2')
hold on
grid on
end
```

Appendix B: MATLAB code to design inverter filter

```
%Inputs
```

V_{LLrms} = 400; % line to line rms voltage

V_{ph} = 400/sqrt(3); % phase rms voltage

P_n = 1.526e3W; % rated active power (Pmpp at STC)

V_{dc} = 700V; % dc-link voltage from the boost converter

f_g = 50Hz; % grid frequency

f_s = 5e3Hz; % inverter switching frequency

%Step1-----Calculate Z_b,L_b,C_b

V_b=V_{LLrms};

P_b=P_n;

I_b=P_n/(sqrt(3)*V_{LLrms});

Z_b=V_{LLrms}^2/P_n;

L_b=Z_b/(2*pi*f_g);

C_b=1/(2*pi*f_g*Z_b);

%Step2-----Calculate C_f (maximum power factor variation seen by the grid is less than 5%)

x=2.5/100;

C_f=x*C_b;

%Step3-----Calculate L_i (deltaIb=V_{dc}/(8*f_s*L_i)) deltaI$_b$ between 10-20%

deltaI$_b$=.2*I_b; %(20% * Imax)

L_i=V_{dc}/(8*f_s*deltaI$_b$);

%Step4-----Calculate L_g

RAF = 20/100; % attenuation factor is 20%

Lg=(RAF+1)/(RAF*C_f*(2*pi*f_s)^2);

%Step5-----Calculate frequency resonance

U_r=sqrt((L_i+L_g)/(L_i*L_g*C_f));

f_{res}=U_r/(2*pi); % resonance frequency

%Step6-----make sure that 10f_g<(f_{res})<f_s/2

f_{res}_Test=(f_{res}>10*f_g) && (f_{res}<f_s/2);

%Step7-----Calculate damping resistor(R_f)

R_f=1/(3*2*pi*f_{res}*C)